

**SIMULATING SEA-SURFACE TEMPERATURE  
EFFECTS ON SOUTHERN AFRICAN RAINFALL  
USING A MESOSCALE NUMERICAL MODEL**

**Steven Jeffery Crimp**

**SIMULATING SEA-SURFACE TEMPERATURE  
EFFECTS ON SOUTHERN AFRICAN RAINFALL  
USING A MESOSCALE NUMERICAL MODEL**

**Steven Jeffery Crimp**

Dissertation submitted to the Faculty of Science, University of the Witwatersrand, for  
completion of the Degree of Master of Science

I declare this dissertation is my own, unaided work, and that it has not been submitted previously as a dissertation or thesis for any degree at any other University.

A handwritten signature in cursive script, appearing to read 'Ling', is centered on the page.

**To Marianne and my family.  
Thank you all.**

## Abstract

The atmospheric response of the Colorado State University Regional Atmospheric Modelling System (RAMS) to sea-surface temperature anomalies is investigated. A period of four days was chosen from 21 to 24 January 1981, where focus was placed on the development and dissipation of a tropical-temperate trough across southern Africa. Previous experiments using this mesoscale numerical model have determined the kinematic, moisture, and thermodynamic nature of these synoptic features. The research in this dissertation focuses specifically on the sensitivity of the numerical model's simulated responses to positive sea-surface temperature anomalies. Three separate experiments were devised, in which positive anomalous temperatures were added to the ocean surface north of Madagascar (in the tropical Indian Ocean), at the region of the Agulhas Current retroflexion, and along the tropical African west coast (in the Northern Benguela and Angola currents). The circulation aspects of each sensitivity test were investigated through the comparison of simulated variables such as vapour and cloud mixing ratios, temperature, streamlines and vertical velocity, with the same variables created by a control simulation. The results indicate that for the first sensitivity test, (the Madagascar anomaly), cyclogenesis was initiated over the area of modified sea temperatures which resulted in a marginal decrease in continental precipitation. The second sensitivity test (over the Agulhas retroflexion) produced a much smaller simulated response to the addition of anomalously warm sea temperatures than the tropical Indian Ocean anomaly. Instability and precipitation values increased over the anomalously warm retroflexion region, and were slowly transferred along the westerly wave perturbation and the South African east coast. The third sensitivity experiment showed a predominantly localised simulated increase in precipitation over Gabon and the Congo, with the slow southward progression of other simulated circulation differences taking place. The small perturbations in each of the simulated meteorological responses are consistent with the expected climate response to anomalously warm sea-surface temperatures in those areas.

## Preface

The climate of southern Africa is maintained by the position of the subcontinent in relation to the major atmospheric circulation features of the southern hemisphere. As a result of its geographical location, rainfall is strongly seasonal over most of the southern subcontinent. However, since the mid 1980's rainfall patterns over South Africa have become increasingly variable, when compared with the period 1951-1980. Debate still rages as to the exact nature of this increase, but the change in variability has served to renew the emphasis on improving the understanding of the factors influencing rainfall over the subcontinent.

Recent research into the forcing effect of sea-surface temperatures has identified associations between the temperature patterns in the tropical Indian, eastern Atlantic and central Pacific Oceans and seasonal rainfall variability over Southern Africa. Although this link has been identified, the effect on South African rainfall is complicated and by no means clear cut. Until recently research has been limited primarily to statistical investigations. However, with the advent and greater availability of more powerful computer processors, sensitivity tests using numerical atmospheric circulation models has become a possibility. The Colorado State University Regional Atmospheric Modelling System represents one such mesoscale numerical model system. Previous experiments with this model have delivered some important insights into the development, structure and dissipation of important rain-bearing synoptic features over southern Africa such as tropical-temperate troughs. A method has therefore become available not only to study synoptic features, but also to investigate the forcing effect of sea-surface temperatures on a meteorological time scale.

This research is aimed at ascertaining the influence that anomalously warm sea-surface temperatures have on a tropical-temperate trough, by:

1. determining the Colorado State University Regional Atmospheric Modelling System's (RAMS) sensitivity to changes in sea-surface temperature;

2. identifying the impacts that the warm ocean anomalies have on the formation, development, and dissipation of the tropical-temperate trough by comparing horizontal wind components ( $u, v$ ), temperature ( $T$ ), streamlines, vapour and cloud mixing ratios, and accumulated convective precipitation with the same variables in a control simulation.

This dissertation comprises of six chapters. **Chapter 1** contains an introduction to the research topic, and provides a necessary background to tropical-temperate troughs, sea-surface temperature anomalies and ocean-atmosphere interactions, in particular with regard to southern African rainfall variability. In **Chapter 2** a brief description of the data sources, research methodology and model features are discussed. Following this the results of the first sensitivity test (the tropical Indian ocean anomaly) are presented in **Chapter 3**. The next two sections, **Chapters 4** and **5** set out the results of the sensitivity experiments at the zone of the Agulhas Current retroflection and the tropical western Atlantic ocean. The synthesis and conclusions regarding the sensitivity experiments are summarised in the final chapter, **Chapter 6**. Sections of this dissertation have been submitted for publication and presented at local conferences. Specifically, **Chapter 3** has been accepted for publication in the South African Journal of Science. Presentations of **Chapters 3, 4** and **5** have been made at the 12<sup>th</sup> and 13<sup>th</sup> Annual Conference of the South African Society of Atmospheric Sciences.

The author would like to thank the following institutes for supplying data:

- a) the European Centre for Medium Range Weather Forecasts (ECMWF), for the Ilb Global analysis atmospheric data sets;
- b) the National Meteorological Centre (NMC) for the radiosonde and surface data sets;
- c) the United Kingdom Meteorological Office (UKMO) for the historical sea surface temperature data sets;

d) the South African Weather Bureau (SAWB) for synoptic charts spanning the case study.

The author would like to personally thank Sue Van den Heever for her willingness to answer a barrage of RAMS questions. Much gratitude is extended to Dr Noel de Villiers, for his technical support and help with the RAMS implementation. The author is also indebted to Dr Simon Mason for his encouragement, insight, and invaluable assistance. Further thanks go to Professor Peter Tyson, Dr Peter D'Abreton, and Alec Joubert for their helpful advice. All model simulations were run on the Cray Y-MP/EL housed at the South African Weather Bureau, and form part of a continued programme funded by the Water Research Commission. The cartographic unit, especially Philip Stickler and Wendy Philips are acknowledged.

A special mention must go to my fiancée, Marianne for her encouragement, patience and perspective throughout the development of this dissertation. Last, but certainly not least I would like to thank my family for their guidance and motivation.

## CONTENTS

Declaration .....	
Dedication .....	
Abstract .....	V
Preface .....	vi-viii

### CHAPTER 1

<b>Background</b> .....	<b>1</b>
<b>Southern African Climate</b> .....	<b>4</b>
<i>Southern African circulation patterns</i> .....	4
<i>Tropical-temperate troughs</i> .....	5
<i>Sea-surface Temperature anomalies and ocean-atmosphere interactions</i> .....	8
<i>Sea-surface Temperature anomalies and southern African rainfall variability</i> .....	9
<b>Hypotheses</b> .....	<b>11</b>

### CHAPTER 2

<b>Data and Methodology</b> .....	<b>13</b>
<b>Model Features and Parameter Options</b> .....	<b>14</b>
<i>Basic equations and time differencing scheme</i> .....	15
<i>Grid structure and boundary conditions</i> .....	15
<i>Cumulus parameterisation</i> .....	17
<b>Observed Synoptic-Scale Conditions</b> .....	<b>17</b>
<b>Control Simulation</b> .....	<b>19</b>

### CHAPTER 3

<b>Tropical Indian Ocean Anomaly (Sensitivity Test 1)</b> .....	<b>23</b>
<b>Results</b> .....	<b>25</b>
<i>Day one (21 January 1981)</i> .....	<b>25</b>
<i>Day two (22 January 1981)</i> .....	<b>28</b>
<i>Day three (23 January 1981)</i> .....	<b>36</b>
<i>Day four (24 January 1981)</i> .....	<b>42</b>
<b>Discussion</b> .....	<b>47</b>

### CHAPTER 4

<b>The Agulhas Current Retroflexion Anomaly (Sensitivity Test 2)</b> .....	<b>51</b>
<b>Results</b> .....	<b>53</b>
<i>Day one (21 January 1981)</i> .....	<b>53</b>
<i>Day two (22 January 1981)</i> .....	<b>53</b>
<i>Day three (23 January 1981)</i> .....	<b>62</b>
<i>Day four (24 January 1981)</i> .....	<b>68</b>
<b>Discussion</b> .....	<b>73</b>

### CHAPTER 5

<b>The Northern Benguela and Angola Current Anomaly (Sensitivity Test 3)</b> ..	<b>82</b>
<b>Results</b> .....	<b>82</b>
<i>Day one (21 January 1981)</i> .....	<b>82</b>
<i>Day two (22 January 1981)</i> .....	<b>84</b>
<i>Day three (23 January 1981)</i> .....	<b>99</b>
<i>Day four (24 January 1981)</i> .....	<b>107</b>
<b>Discussion</b> .....	<b>114</b>

## CHAPTER 6

<b>Synthesis and Conclusions</b> .....	<b>115</b>
<b>The Tropical Indian Ocean Anomaly (Sensitivity Test 1)</b> .....	<b>117</b>
<b>The Agulhas Current Retroflexion Anomaly (Sensitivity Test 2)</b> .....	<b>118</b>
<b>The Tropical Western Atlantic Ocean (Sensitivity Test 3)</b> .....	<b>119</b>
<b>References</b> .....	<b>122</b>

# CHAPTER I

## Background

The southern African subcontinent is positioned between two quasi-stationary oceanic anticyclones, circumpolar westerlies to the south, and tropical disturbances to the north. Variation in the location and intensity of the anticyclones, along with changes in frequency and paths of westerly disturbances, as well as tropical easterly disturbances, serve as the main influences on rainfall variability over the region. As South Africa's growing population places increasing pressure on already limited water resources a more accurate understanding and prediction of variations in precipitation is necessary. Research in the past and especially in the present has for the most part, been focused on achieving this goal.

Initially research was focused on the generalised classification of rainfall-producing systems and was limited to the identification of pressure systems and distinctive air flow patterns from surface data only. Recent research, with the help of satellite and general circulation model data, has succeeded in generating a more definitive classification of rain-bearing features (Fig 1.1) (Harangozo and Harrison, 1983; Harrison, 1984a,b; Tyson, 1987; D'Abreton, 1992). With this classification system in place tropical-temperature troughs were identified as having a substantial role in southern African rainfall variability (Fig 1.2) (Harrison 1984a, 1984b; Tyson, 1987; Preston-Whyte and Tyson, 1988; D'Abreton, 1992).

With the generalised classification of circulation types defined, the most important rain-producing systems for the country's interior were found to be tropical-temperate troughs. Further research showed that during early summer months temperate forcing mechanisms exhibit greater control over rainfall variability than tropical mechanisms (Harrison 1984a, 1984b; Tyson, 1987; Preston-Whyte and Tyson, 1988). The opposite was found to be true during late-summer. As cloud bands or tropical-temperate troughs combine both temperate and tropical synoptic features

predominantly during late summer, their frequency and duration account for a sizable portion of southern African rainfall variability. Factors affecting the frequency and duration of cloud band events have been linked to the phase of the Southern Oscillation and are indirectly linked to sea-surface temperature anomaly patterns. The following sections of this chapter deal with atmospheric circulation patterns of southern Africa with particular emphasis on tropical-temperate troughs, boundary layer interactions and a discussion of the effect of sea-surface temperatures on rainfall variability.

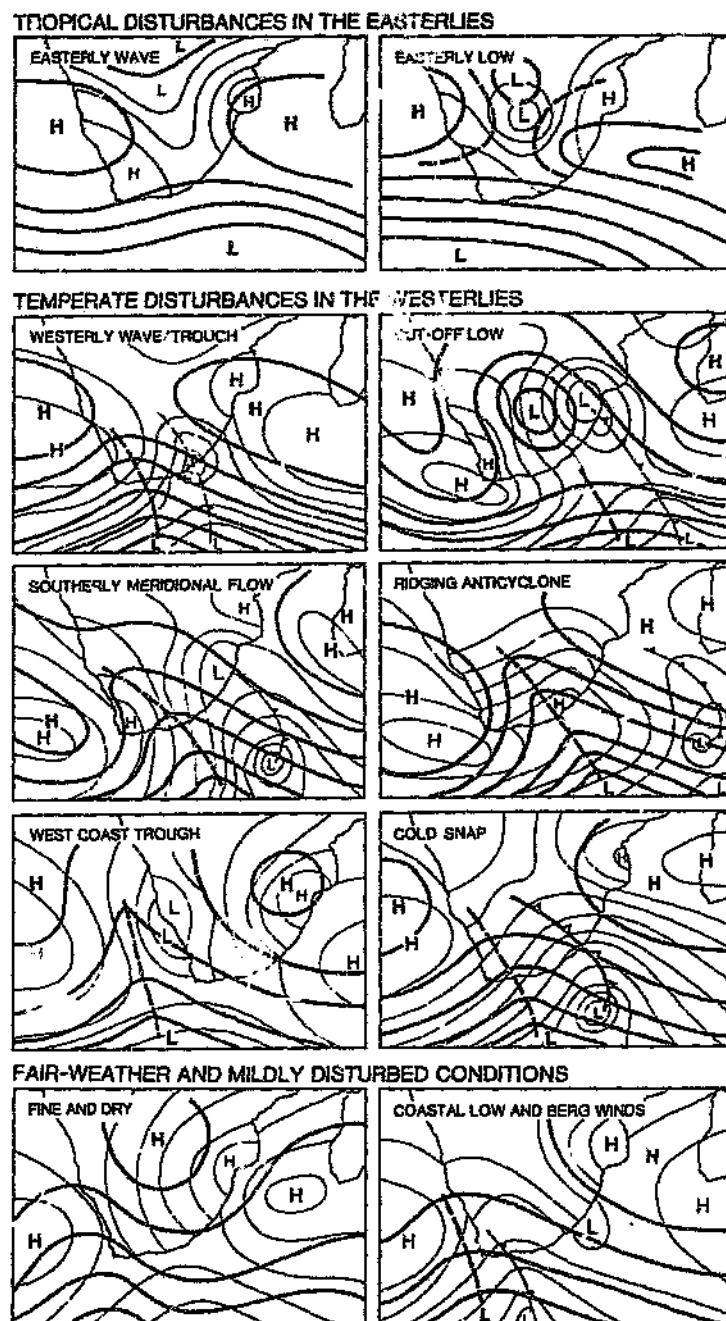


Figure 1.1 A generalised classification of circulation types over southern Africa (after Tyson, 1986).

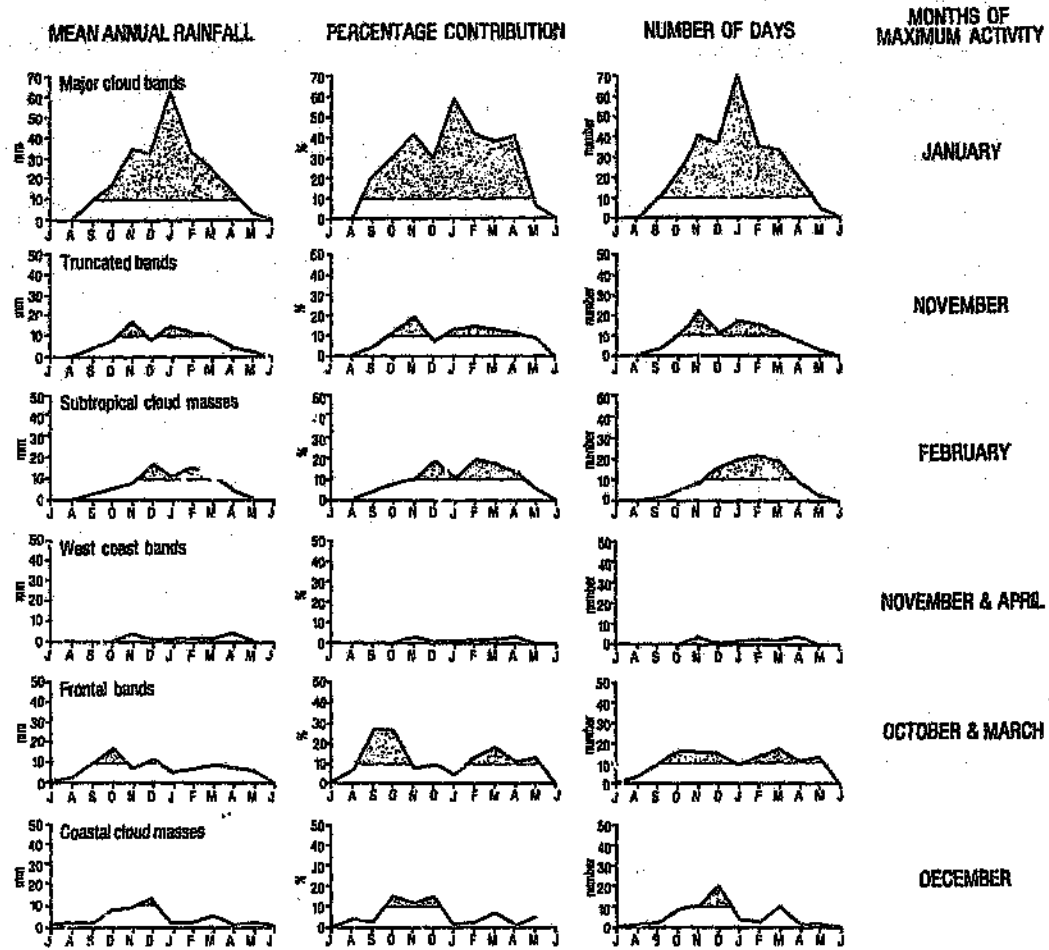


Figure 1.2 Annual cycles of significant rainfall from the classified synoptic circulation (after Tyson, 1986)

## Southern African Climate

### *Southern African circulation patterns*

The climate of southern Africa is, for the most part, maintained by its position within the southern hemisphere subtropical region and its situation between the cold South Atlantic Ocean and warmer Indian Ocean. The surface circulation effecting the climate of the subcontinent is generated by an interaction of the tropical, subtropical and mid-latitude pressure systems (Lindesay, 1988a,b). The subtropical pressure system is made up of a discontinuous high pressure belt formed from the two semi-permanent oceanic high pressure systems, in the Atlantic and Indian oceans respectively, and a continental high pressure. The South Atlantic, South Indian and Continental anticyclones are created and maintained by the descending limbs of the thermally direct Hadley and thermally indirect Ferrel cells as well as the Walker circulation. Although the oceanic anticyclones are described as semi-permanent their latitudinal and longitudinal positions vary both on a seasonal and daily time scale. During the austral winter both anticyclones migrate up to  $6^{\circ}$  in a northerly direction (Tyson, 1986). Thus the variation in longitudinal position of the above mentioned atmospheric circulation cells is responsible for the continued moisture input along the east coast and stability along the west coast. The southern and northern limits of the subtropical high pressure belt marks the boundary between the mid-latitude and tropical region respectively.

Within the mid-latitude low pressure belt, the eastward propagation of depressions and lows within the circumpolar westerly flow accounts for the winter rainfall in the southwestern regions of the country. The seasonal variation in the northern extent of the circumpolar westerly flow is dependent on the above mentioned northward shift of the oceanic anticyclones (van Loon, 1972; Trenberth, 1981; Lindesay, 1992). The quantity and severity of temperate zone disturbances are controlled primarily by the amplitude, phase angle and wave number of the westerly circumpolar circulation (van Loon, 1972; Trenberth, 1981).

The inter-hemispheric boundary between the subtropical and tropical regions is identified as the Intertropical Convergence Zone (ITCZ) (Taljaard, 1972; Tyson,

1986). Its position between the subtropical highs, and tropical easterly flow allows the zone to be maintained by three convergent airmasses (Taljaard, 1972; Tyson, 1986). These airmasses are: the recurved southwesterly South Atlantic air at 12°S, the northeasterly monsoon airflow, and the tropical easterlies (Torrance, 1972, 1979; D'Abreton, 1992). The position of the Intertropical Convergence Zone oscillates hemispherically over the African continent on a seasonal time scale (Tyson, 1986). During the months of January to July the ITCZ can be found in the Northern Hemisphere, while during August to December the zone of convergence is located within the Southern Hemisphere (Tyson, 1986). As its name suggests the ITCZ is a region of intense surface convergence and hence pronounced convective activity. Tropical surface sensible and latent heat fluxes along with the ascending limb of the Walker circulation, maintain the convective instability and thus promote precipitation in this region. The ITCZ and tropical zone are thus important moisture sources for the southern African continent. The interaction of the mid-latitude and tropically generated disturbances produce widespread summer rains over the majority of the subcontinent. During the austral winter the interaction of mid-latitude and tropical features is less likely to occur due to the northerly migration of the tropical zone of convergence. The coupling, by means of a sub-tropical trough, gives rise to what is termed a tropical-temperate trough or cloud band (Harangozo and Harrison, 1983; Tapp and Barrell, 1984; Harrison, 1984b; Harangozo, 1989).

#### *Tropical-temperate troughs*

The earliest identification of tropical and temperate interactions that cause significant rainfall events, were recognised by the Australian researchers Hunt, Taylor and Quayle in a publication entitled 'The Climate and Weather of Australia' in 1913. Their research described a 'trough-like depression, lying in a north-south direction', connecting with the tropical low pressure belt, and a concentration of precipitation activity along the trough front (Hunt *et al.*, 1913). Later quantitative studies by Quayle, Foley, and Hill recognised that 'meridional troughs', as they were termed, formed an effective linkage for the transport of tropical moisture to mid-latitude synoptic systems.

With the advent of satellite technology by the late 1960s the nature and extent of the 'meridional troughs' could be identified. By the early 1980s many conflicting definitions existed, so in order to standardise the process of identification, cloud masses had to fulfill a number of conditions in order to be defined as cloud bands. These conditions stipulate that a cloud band must:

- (1) have a zonal extent of  $25^{\circ}$  of longitude or more;
- (2) have a meridional extent of at least  $10^{\circ}$  of latitude;
- (3) have a tropical origin between the Equator and  $20^{\circ}\text{N}$  or  $20^{\circ}\text{S}$ ;
- (4) deliver a consistent texture when viewed as a satellite image,  
i.e. continuous cloud cover from origin to end point  
(Meehl, 1988; Wright, 1988; Kuhnelt, 1989).

Research from the beginning of this century until the early 1980's has identified the global extent of cloud band activity and has allowed climatologists and meteorologists to focus on the localised impacts of these structures. Tropical-temperate troughs and their associated cloud bands are the largest rainfall contributors over the summer rainfall region of South Africa and Zimbabwe (Harangozo and Harrison, 1983; Harrison, 1984b; Tyson, 1986; Diab *et al*, 1991; van den Heever, 1995). This fact motivated the extensive investigation of their structure and formation (Harangozo and Harrison, 1983; Harrison, 1984b; Harangozo, 1989; Lindsay and Jury, 1991; D'Abreton, 1992, van den Heever, 1995). It was found that these systems develop most frequently during the second half of the summer season during the period December to March, when the southern position of the Inter-tropical Convergence Zone allows for a more regular interaction with the westerly wave band.

The southern African synoptic circulation associated with tropical-temperate trough development, is borne from the linkage of three distinct synoptic features, namely a tropical low, a subtropical trough and a westerly wave (Fig 1.3) (Harangozo and

Harrison, 1983). The tropical-temperate trough facilitates the transport of moisture and energy poleward, and hence has a significant influence on summer rainfall over southern Africa (Harrison, 1984b).

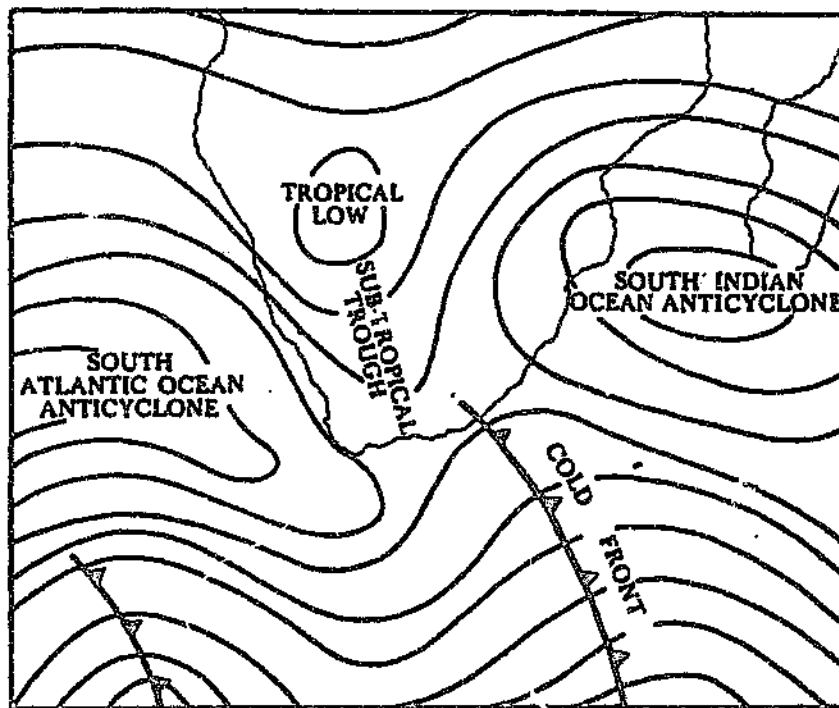


Figure 1.3 Schematic representation of the surface synoptic circulation's making up a tropical-temperate trough (after Harangozo and Harrison, 1983).

During seasons of anomalously high rainfall isohets are aligned in a north-west, to south-east direction, as opposed to the north-east, to south-west alignment exhibited during below normal rainfall periods (Barclay *et al.*, 1993). The propagation speed of the mid-latitude disturbance is slower, along with greater wavelength and amplitude growth during anomalously high rainfall periods (Barclay *et al.*, 1993). This means that tropical-temperate troughs that develop during wet periods are sustained for two to three days with more intense convection and hence greater precipitation (Barclay *et al.*, 1993). The larger scale atmospheric circulation controlling tropical-temperate trough development shows an eastward shift in the preferred location of surface convergence during dry conditions (Harangozo and Harrison, 1983; Harrison, 1986; Tyson, 1986; Jury, 1992, 1996). Hence convection decreases over the subcontinent but increases over the tropical Indian Ocean east of Madagascar (Jury and Pathack, 1991; Jury, 1992). This longitudinal shift in convection is the result of

the response of the Hadley circulation to changes in sea-surface temperatures in the equatorial Pacific, Indian and Atlantic oceans.

*Sea-surface temperature anomalies and ocean-atmosphere interactions*

The thermal and dynamic properties of oceans make them extremely important energy sources and sinks. The fact that water is a fluid complicates the energy exchange at the ocean/atmosphere interface (Fig 1.4).

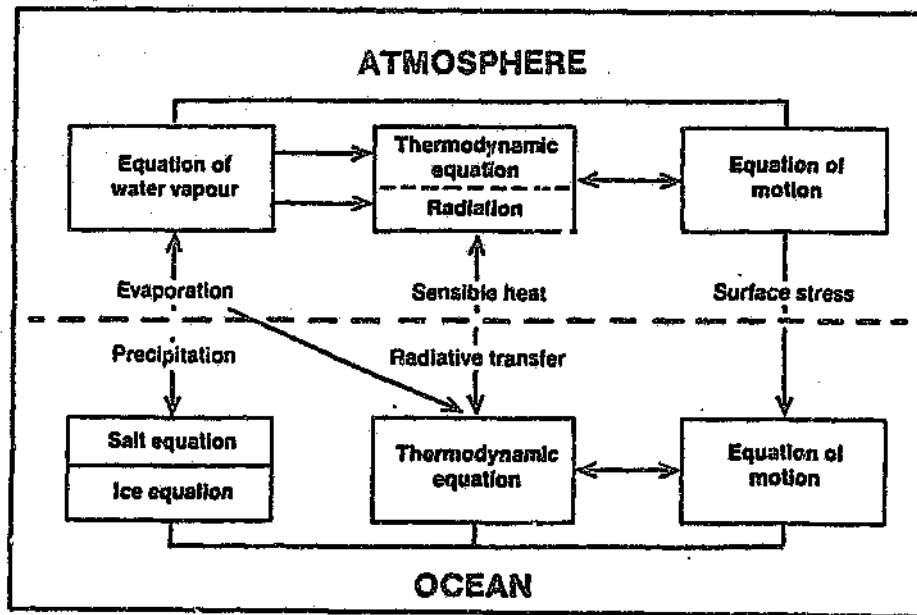


Figure 1.4 A schematic representation of the interaction of the atmosphere and ocean (after Gates, 1979).

The atmosphere interacts with the sea surface through a complex balance of heat fluxes, transfer of momentum, and turbulent mixing, which plays a significant role in the determination of climate on daily, seasonal and longer time scales. In recent years

increased attention has been given to the association between sea-surface temperature, local southern African atmospheric circulation and rainfall variability (Nicholls, 1984; Folland *et al.*, 1986; Walker, 1989, 1990). South African rainfall distribution is strongly correlated to sea-surface temperature fields and surface heat flux characteristics of the adjacent oceans. Maximum annual rainfall figures are found along the eastern and southeastern coasts of South Africa where sea-surface temperatures and hence latent and sensible heat fluxes are high (Tyson, 1986). On the west coast by comparison the low annual rainfall occurs in the oceanic region with the lowest sea-surface temperatures (Tyson, 1986). The tropical atmospheric response to sea-surface temperature anomalies are thought to be of a greater order of magnitude than mid-latitude regions, as a result of a significantly greater incidence of convection and the absence of the coriolis parameter (Shukla, 1986). Over areas of high sea-surface temperatures, atmospheric heat anomalies occur because of large latent energy supply and pre-existing convective motion (Webster, 1981). The low-level convergence that develops serves to maintain the supply of latent energy and thus promotes continued convection (Trenberth, 1991).

In the mid-latitudes the atmospheric response to warm oceanic anomalies differs from in the tropics (Bjerknes, 1969; Newell, 1979; Harrison 1984a, Love, 1985b). Usually the response is restricted to shallow sensible heating, with significant latent heating impacting only on pre-existing cyclogenesis and vertical instability (Lindesay, 1988a; Walker and Lindesay, 1988; Walker, 1990; Jury and Pathack, 1991; Mason, 1995).

#### *Sea-surface temperature anomalies and southern African rainfall variability*

Once the energy transfer mechanisms of the boundary layer are understood, it is important to fit this knowledge into the context of sea-surface temperatures and their effect on southern African rainfall variability. Researchers have discovered that summer rainfall is positively correlated with sea-surface temperatures in the Agulhas Current retroflexion region, the northern Benguela Current, and negatively correlated with the tropical Indian Ocean east of Madagascar (Fig 1.5) (Walker, 1989, 1990).

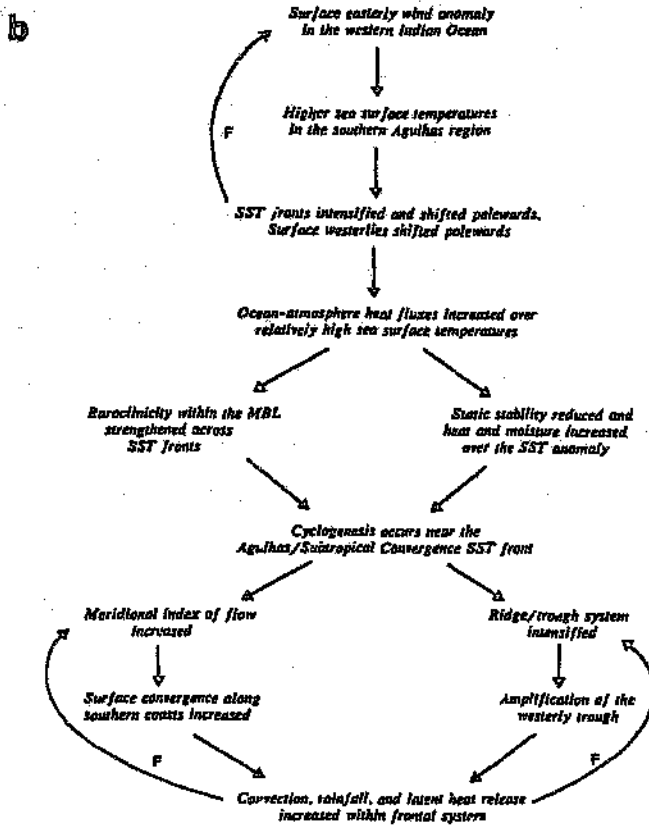
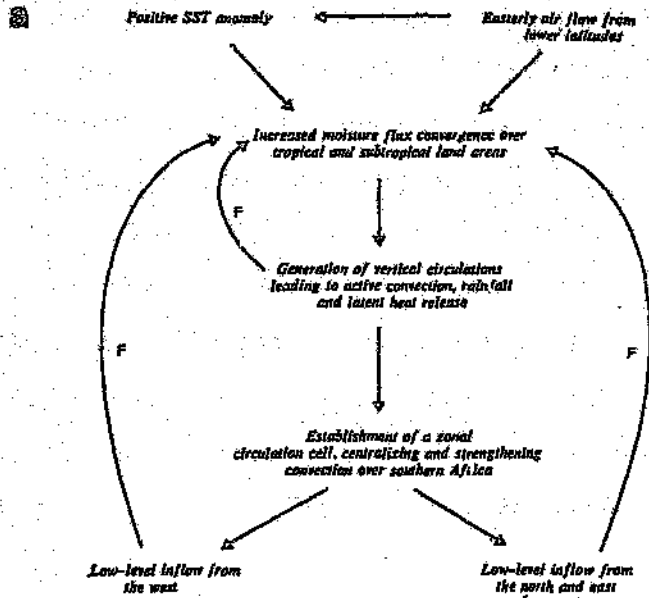


Figure 1.5 Possible ocean/atmosphere interactions along (a) the east coast and (b) the south coast of southern Africa for wet case scenarios (after Walker, 1989).

In the tropical Indian Ocean the development of positive sea-surface temperatures promotes the development of cyclogenesis north of Madagascar (Walker, 1989, 1990; Mason, 1992). The presence of enhanced cyclogenesis causes moisture redirection to the region of instability, thus reducing moisture availability over the subcontinent (Walker, 1989, 1990; Mason, 1992). On the east coast of South Africa warmer sea-surface temperatures have been found to precede and accompany higher rainfall conditions (Walker 1989). The warmer atmospheric boundary layer and heightened instability are translated inland by the tropical easterly flow producing higher moisture convergence over the immediate interior (Walker, 1989, 1990; Mason, 1992). Warm anomalies developing at the Agulhas retroflect are found to influence the atmospheric boundary layer by generating strong surface heat fluxes, and thus again enhancing instability and moisture levels (Walker, 1989, 1990). The presence of positive anomalies both to the east and south of South Africa increase the likelihood of tropical-temperate trough development by increasing moisture availability and by increasing the amplitude of the westerly wave (Walker, 1989, 1990).

Although the forcing effect of the warm sea-surface temperatures is well known on a climatological time scale the interactive mechanisms are less well understood at the meteorological scale. Earlier experiments with the Regional Atmospheric Modelling System, have provided accurate simulations of Southern African meteorology (van den Heever, 1995). However, investigations concerning the response of tropical-temperate troughs to perturbations in sea-surface temperature proved inconclusive (van den Heever, 1995). The importance of sea-surface temperature sensitivity experiments is thus to provide evidence concerning oceanic-atmospheric boundary layer interactions on a meteorological time scale.

### Hypotheses

The uncertainty surrounding the forcing effect of warm oceanic anomalies at a meteorological time scale has become an area of interest for modellers. By providing an overall assessment of the RAMS model's sensitivity to warm anomalies, the stage will be set for investigations into the local circulation changes brought about by observed anomalies. The hypotheses tested in this dissertation are:

- (a) The RAMS model is adequately sensitive to respond to warm oceanic anomalies.
  
- (b) The model Sensitivity simulation will closely parallel what is expected at the climatological time scale.

.....

As South Africa's growing population places increasing pressure on already limited water resources a more accurate understanding and prediction of both inter- and intra-annual precipitation have become essential. With the investigation into southern African rain-producing systems, tropical-temperate troughs have been identified as the single most important contributor to rainfall over the southern African interior during late summer. The variability of sea-surface temperatures around southern Africa have been correlated to changes in rainfall patterns on seasonal time-scales. Thus the development of sea temperature anomalies surrounding South Africa is thought to be an overriding factor in seasonal rainfall variability. The ability to simulate atmospheric simulation on shorter time scales using mesoscale numerical models has become possible. The use of the Regional Atmospheric Modelling System to investigate the atmospheric response to sea-surface temperature anomalies is presented in the following chapters.

## CHAPTER II

### Data and Methodology

The Regional Atmospheric Modelling System (RAMS) was used to visualise the formation and dissipation of a tropical-temperate trough for the period 21 to 24 January 1981. The model, a three dimensional, modular scheme, can simulate atmospheric circulation on a range of spatial scales from hundreds of metres to thousands of kilometres in extent. RAMS is comprised of three components: an isentropic analysis package (ISAN), an atmospheric modeling package (MODEL) and a visualisation and analysis package (VAN). MODEL performs the simulation based on a full set of primitive atmospheric dynamical equations (Walko and Tremback, 1991).

ISAN creates a three dimensional atmospheric grid to moderate the boundary conditions throughout the simulation (Davies, 1983; Pielke *et al.*, 1992). The three dimensional field is compiled using pressure, horizontal ( $u$ ,  $v$ ) and vertical ( $w$ ) wind components, and relative humidity. In order to create more accurate simulations, long term sea-surface temperatures are interpolated to the surface grid level (Parker, 1987; Parker and Folland, 1988). An isentropic co-ordinate system was favoured over and above other systems as it concentrates isentropes, thus providing easier recognition of discontinuities and synoptic scale air flow variability between stations (Pielke, 1992). The isentropic levels chosen were defined from the surface to 300 K at an interval of 2 K, then from 300 K to 400 K at an interval of 5 K, and finally from 400 K to 500 K at an interval of 10 K (van den Heever, 1995).

Once ISAN has created the global isentropic grid the user must define the domain limits in order for specific co-ordinate extraction to take place in the modelling subroutine. Atmospheric variables and topography are then transferred to the model

domain grid by using the overlapping polynomial interpolation (Pielke, 1992). For the experiments the study domain was set from the equator to  $50^{\circ}\text{S}$ , and from  $20^{\circ}\text{W}$  to  $70^{\circ}\text{E}$ . The grid contained 85 reference points in the north-south direction and 83 reference points in the east-west direction, which translated to a resolution of approximately 80 km.

The European Centre for Medium Range Weather Forecasts (ECMWF) IIb Global Analysis Data Set, the National Meteorological Centre (NMC) Global surface data set (both 2.5 degree resolution), and long term mean sea-surface temperature data from the United Kingdom Meteorological Office (1 degree resolution) (Parker, 1987; Parker and Folland, 1988) were used in order to initialise RAMS for a simulation of a tropical-temperate trough for the period 21 to 24 January 1981. The first of three sensitivity simulations was initialised from a modified data set that included a  $+2^{\circ}\text{C}$  sea-surface temperature anomaly and a  $+1^{\circ}\text{C}$  anomaly imposed on the boundaries of the perturbed sea-surface temperatures field to minimise any unwanted effects of strong sea-surface temperature gradients (Cione and Raman, 1995). The anomalies were added to an area north of Madagascar centred between the  $10^{\circ}\text{N}$  latitude and  $20^{\circ}\text{S}$  latitude and east of  $50^{\circ}\text{E}$ . The second sensitivity test utilised the same anomaly fields but placed between the  $33^{\circ}\text{S}$  and  $40^{\circ}\text{S}$  latitudes and  $14^{\circ}\text{E}$  and  $24^{\circ}\text{E}$  longitudes in the Agulhas retroflection region. In the third sensitivity test the anomalies were placed between  $4^{\circ}\text{N}$  and  $20^{\circ}\text{S}$ , and east of  $6^{\circ}\text{W}$  in the tropical western Atlantic Ocean region. All the model features and optional parameters were fixed for both the control and sensitivity simulations in order to identify circulation differences produced solely by the modified sea-surface temperature fields.

### Model Features and Parameter Options

In order to create accurate model simulations for each case study, dynamical equations and parameterisations are set according to the specific nature and objectives of the investigation (Manton *et al.*, 1977). Numerous parameters were tested for this set of simulations and for previous experiments. In the following sections model features and

parameter options will be compared and discussed, in order to substantiate the usage of particular model settings.

#### *Basic equations and time differencing scheme*

The RAMS model can be run hydrostatically (Triploi and Cotton, 1980) or non-hydrostatically (Tremback and Kessler, 1985; Tremback *et al.*, 1985; Pielke *et al.*, 1992; Snook *et al.*, 1995). Previous experiments utilising both the non-hydrostatic and hydrostatic modelling option determined that for coarse resolution simulations (greater than 120 kms), both modes gave virtually the same results (van den Heever, 1995). However, where high resolutions (less than 80 kms) were required for simulating deep convection or flow over significant topographic features the non-hydrostatic mode provided more accurate simulations. The need for simulating deep convection during the sensitivity tests is paramount, thus encouraging the use of the non-hydrostatic option.

The operational processes such as advection, convection and precipitation rates are controlled and updated by a time-differencing scheme. When the RAMS model is run non-hydrostatically the leapfrog time-differencing scheme is the default setting. The update iteration was set at 90 seconds for the case studies in order to maintain computational stability.

#### *Grid structure and boundary conditions*

Horizontal, and vertical co-ordinates are imposed onto a single staggered Arakawa C grid (Messinger and Arakawa, 1976; Fox-Rabinovitz, 1991). The horizontal co-ordinates are taken from the polar stereographic co-ordinate system compensating for the curvature of the earth surface. The vertical co-ordinate scheme uses the  $\sigma_z$  terrain following system (Gal-Chen and Somerville, 1975b; Clark, 1977; Mahrer and Pielke, 1977; Zanjic and Zanjic, 1993). For the sensitivity tests 30 vertical atmospheric layers were defined. At the surface the initial vertical depth was set at 300 m. Each successive level is stretched by a ratio of 1.1 until a maximum depth of 750 m is

reached, after which the vertical depth is fixed at 750 m (Gal-Chen and Somerville, 1975; Clark, 1977).

Lateral boundary conditions are maintained using the Klemp and Wilhelmson (1978a,b) radiative boundary condition which allows synoptic features to propagate out of the domain at a velocity determined by the user (Perkey and Kreitzberg, 1976; Clark, 1977; Klemp and Wilhelmson, 1978a). The continual update of the position of different features is monitored and controlled by a fourth or second order advection scheme. For this study the second order advection scheme was chosen as less processing time was utilised and the differences between the two orders are small (Klemp and Wilhelmson, 1978b; Cram, 1990).

The synoptic-scale boundary forcing was performed by the Davies nudging condition (Davies, 1983). The Davies condition causes computed values created at and near the boundary, during the simulation, to be forced to the observed values contained within isentropic grid files. The extent of the forcing and strength of nudging inwards by the lateral boundary is set by the user. Previous tests determined that optimal forcing conditions exist when a region of five grid points wide with weighting values of 0,15; 0,09; 0,05; 0,02; and 0,01 were used (van den Heever, 1995). These nudging values are set to a minimum for the control and sensitivity experiments in order to limit the control observed values have on the model simulations. The non-hydrostatic configuration of the model maintains the upper boundary as a rigid lid and the vertical velocity of propagated gravity waves towards this boundary is reduced to zero (Cram 1990).

The lower boundary is maintained by a 10 level Tremback and Kessler soil model that extends to a soil depth of 50 cm (McCumber and Pielke, 1981; Tremback and Kessler, 1985). At a depth of 10 cm the soil temperatures are set at 4 K lower than the surface temperature, 8 K lower at a depth of 30 cm below surface, and 10 K lower than the surface at a depth of 50 cm (van den Heever, 1995).

### *Cumulus parameterisation*

The modified Kuo cumulus parameterisation scheme controls the model cloud physics (Cram, 1990; Flatau *et al.*, 1993). The scheme allows for vertical and horizontal redistribution of moisture and heat on a coarse grid structure. In most cases, mesoscale models require a number of grid cells of horizontal size of less than 1 to 2 km, in order to resolve convective potential (Cram, 1990). Coarse resolution models would thus find it impossible to realise vertical motion for areas of localised instability. The RAMS model contains a convective parameterisation scheme that makes convective adjustments on coarse grid resolutions. Cloud features, such as lifting condensation levels are calculated from vertical motion and moisture convergence within the vertical cross-section. The minimum updraft required at the cloud base to facilitate convection, is specified as  $0,5 \text{ cms}^{-1}$ . The update frequency for this parameterisation was set to 1800 seconds (van den Heever, 1995).

### **Observed Synoptic-Scale Conditions**

The period 21 to 24 January 1981 forms an interesting case study for investigation as it marks the formation of a tropical-temperate trough during a particularly high wet phase of the Southern Oscillation. Cloud cover persists for the entire four day period, with highest precipitation values recorded on the day the tropical-temperate trough becomes fully coupled.

On 21 January 1981 (Day 1), moist tropical air was in circulation around a low pressure centred over the Botswana/Namibian border, with thundershowers experienced over the northern and central parts of the country (Fourie, 1981). A westerly wave was situated to the south of the subcontinent, with little effect on the presiding weather conditions (Fig. 2.1a). By 22 January 1981 (Day 2), the westerly wave had moved to the south of Madagascar, and had been replaced by a second westerly wave perturbation (Fourie, 1981). The subtropical trough had intensified and

moved southward. No interaction between the westerly wave and subtropical trough had taken place at this time (Fig. 2.1b).

The tropical-temperate trough had developed by 23 January (Day 3), through the linking of the tropical low, a subtropical trough and a westerly wave perturbation (Fig. 2.1c) (Fourie, 1981). Recorded rainfall values indicated widespread precipitation over the majority of the subcontinent. The tropical-temperate trough began to dissipate on the morning of 24 January (Day 4), although cloud cover still persisted over the southern regions of South Africa and immediate interior (Fourie, 1981). Precipitation was reduced and more isolated as the temperate link between subtropical trough and westerly wave had broken (Fig. 2.1d).

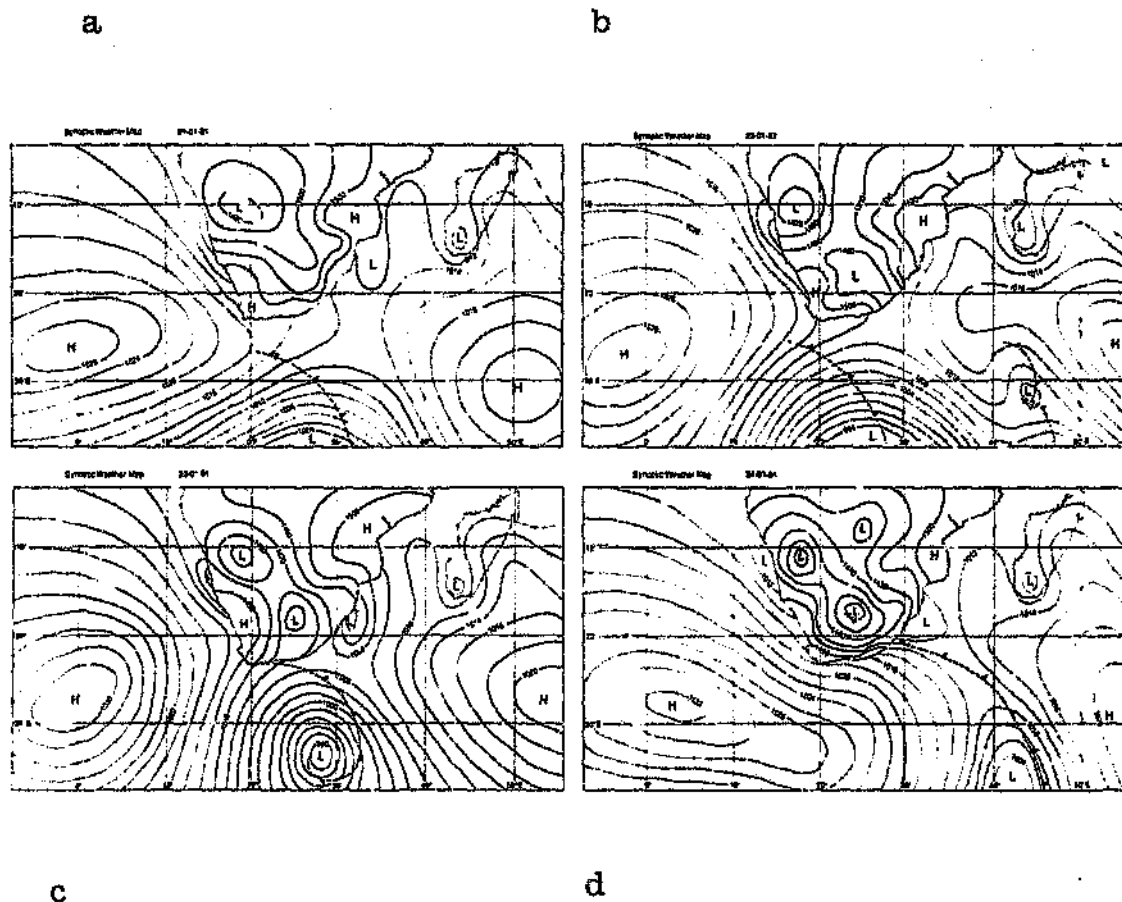


Figure 2.1(a,b,c,d) A schematic representation of synoptic conditions for the period 21 to 24 January 1981.

During the simulation period 21-24 January 1981 the circumpolar westerly circulation was dominated by a wave six structure (Fourie, 1981). This served to increase the overall amplitude of the westerlies and thus aid the formation of the tropical-temperate trough, by enhancing baroclinicity and thus under-cutting of warm moist tropical air.

### Control Simulation

Previous experiments (van den Heever, 1995), have proved that the RAMS numerical model can accurately simulate the atmospheric circulation of this particular case study, but it is important to consider the sequence of events portrayed by the control simulation. Simulated synoptic features are viewed at the 146 m and 807 m sigma levels for the control simulation and for the sensitivity experiments. These two levels were singled out as the magnitude of the sea-surface temperature anomalies are small and the time frame of the simulations are limited. These factors limit the atmospheric response of the numerical model and thus few circulation differences are found above the 807,2m sigma level. These two levels, therefore, represent the surface and the vertical extent of the atmospheric response.

At 1200 UTC on 21 January 1981, the control streamline output indicates the southerly position of the South Atlantic High pressure system and the South Indian High pressure system at 32°S and 42°S respectively, this equates well with synoptic data for that day. A westerly wave perturbation was also simulated, having an approximate longitudinal position of 35°E. In the tropical regions low pressures are positioned over the Indian Ocean north of Madagascar and on the continent over the Namibia/Angola border. Later in the day the control simulation shows that the tropical low over the subcontinent intensified and was now positioned further south. A trough of low pressure was beginning to form within the borders of South Africa.

On the second day of the simulation the sub-tropical trough over South Africa appeared fully developed and began to move eastwards as the day progressed. Directly to the north of the continental tropical low a strong zone of convergence formed. Enhanced vertical instability was present in this area, along with high moisture

availability and cloud development. This was caused by the cool dry recurved southeasterly air mass that encroached and undercut the warm moist tropical northeasterly air mass from the eastern regions of tropical Africa.

For the evening of 22 January the RAMS model simulated the further intensification of the sub-tropical trough, and the strengthening of the tropical low, (now within the borders of Namibia). The convergence to the north of this low shifted eastwards towards the centre of the Angolan interior. The approach of a second westerly wave perturbation was simulated, with the first wave disturbance continuing its eastward trajectory.

By the third day of the model simulation, the sub-tropical trough, the tropical low, and the second westerly wave perturbation appeared to have coupled forming a tropical-temperate trough. Intense convergence was found around the trough, with weaker southwesterly flow from the tropical low. At this point a strong equatorial low pressure system began to develop near the Angola/Zaire border. When comparing the simulated streamlines with the hypothesised regions of maximum moisture contributions for wet years (D'Abreton and Lindsay, 1993; D'Abreton, 1992; Harrison, 1986), a good correlation can be found (Fig 2.2). The recurved south westerly wind off the South Atlantic High (A), the westerly winds from the westerly wind disturbance (B), the north easterly winds from tropical Africa (C), the easterly winds from the tropical Indian Ocean (D), and the poleward air flow along the cloud band (E) are all present and simulated in this model iteration. The importance of these areas of moisture input become apparent when viewing the results of the individual sensitivity experiments.

Later on 23 January, the simulated equatorial low further intensified and began to reduce air flow to the low located along the Angolan/Namibian west coast. By evening the model simulated the dissipation of this low, with moisture then transported to the sub-tropical trough and westerly wave perturbation from the predominant zone of convergence extending from the developing equatorial low.

On the final day of the simulation the tropical-temperate trough dissipated through the decoupling of the tropical low, subtropical trough and the westerly wave disturbance. The perturbation continued its easterly circumpolar circulation maintaining only a tentative connection with the southern African continent. Strong convergence prevailed along the east coast of South Africa, however the sub-tropical trough had dissipated. The last period of simulation output indicated the predominance of the equatorial low over the central African continent at 10°S.

Control Simulation  
 January 23 1981

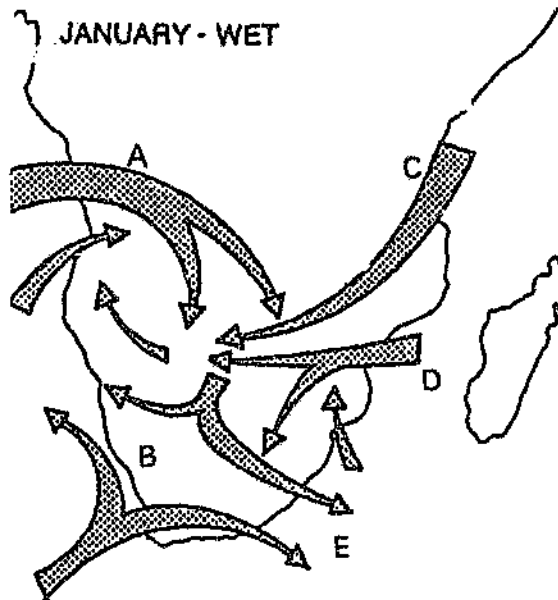
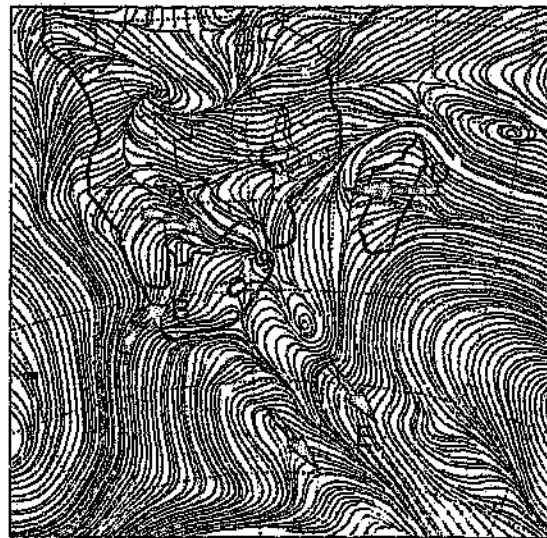


Figure 2.2 A comparison of the streamline simulation on 23 January 1981 at 2100 UTC with a schematic representation of the main vertically integrated vapour fluxes for a wet January scenario (flux schematic taken from D'Abreton, 1993).

.....

The RAMS numerical model is a three dimensional modular scheme, that can simulate atmospheric circulation on a number of spatial scales from hundreds of metres to thousand of kilometres. RAMS is comprised of three components: an isentropic package (ISAN), an atmospheric modelling package (MODEL) and a visualisation package (VAN). The model was initialised from ECMWF atmospheric data, NMC global surface data, and UKMO mean sea-surface temperature data. Three separate sensitivity experiments were devised, in which positive anomalous sea-surface temperatures were added to the ocean north of Madagascar, at the region of the Agulhas Current retroflexion, and along the tropical African west coast. A further control experiment was run that simulated the atmospheric circulation for the study period 21 to 24 January 1981 very well. The results of the sensitivity simulations are found in the following chapters.

## Chapter III

### The Tropical Indian Ocean Sea-surface Temperature Anomaly (Sensitivity Test 1)

Sea-surface temperatures have a direct effect on the atmospheric boundary layer, through a complex balance of energy fluxes and momentum transfer. Over intra-annual and inter-annual time scales the variability of sea-surface temperatures surrounding the subcontinent has demonstrated a causative link with variations in rainfall (Walker, 1989; Mason, 1992). The tropical Indian Ocean in particular exhibits strong control over late summer precipitation, as it forms an important water vapour source to the subcontinent by means of easterly transport (D'Abreton, 1992). Anomalously warm sea-surface temperatures result in reduced divergence of water vapour from the Indian Ocean to the African subcontinent as moisture is redirected to regions of heightened instability by the development of cyclonic vorticity. This causes a reduction in precipitation over the country due to lower moisture availability. Although these investigations have helped to develop some understanding of the importance of the tropical Indian Ocean as both a late summer moisture source and as a control on the longitudinal position of the African convective centre (Jury and Pathack, 1991; Lindsay and Jury, 1991; Mason, 1992; Jury, 1993), limited research efforts have investigated the influence this oceanic region has on a shorter time scale. Most research has been confined to statistical analyses, through correlation and cross-spectral techniques, and to investigations of inter-annual fluctuations of the ocean-atmosphere system, through the investigation of the Southern Oscillation and its global teleconnections (Bjerknes, 1969; Harrison, 1984b; Cane, 1986; Nicholson and Entekhabi, 1987; Lindsay, 1988a, 1988b; Harangozo, 1989; Walker, 1989; Jury and Pathack, 1991; Lindsay and Jury, 1991; Mason, 1991, 1995; Jury, 1993). With this in mind an attempt is made in this dissertation to investigate the effect the tropical Indian Ocean has on precipitation over a much smaller time frame (4 days) by testing the

sensitivity of the Regional Atmospheric Modelling System to imposed sea temperature anomalies.

In the tropical Indian Ocean, north east of Madagascar, the observed mean sea-surface temperature data set from the United Kingdom Meteorological Office (Parker, 1987; Parker and Folland, 1988), was modified to include a positive  $2^{\circ}\text{C}$  increase in existing sea-surface temperatures. Ocean temperatures on the boundary of the perturbed sea-surface temperature field were increased by  $1^{\circ}\text{C}$  in order to minimise any unwarranted effects of a strong temperature gradient (Fig 3.1).

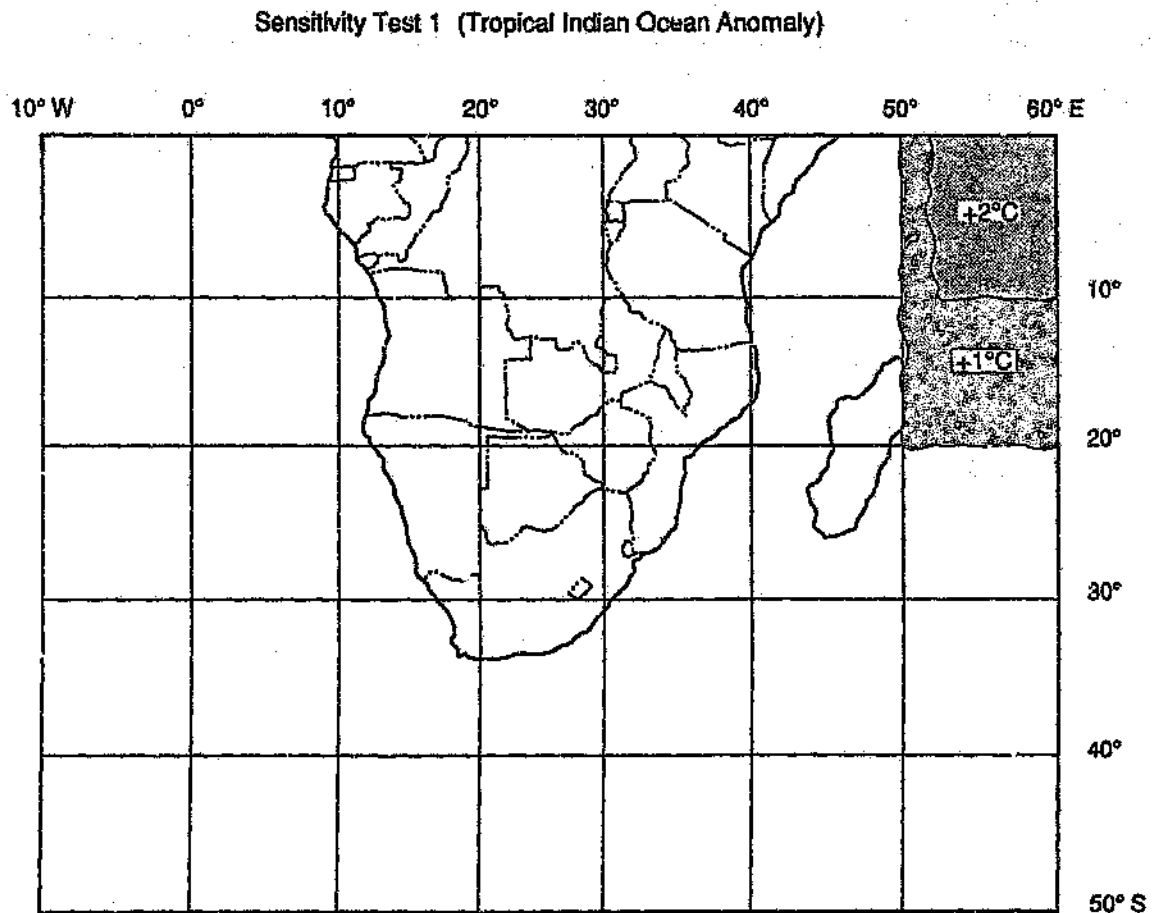


Figure 3.1 Representation of the first anomaly location, whereby a positive  $2^{\circ}\text{C}$  anomaly was placed north of  $10^{\circ}\text{N}$  and a positive  $1^{\circ}\text{C}$  anomaly placed on the boundary of the  $2^{\circ}\text{C}$  perturbed field.

## Results

The sensitivity of the RAMS simulation of the tropical-temperate trough, to a tropical Indian Ocean positive sea-surface temperature anomaly event is ascertained by the comparison of control and sensitivity wind components ( $u, v$ ), streamlines, temperature, vertical velocity ( $w$ ), vapour and cloud mixing ratios, and accumulated convective precipitation, at the surface (146,4 m) and the (807,2 m) near surface levels. These levels were chosen for comparison as it would be unrealistic to expect any significant changes in the upper-level dynamics over a 4-day period. The control and sensitivity simulations were initialised using the same parameterisation and data except for the sea-surface temperature anomaly imposed in the sensitivity sea-surface temperature data set. Differences in simulation are thus the product of different sea-surface temperatures only.

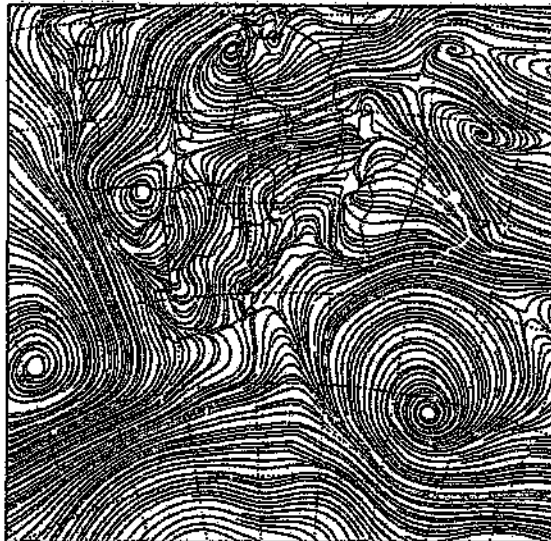
### *Day one*

At the start time of the simulation (1200 UTC, 21 January 1981), all the atmospheric components simulated in the sensitivity test were compared to the control at the 146,4 m sigma level, but no differences were identified (Fig 3.2 a,b). This is however not surprising as the initialisation of both the control and sensitivity simulations takes place from the same ECMWF atmospheric data sets. This data set provides the model with the 3-D atmospheric fields needed at the initial time-step. After the first time-step has been completed the ECMWF data sets are used only to maintain the lateral boundary conditions through the application of a nudging technique, and thus allowing simulation differences to develop. Both simulations model the moist air in circulation over Namibia, and around the tropical low, as well as the approximate positions of the quasi-stationary high pressures and westerly wave perturbations (Fig 3.3 a,b).

After nine hours of simulated time have elapsed (2100 UTC) the sensitivity output at the 146,4 m level begins to diverge from the control. The imposition of the sea-surface temperature anomaly produced an initial strengthening of easterly flow to the east of Madagascar from between 4 to 5  $\text{ms}^{-1}$  in the control simulation to between 5 to

Control Run

January 21 1981

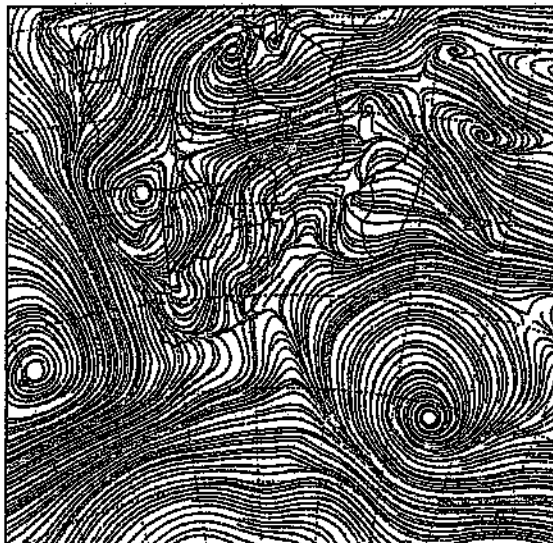


$z = 146.4 \text{ m}$

$t = 1200 \text{ UTC}$

Sensitivity Test 1

January 21 1981



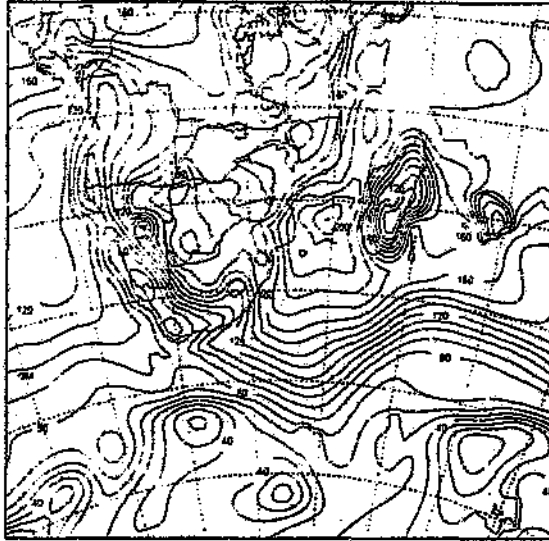
$z = 146.4 \text{ m}$

$t = 1200 \text{ UTC}$

Figure 3.2 Streamline diagrams for (a) the control and (b) the sensitivity simulations at the 146,4 m sigma level for 1200 UTC on 21 January 1981.

Control Run

January 21 1981



VAPOR AND CLOUDS

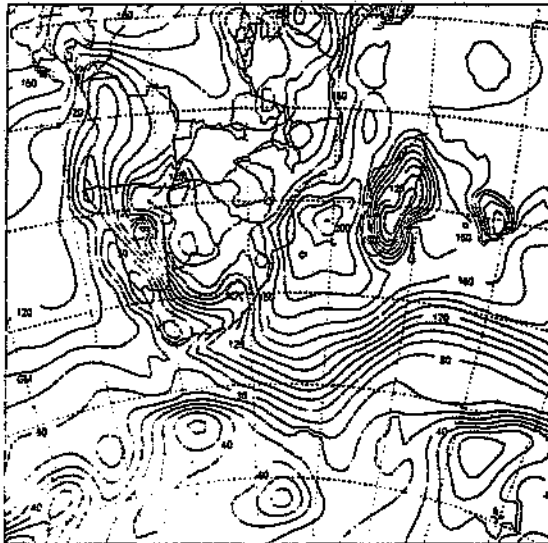
File: 010000-01  
File: 010000-01  
File: 010000-02  
File: 010000-03

z = 146.4 m

t = 1200 UTC

Sensitivity Test 1

January 21 1981



VAPOR AND CLOUDS

File: 010000-01  
File: 010000-01  
File: 010000-02  
File: 010000-03

z = 146.4 m

t = 1200 UTC

Figure 3.3 Vapour and cloud mixing ratios ( $\text{g}\cdot\text{kg}^{-1}\times 10^{-6}$ ) for (a) the control and (b) the sensitivity simulations at the 146.4 m sigma level for 1200 UTC on 21 January 1981.

6  $\text{ms}^{-1}$  in the sensitivity test (Fig 3.4 a,b). Concomitant to the marginal strengthening of the easterly flow is an increase in simulated instability from a control value of 0,018  $\text{cms}^{-1}$  to a sensitivity value of 0,021  $\text{cms}^{-1}$  in the same area, and an increase in vapour and cloud mixing ratios south of  $10^{\circ}\text{S}$ . Isolated areas to the east of Madagascar recorded higher convective precipitation values of 3,6 mm in the sensitivity test compared to 2,8 mm in the control simulation (Fig 3.5 a,b).

At the same time, at the 807,2 m level, easterly flow over the central regions of Madagascar and the Mozambique Channel strengthened (Fig 3.6 a,b). Vertical velocity, vapour and cloud mixing ratios, and accumulated convective precipitation simulated increases of the same magnitude as near the surface (Fig 3.7 a,b).

#### *Day two*

On 22 January (0600 UTC) at the 146,4 m level the easterly wind component anomaly to the east of Madagascar continued to strengthen. North of  $10^{\circ}\text{S}$  the easterly component reduced, making way for the intrusion of northwesterly flow into the region north of Madagascar (Fig 3.8 a,b). At 0600 UTC cyclogenesis appears for the first time to the west of the modified sea-surface temperatures. Vertical velocity strengthened along the east coast of Madagascar with a maximum value of 0,028  $\text{cms}^{-1}$  as opposed to the control value of 0,021  $\text{cms}^{-1}$ . The maximum subcontinent precipitation values recorded decreased from 13,6 mm in the control simulation to 12,8 mm in the sensitivity experiment. Accumulated convective precipitation increased to the east and northeast of Madagascar from between 1,6 mm and 2,4 mm in the control simulation to between 2,4 mm and 3,2 mm in the sensitivity test (Fig 3.9 a,b).

At 2100 UTC on 22 January a comparison of the control and sensitivity simulations at 146,4 m revealed that the recurved northwesterly flow further increased its westward extent along  $10^{\circ}\text{S}$  (Fig 3.10 a,b). An intensification of the developing cyclogenesis is found to the west of the modified sea-surface temperatures, with a low pressure cell developing at the mouth of the Mozambique Channel. Surface divergence appeared for the first time along the  $40^{\circ}\text{E}$  line of longitude deflecting moist tropical air away from the subcontinent and towards the developing low pressure. Vapour and cloud

Control Run

January 21 1981



U

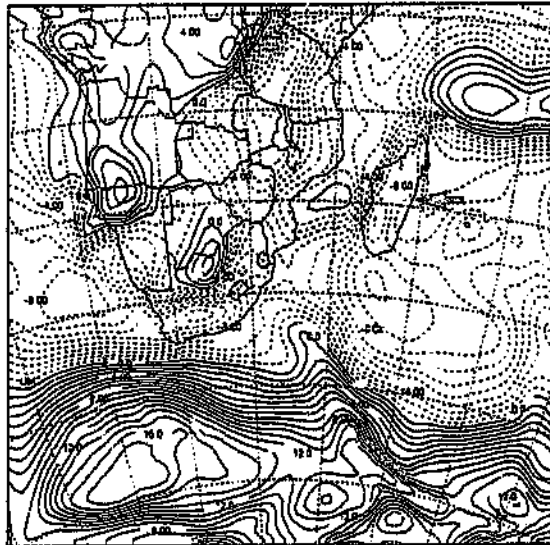
z = 146.4 m

t = 2100 UTC

1000-10200-02  
1000-10200-02  
1000-10200-02  
1000-10200-02

Sensitivity Test 1

January 21 1981



U

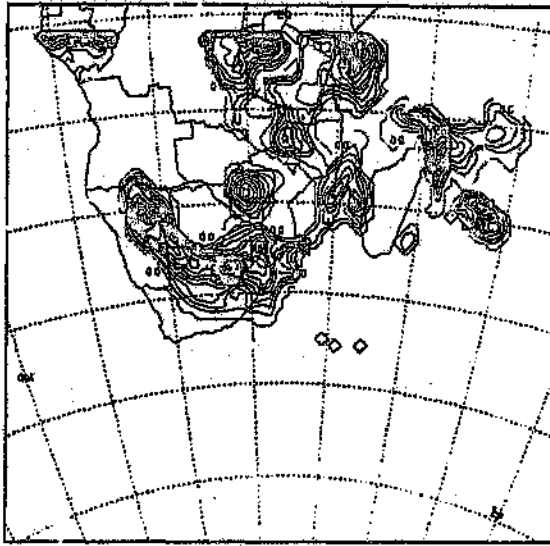
z = 146.4 m

t = 2100 UTC

1000-10200-02  
1000-10200-02  
1000-10200-02  
1000-10200-02

Figure 3.4 U components (in  $m.s^{-1}$ ) for (a) the control and (b) the sensitivity simulations at the 146,4 m sigma level for 2100 UTC on 21 January 1981.

Control Run  
January 21 1981



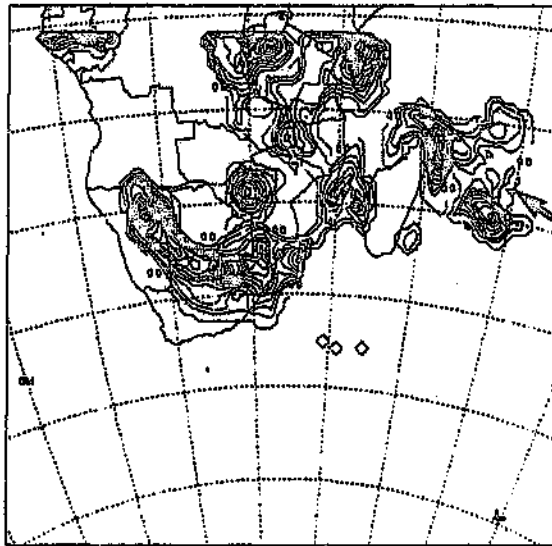
accum conv pop

z = 146.4 m

t = 2100 UTC

File: 000000-01  
to: 0.75000-01  
by: 0.00000-01  
map: 1.0.0000-01

Sensitivity Test 1  
January 21 1981



accum conv pop

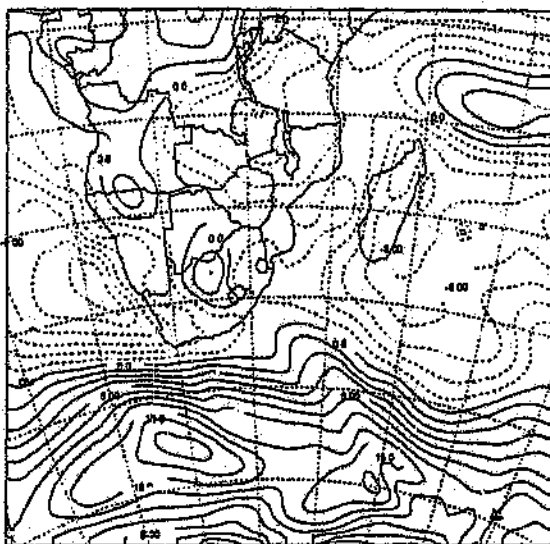
z = 146.4 m

t = 2100 UTC

File: 000000-01  
to: 0.75000-01  
by: 0.00000-01  
map: 1.0.0000-01

Figure 3.5 Accumulated convective precipitation (in mm) for (a) the control and (b) the sensitivity simulations at the 146.4 m sigma level for 2100 UTC on 21 January 1981.

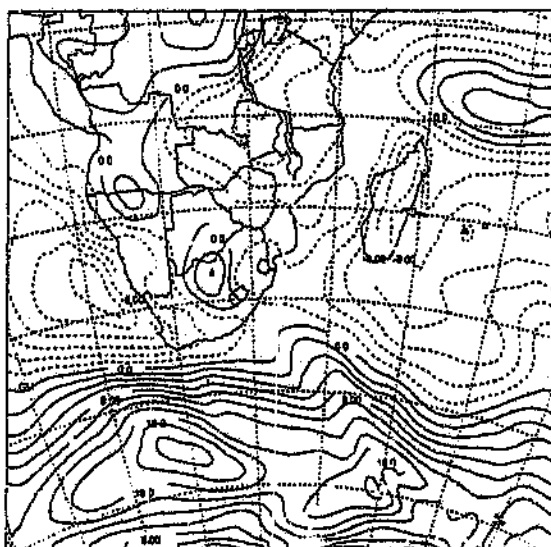
Control Run  
January 21 1981



Run: 1205-01  
M: 0 2000-01  
P: 0 2000-01  
Time: 18 00:00:00

U  
z = 807.2 m      t = 2100 UTC

Sensitivity Test 1  
January 21 1981



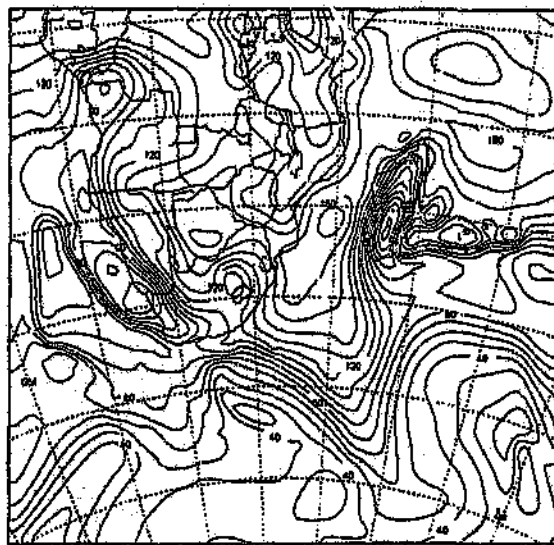
Run: 1205-01  
M: 0 2000-01  
P: 0 2000-01  
Time: 18 00:00:00

U  
z = 807.2 m      t = 2100 UTC

Figure 3.6 U components (in  $\text{m}\cdot\text{s}^{-1}$ ) for (a) the control and (b) the sensitivity simulations at the 807,2 m sigma level for 2100 UTC on 21 January 1981.

Control Run

January 21 1981



VAPOUR AND CLOUDS

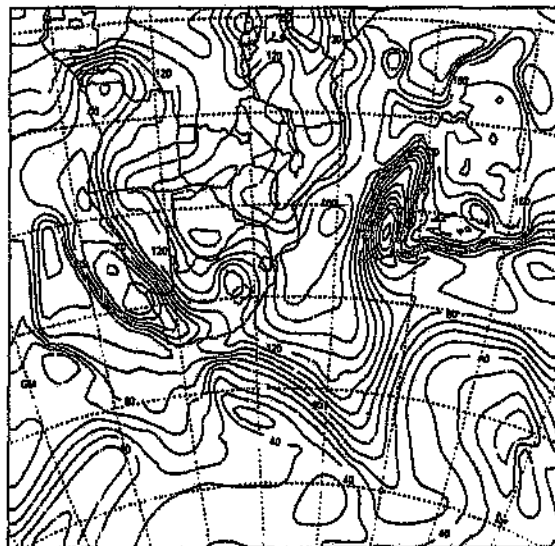
z = 807.2 m

t = 2100 UTC

Scale 0 10000-00  
0 10000-00  
0 10000-00  
Scale 0 10000-00

Sensitivity Test 1

January 21 1981



VAPOUR AND CLOUDS

z = 807.2 m

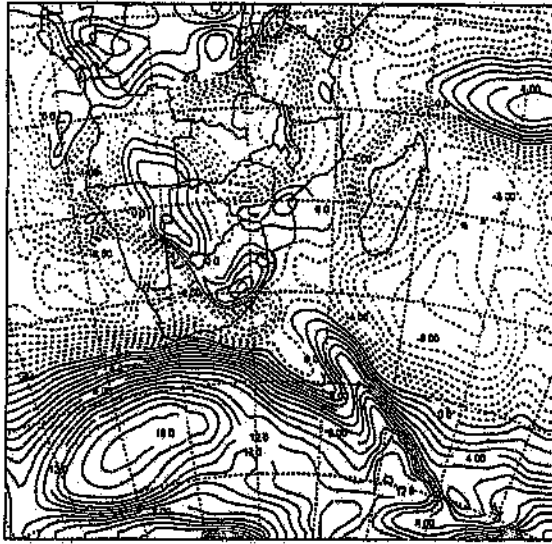
t = 2100 UTC

Scale 0 10000-00  
0 10000-00  
0 10000-00  
Scale 0 10000-00

Figure 3.7 Vapour and cloud mixing ratios (in  $\text{g kg}^{-1} \times 10^{-4}$ ) for (a) the control and (b) the sensitivity simulations at the 807.2 m sigma level for 2100 UTC on 21 January 1981.

Control Run

January 22 1981



U

z = 146.4 m

t = 0600 UTC

NOAA-NCEP  
1981-01-22 06:00 UTC  
U (m/s) at 146.4 m

Sensitivity Test 1

January 22 1981



U

z = 146.4 m

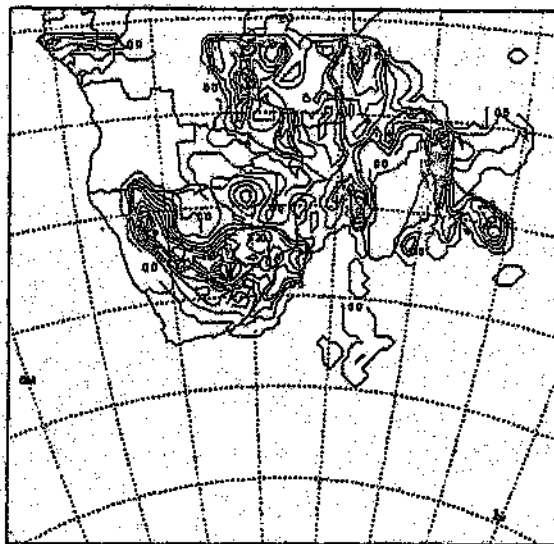
t = 0600 UTC

NOAA-NCEP  
1981-01-22 06:00 UTC  
U (m/s) at 146.4 m

Figure 3.8 U components (in  $m \cdot s^{-1}$ ) for (a) the control and (b) the sensitivity simulations at the 146.4 m sigma level for 0600 UTC on 22 January 1981.

Control Run

January 22 1981



accum conv pcp

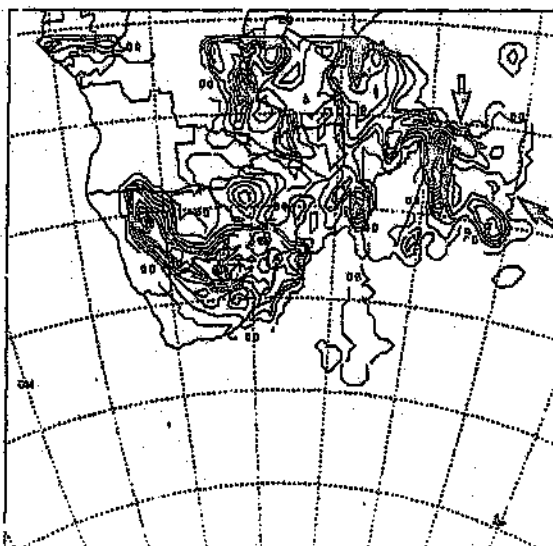
##= 0.0000-00  
##= 1.0000-00  
##= 2.0000-00  
##= 3.0000-00  
##= 4.0000-00  
##= 5.0000-00  
##= 6.0000-00  
##= 7.0000-00  
##= 8.0000-00  
##= 9.0000-00  
##= 10.0000-00

z = 146.4 m

t = 600 UTC

Sensitivity Test 1

January 22 1981



accum conv pcp

##= 0.0000-00  
##= 1.0000-00  
##= 2.0000-00  
##= 3.0000-00  
##= 4.0000-00  
##= 5.0000-00  
##= 6.0000-00  
##= 7.0000-00  
##= 8.0000-00  
##= 9.0000-00  
##= 10.0000-00

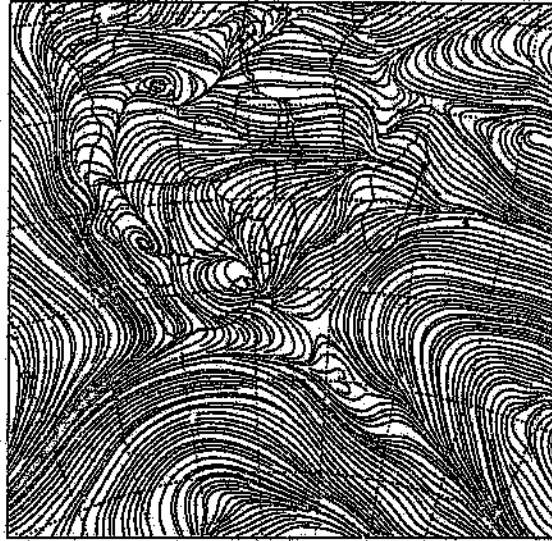
z = 146.4 m

t = 600 UTC

Figure 3.9 Accumulated convective precipitation (in mm) for (a) the control and (b) the sensitivity simulations at the 146.4 m sigma level for 0600 UTC on 22 January 1981.

Control Run

January 22 1981

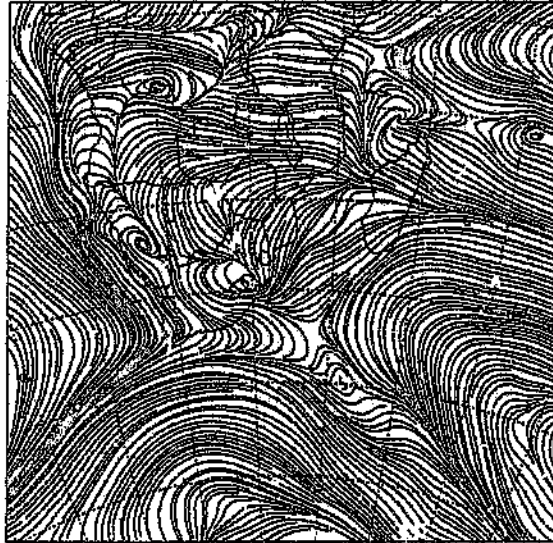


$z = 146.4 \text{ m}$

$t = 2100 \text{ UTC}$

Sensitivity Test 1

January 22 1981



$z = 146.4 \text{ m}$

$t = 2100 \text{ UTC}$

Figure 3.10 Streamline diagrams for (a) the control and (b) the sensitivity simulations at the 146.4 m sigma level for 2100 UTC on 22 January 1981.

mixing ratios indicate a greater moisture availability north of Madagascar i.e. a greater southerly extent of the  $0,017 \text{ g.kg}^{-1}$  contour line (Fig 3.11 a,b). Lower continental precipitation values were recorded due to the reduction of moist tropical flow from the east with control values over Durban approximately 9 mm as opposed to 11 mm in the experiment. Increased convergence and orographic impetus along the east coast of Madagascar produced higher convective precipitation in the area, as well as along the north coast with values of 5 mm in the control compared to 8 mm in the sensitivity test (Fig 3.12 a,b).

Trends at the 807 m level, for the same period, indicate a continued westerly expansion of the recurved northwesterly flow. The upper-level easterly flow at approximately  $5^{\circ}\text{S}$  strengthened and produced a concomitant intensification of the low pressure system found at  $10^{\circ}\text{S}$  (Fig 3.13 a,b). Vertical instability is higher along the north and northeast coasts of Madagascar due to the proximity of the low pressure system with highest recorded values of  $0,028 \text{ cms}^{-1}$  for the control simulation and  $0,042 \text{ cms}^{-1}$  for the sensitivity experiment, along with heightened easterly winds (Fig 3.14 a,b).

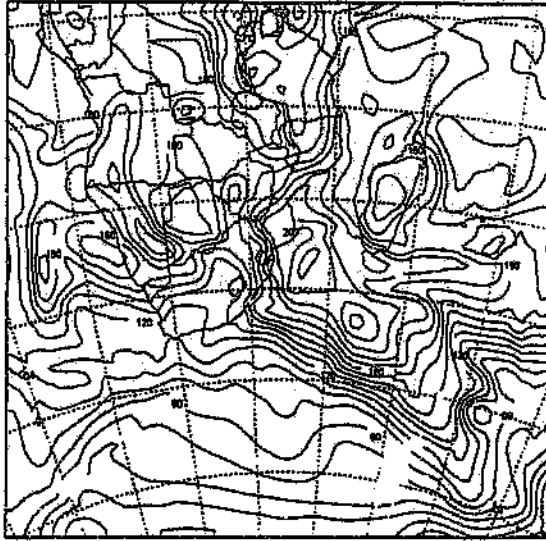
Vertical velocities for the sensitivity simulation are lower along the east coast of South Africa with values of  $0,077 \text{ cms}^{-1}$  compared to  $0,084 \text{ cms}^{-1}$ , possibly due to stronger northwesterly winds in the area. Vapour and cloud mixing ratio values remained higher over the modified sea-surface temperature field, as a result of the modification of the saturated mixing ratios by the warmer sea-surface temperature anomalies. At 2100 UTC on 22 January the higher atmospheric comparison level of the sensitivity experiment exhibits departures from the control simulation in the subtropical areas, and to a lesser extent in temperate areas.

### *Day three*

By the third day (0900 UTC) of the sensitivity test, the simulated low pressure, to the north of Madagascar had intensified. The recurved northwesterly winds continued their expansion westward reaching the east coast of Africa (Fig 3.15 a,b). The easterly winds remained stronger than the simulated winds of the control experiment along the

Control Run

January 22 1981



VAPOUR AND CLOUDS

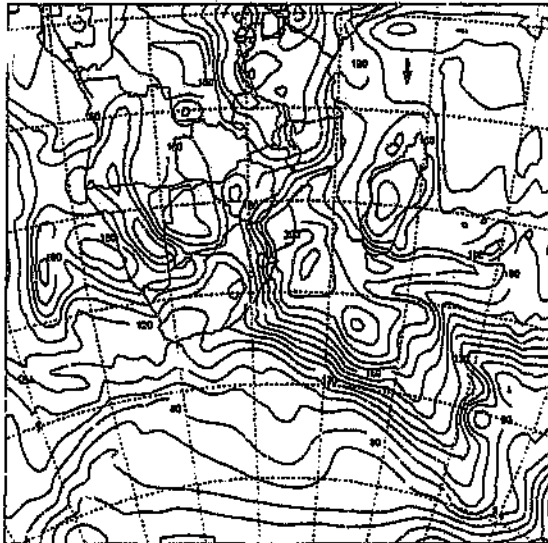
z = 146.4 m

t = 2100 UTC

--- 100  
- - - 200  
... 300

Sensitivity Test 1

January 22 1981



VAPOUR AND CLOUDS

z = 146.4 m

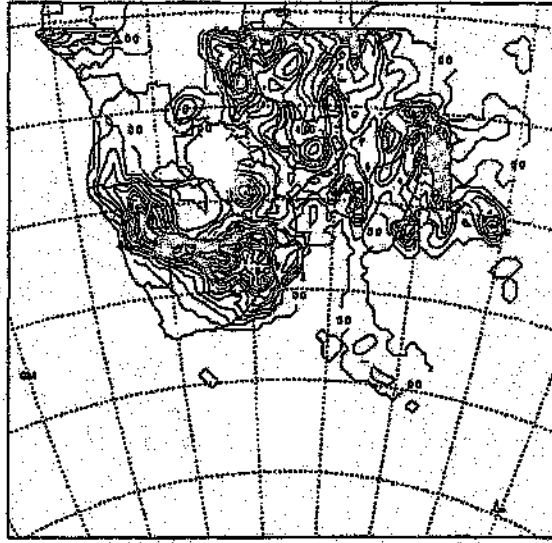
t = 2100 UTC

--- 100  
- - - 200  
... 300

Figure 3.11 Vapour and cloud mixing ratios (in  $\text{g.kg}^{-1} \times 10^{-4}$ ) for (a) the control and (b) the sensitivity simulations at the 146.4 m sigma level for 2100 UTC on 22 January 1981.

Control Run

January 22 1981



accum conv pcp

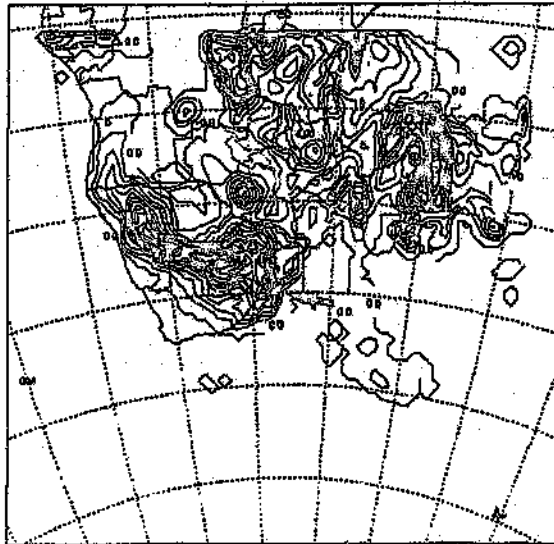
z = 146.4 m

t = 2100 UTC

Jan 22 0000-00  
146.4 2100-00  
By 11 0000-01  
Name "0 0000-01"

Sensitivity Test 1

January 22 1981



accum conv pcp

z = 146.4 m

t = 2100 UTC

Jan 22 0000-00  
146.4 2100-00  
By 11 0000-01  
Name "0 0000-01"

Figure 3.12 Accumulated convective precipitation (in mm) for (a) the control and (b) the sensitivity simulations at the 146.4 m sigma level for 2100 UTC on 22 January 1981.

Control Run

January 22 1981



$z = 807.2 \text{ m}$

$t = 2100 \text{ UTC}$

Sensitivity Test 1

January 22 1981



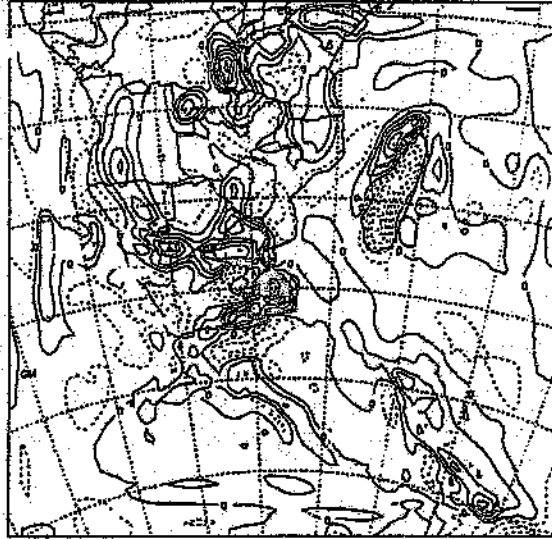
$z = 807.2 \text{ m}$

$t = 2100 \text{ UTC}$

Figure 3.13 Streamline diagrams for (a) the control and (b) the sensitivity simulations at the 807.2 m sigma level for 2100 UTC on 22 January 1981.

Control Run

January 22 1981



File: 2022-01  
14 07 00 01  
by: 07022-03  
Date: 14 07 00 01

W

z = 807.2 m

t = 2100 UTC

Sensitivity Test 1

January 22 1981



File: 2022-01  
14 07 00 01  
by: 07022-03  
Date: 14 07 00 01

W

z = 807.2 m

t = 2100 UTC

Figure 3.14 Vertical velocities (in  $\text{cm.s}^{-1} \times 10^{-4}$ ) for (a) the control and (b) the sensitivity simulations at the 807,2 m sigma level for 2100 UTC on 22 January 1981.

Control Run

January 23 1981



$z = 146.4 \text{ m}$

$t = 900 \text{ UTC}$

Sensitivity Test 1

January 23 1981



$z = 146.4 \text{ m}$

$t = 900 \text{ UTC}$

Figure 3.15 Streamlines diagrams for (a) the control and (b) the sensitivity simulations at the 146.4 m sigma level for 0900 UTC on 23 January 1981.

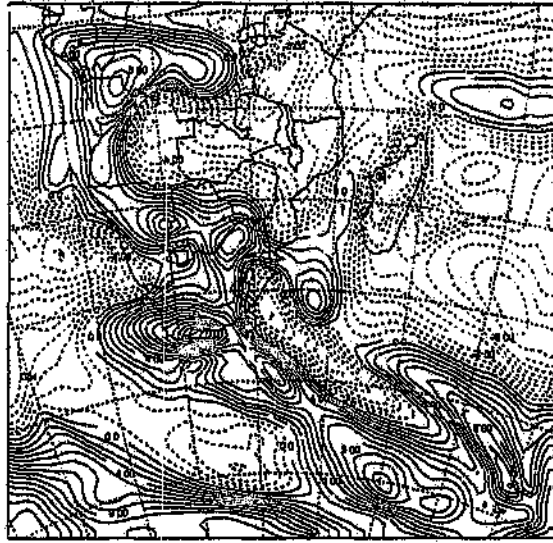
east coast of Madagascar and within the Mozambique Channel. Surface divergence (146,4 m) along 40°E became more prominent, further reducing moisture input to the continental tropical low centered over the Namibia/Botswana border. The presence of strong divergence at the 146,4 m level aided in reducing precipitation over the subcontinent but also enhanced the vertical instability of the developing low, by diverting more water vapour into the area of convection. Later that day (2100 UTC) the tropical-temperate trough became fully developed. The westerly wind component at the 146,4 m level extended down the Mozambique Channel with continued characteristically strong easterly flow along the east coast of Madagascar i.e. 7 ms<sup>-1</sup> simulated in the sensitivity simulation compared to 6 ms<sup>-1</sup> simulated in the control simulation (Fig 3.16 a,b). Simulated control and sensitivity instability values remained the same on the west and east coasts, but over the central parts of southern Africa sensitivity values were lowered due to the reduction of moisture from over the tropical Indian Ocean. Moisture availability continued its higher trend over Madagascar and the modified sea-surface temperature field with precipitation values showing a marked increase of maximum values of 46 mm for the sensitivity simulation compared with 36 mm in the control simulation (Fig 3.17 a,b).

#### *Day four*

By the final day, the sensitivity simulation modelled the dissipation of the tropical-temperate trough through the easterly migration of the westerly wave perturbation. The low pressure circulation simulated from the second day of the sensitivity test weakened and moved southwards along the Mozambique Channel (Fig 3.18 a,b). A consistently stronger easterly flow to the east of Madagascar was maintained with continually higher vapour and cloud mixing ratios indicative of greater moisture availability over Madagascar and the tropical Indian Ocean. Lower vapour and cloud mixing ratios along the east coast of southern Africa indicate the reduction of moisture availability in this area. This can be seen by the reduction in extent of the 0,023 g.kg<sup>-1</sup> contoured area over Durban (Fig 3.19 a,b). On 24 January at 1200 UTC higher accumulated convective precipitation values for the sensitivity experiment were recorded over the tip of Madagascar and tropical Indian Ocean (51 mm versus 42 mm), along with a decrease in precipitation on the southern African subcontinent

Control Run

January 23 1981



Plot: U1000-01  
148 1000-01  
by: 0 1000-01  
date: \* 0 1000-01

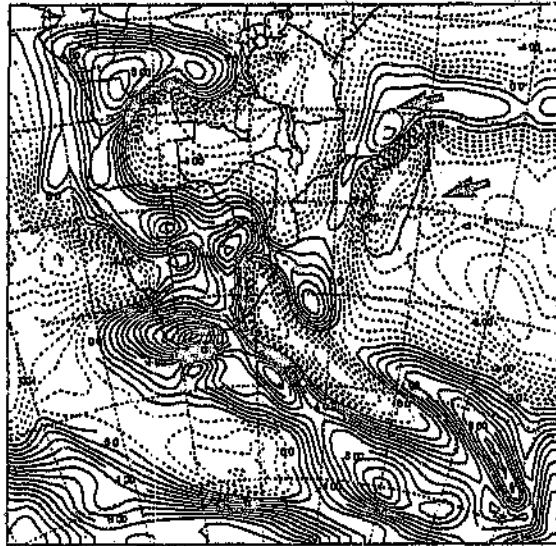
U

z = 146.4 m

t = 2100 UTC

Sensitivity Test 1

January 23 1981



Plot: U1000-01  
148 1000-01  
by: 0 1000-01  
date: \* 0 1000-01

U

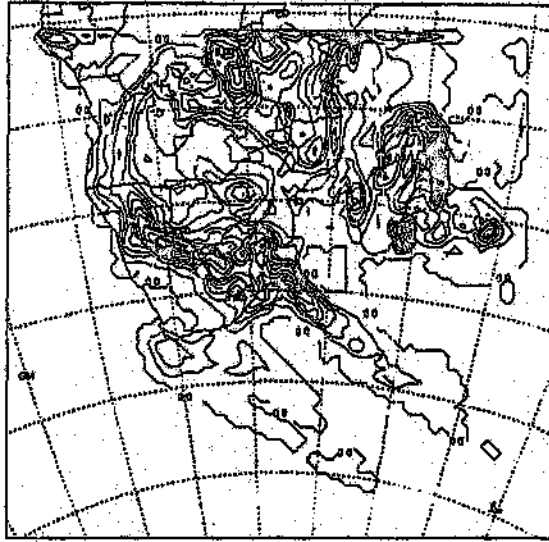
z = 146.4 m

t = 2100 UTC

Figure 3.16 U components (in  $m \cdot s^{-1}$ ) for (a) the control and (b) the sensitivity simulations at the 146,4 m sigma level for 2100 UTC on 23 January 1981.

Control Run

January 23 1981



accum conv pop

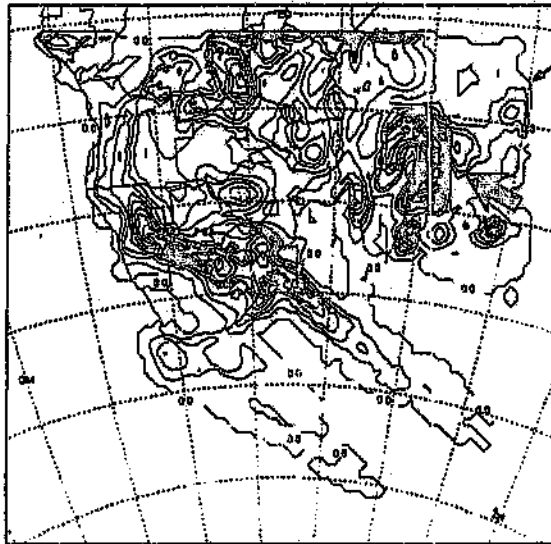
Run 0 22028-02  
to 0 22029-02  
by 0 22029-02  
date 14 1981-01

z = 146.4 m

t = 2100 UTC

Sensitivity Test 1

January 23 1981



accum conv pop

Run 0 22028-02  
to 0 22029-02  
by 0 22029-02  
date 14 1981-01

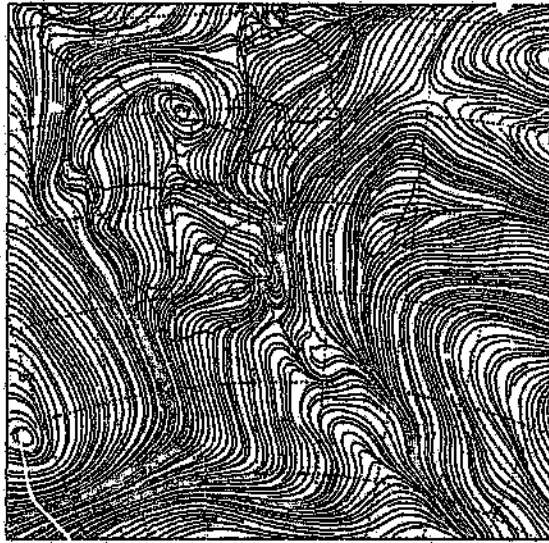
z = 146.4 m

t = 2100 UTC

Figure 3.17 Accumulated convective precipitation (in mm) for (a) the control and (b) the sensitivity simulations at the 146.4 m sigma level for 2100 UTC on 23 January 1981.

Control Run

January 24 1981



$z = 146.4 \text{ m}$

$t = 1200 \text{ UTC}$

Sensitivity Test 1

January 24 1981



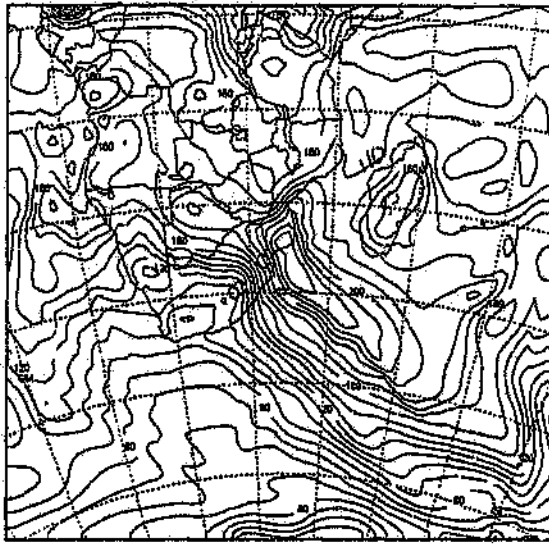
$z = 146.4 \text{ m}$

$t = 1200 \text{ UTC}$

Figure 3.18 Streamlines diagrams for (a) the control and (b) the sensitivity simulations at the 146.4 m sigma level for 1200 UTC on 24 January 1981.

Control Run

January 24 1991



VAPOUR AND CLOUDS

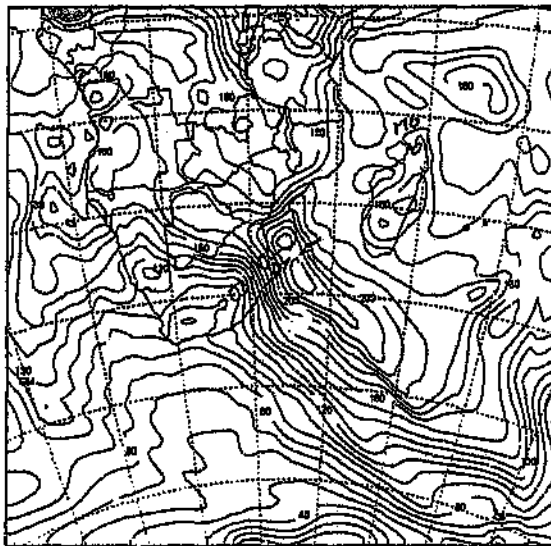
from 0 22000-02  
to 0 22000-01  
by 0 12000-02  
level \* 0 02000-02

z = 146.4 m

t = 1200 UTC

Sensitivity Test 1

January 24 1991



VAPOUR AND CLOUDS

from 0 22000-02  
to 0 22000-01  
by 0 12000-02  
level \* 0 02000-02

z = 146.4 m

t = 1200 UTC

Figure 3.19 Vapour and cloud mixing ratios (in  $\text{g kg}^{-1} \times 10^{-6}$ ) for (a) the control and (b) the sensitivity simulations at the 146,4 m sigma level for 1200 UTC on 24 January 1991.

from 24 mm in the control simulation to 18 mm in the sensitivity over Durban (Fig 3.20 a,b).

Higher-level (807,2 m) simulated circulation at 1200 UTC possessed similar trends to surface patterns. The moisture availability did, however, differ quite significantly from the control simulation with higher values to the east of Madagascar and within the Mozambique Channel (Fig 3.21 a,b).

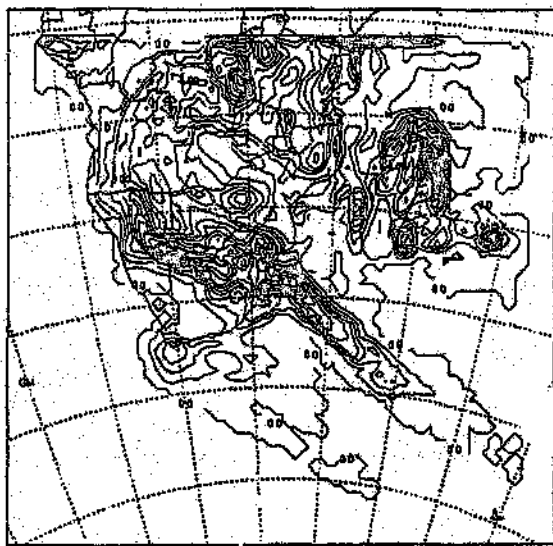
### Discussion

The modification of sea-surface temperatures in the tropical Indian Ocean, by the addition of a positive 2°C anomaly core bounded by a positive 1°C anomaly, had little effect on the overall formation and dissipation of the simulated tropical-temperate trough. Localised differences were, however significant with sea-surface temperature modification producing zones of heightened instability and cyclogenesis. The westerly wind component situated on the 5°S latitude increased its westerly extent and on reaching the African east coast proceeded to move down the Mozambique Channel. The presence of increased moisture availability due to the development of surface divergence along 40°E and instability due to the increased temperature anomalies heightened the development of cyclogenesis over the tropical Indian Ocean. The development of both divergence at 40°E and the tropical low at approximately 10°S reduced atmospheric moisture input from the tropical Indian Ocean to the subcontinent, as the pathway of moisture transport was redirected to the Mozambique Channel. Easterly winds, to the east of Madagascar remained stronger throughout the simulation due to the development of the quasi-stationary low pressure.

Very few differences were found in the 807,2 m level: those that were simulated in the sensitivity simulation were consistent with the larger sensitivity simulation differences found near the surface (146,4 m). Departures from the model control iteration took much longer to translate to the continental regions and temperate zone, particularly in

Control Run

January 24 1981



accum conv pcp

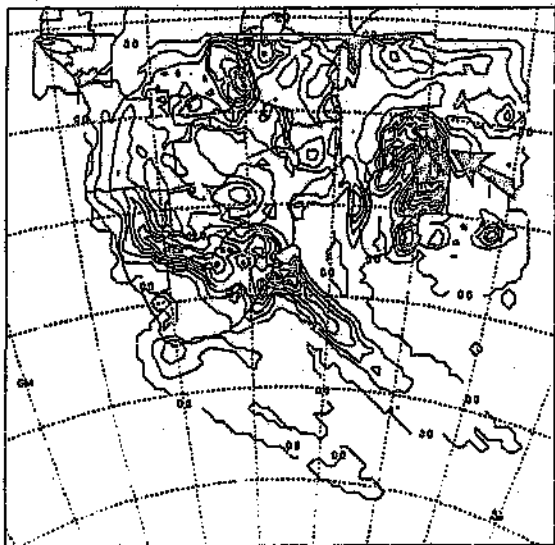
z = 146.4 m

t = 1200 UTC

From G22001-02  
to G22001-02  
by G22001-02  
www.G22001-02

Sensitivity Test 1

January 24 1981



accum conv pcp

z = 146.4 m

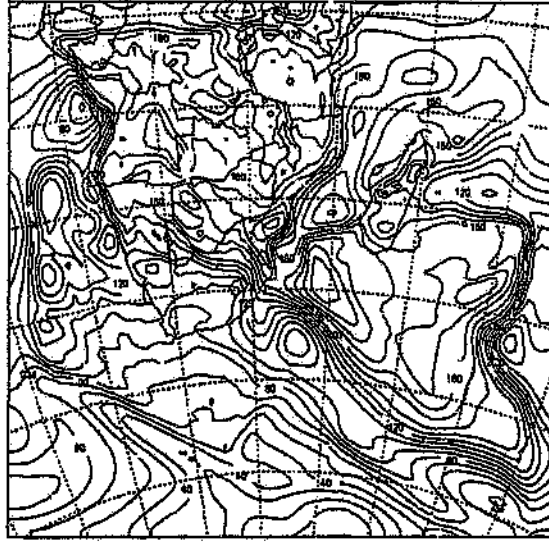
t = 1200 UTC

From G22001-02  
to G22001-02  
by G22001-02  
www.G22001-02

Figure 3.20 Accumulated convective precipitation (in mm) for (a) the control and (b) the sensitivity simulations at the 146.4 m sigma level for 1200 UTC on 24 January 1981.

Control Run

January 24 1981



Plot of 020000-02  
-01 2000-01  
-01 1000-02  
-01 1000-02

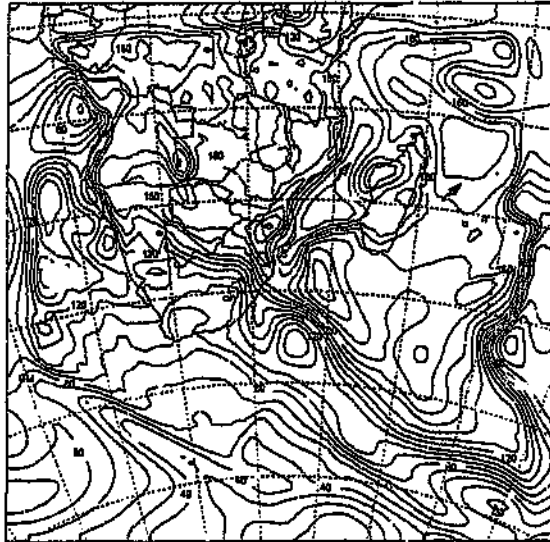
VAPOUR AND CLOUDS

z = 307.2 m

t = 1200 UTC

Sensitivity Test 1

January 24 1981



Plot of 020000-02  
-01 2000-01  
-01 1000-02  
-01 1000-02

VAPOUR AND CLOUDS

z = 307.2 m

t = 1200 UTC

Figure 3.21 Vapour and cloud mixing ratios (in  $\text{g.kg}^{-1} \times 10^{-4}$ ) for (a) the control and (b) the sensitivity simulations at the 307,2 m sigma level for 1200 UTC on 24 January 1981.

sensitivity experiment were constant with inter-annual atmospheric circulation changes found in dry years around the subcontinent. (D'Abreton, 1992; Mason, 1992, 1993, 1994; Jury *et al.*, 1991a,b; Barclay *et al.*, 1993; Jury, 1996).

## Chapter IV

### The Agulhas Current Retroflection Anomaly (Sensitivity Test 2)

The oceanic region to the south of the subcontinent is thought to play a decisive role in weather modification on relatively short time scales (Walker, 1989). Research has indicated that the development of positive anomalies to the south of the subcontinent serve to strengthen the sea-surface temperature gradient in this area (Walker, 1989). Positive sea-surface temperature increases in the Agulhas retroflection region also produce heightened surface fluxes, particularly sensible heating (Walker, 1989; Jury, 1993). Thus the combination of both an increased sea-surface temperature gradient and enhanced heat fluxes, facilitate the reduction of low-level stability, which in turn increases surface convergence, convection and finally precipitation within the westerly wave disturbance (Walker, 1989; Mey *et al*, 1990)

The second sensitivity test represents a modification of the long term mean sea-surface temperatures within the zone of the Agulhas Current retroflection (Fig 4.1), in order to test whether circulation changes in the sensitivity experiment coincide with the conceptualised changes proposed by previous research (Walker, 1989). The second sensitivity simulation was run for the same period as the first, from 21 to 24 January 1981. The sensitivity simulation was then compared with the control simulation by the analysis of wind components ( $u, v$ ), streamlines, temperatures, vertical velocity ( $w$ ), vapour and cloud mixing ratios, and accumulated convective precipitation at the 146,4 m and 807,2 m sigma levels.

### Sensitivity Test 2 (Agulhas Current Retroflexion Anomaly)

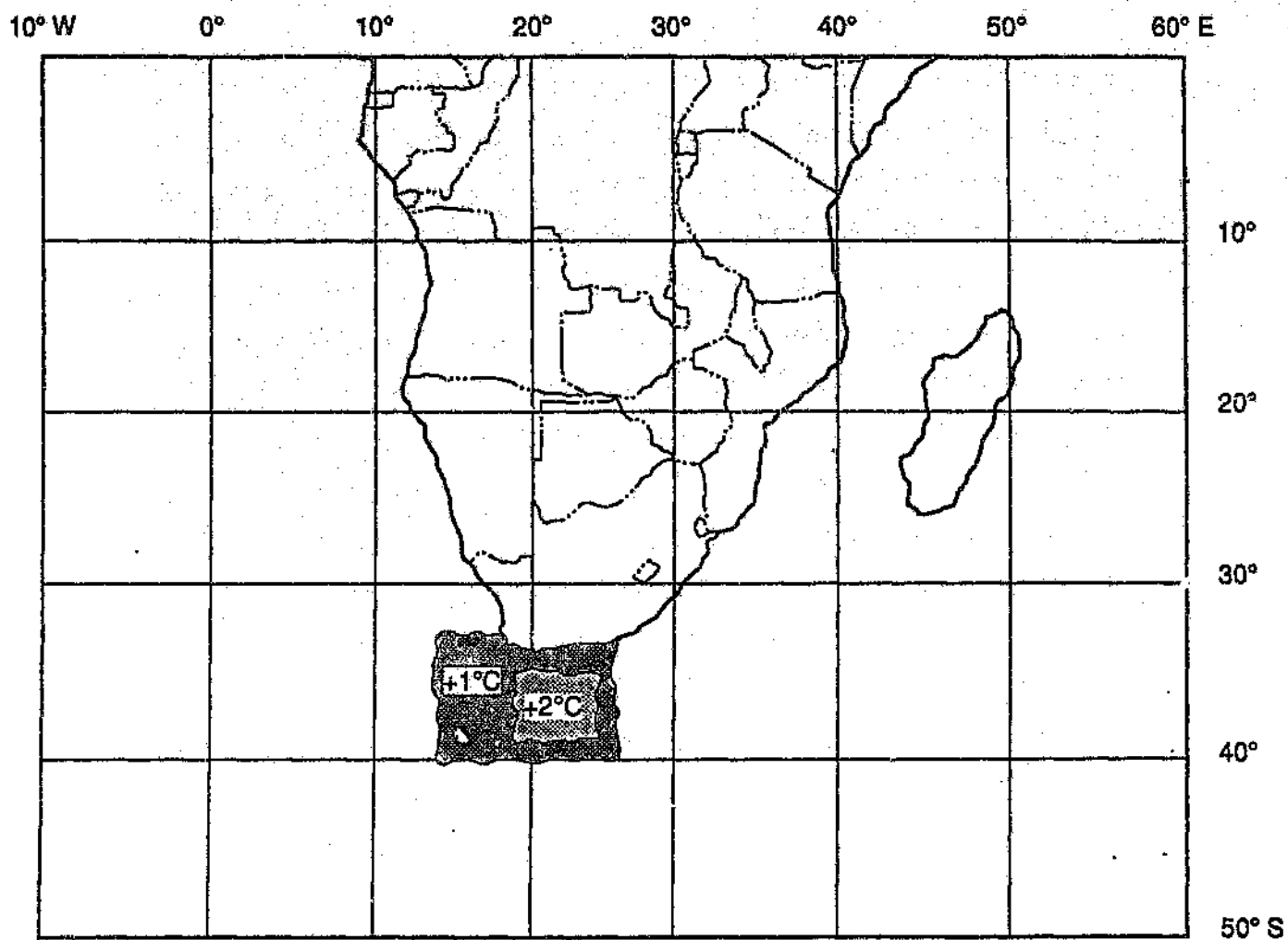


Figure 4.1 Representation of the second sensitivity test, whereby a positive 2°C anomaly and positive 1°C anomaly were added to the Agulhas current region of retroflexion.

## Results

### *Day one*

When the Agulhas Current retroflection anomaly experiment was compared to the control simulation, the initial time-step (1200 UTC) exhibited no circulation or atmospheric parameter differences. As for the control and first sensitivity experiment, the South Atlantic and South Indian Highs were positioned relatively far south at 35°S and 42°S respectively. Two prominent tropical lows were simulated over the continent, with significant moisture availability in these areas. High vapour and cloud mixing ratio values were also simulated over Madagascar and over the tropical Indian Ocean to the east. Easterly winds were predominant to the east of Madagascar along with westerly winds in the temperate latitudes. At 2100 UTC on the first day of the simulation small disparities between the control and sensitivity test become apparent at the 146,4 m sigma<sub>2</sub> level. A marginal decrease in onshore flow along the south coast became evident along with a slight increase in the availability of moisture found along the west coast of South Africa. When comparing the magnitude of change with the tropical Indian Ocean anomaly simulation, the Agulhas retroflection anomaly experiment exhibits a much smaller response over the same time period. This may be the result of the mid-latitude atmospheric circulation requiring a longer reaction time to the development of sea-surface temperature anomalies.

### *Day two*

On the second day of the simulation (0600 UTC) the weaker onshore flow continued (Fig 4.2 a,b), allowing the southeasterly extension of the 294 K contour line along the west coast of South Africa, bringing an increase in air temperature to the area. Over the region of sea-surface temperature modification vertical velocities exhibited a slight increase, by the southwest displacement of the 0,003 cms<sup>-1</sup> vertical velocity contour line (Fig 4.3 a,b), indicating that instability was beginning to under-cut the low-level stability in the area. The combination of weaker onshore flow and air temperature increase served to perpetuate the growth of instability over the anomalous sea-surface

Control Run

January 22 1981



$z = 146.4 \text{ m}$

$t = 600 \text{ UTC}$

Sensitivity Test 2

January 22 1981



$z = 146.4 \text{ m}$

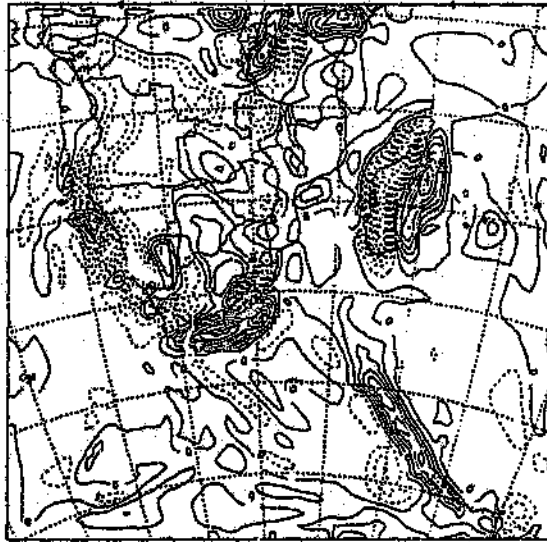
$t = 600 \text{ UTC}$

Figure 4.2 Streamline diagrams for (a) the control and (b) the sensitivity simulations at the 146.4 m sigma level for 0600 UTC on 22 January 1981.

Control Run

January 22 1981

0600



0600  
0600  
0600  
0600  
0600

W

z = 146.4 m

t = 0600 UTC

Sensitivity Test 2

January 22 1981



0600  
0600  
0600  
0600  
0600

W

z = 146.4 m

t = 0600 UTC

Figure 4.3 Vertical velocities (in  $\text{cm.s}^{-1} \times 10^{-4}$ ) for (a) the control and (b) the sensitivity simulations at the 146.4 m sigma level for 0600 UTC on 22 January 1981.

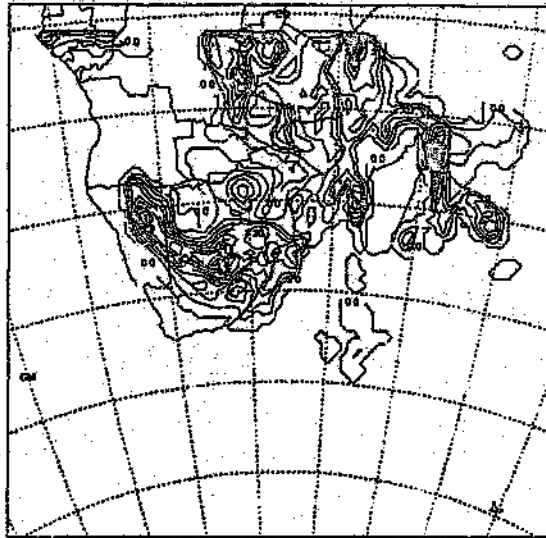
temperature field. Accumulated convective precipitation recorded higher simulated values over the South Africa/Botswana border for this sensitivity simulation period with control values of 5,6 mm versus values of 6,4 mm. The increase had no effect on precipitation up to the period 0600 UTC (Fig 4.4 a,b).

By 1500 UTC southeasterly winds along the west coast strengthened, producing a marginal increase in convergence over Angola and Namibia, as well as a stronger cyclonic circulation over central Namibia (Fig 4.5 a,b). The subtropical trough situated over the northern half of South Africa indicated the same pattern of change as the streamlines, with higher positive vertical velocities at the eastern limits, the west coast of southern Angola, and northern Namibia. Localised increases in instability are found over the area of modified sea-surface temperatures (Fig 4.6 a,b). Moisture availability increased over the eastern boundary of the modified sea-surface temperature field with the southerly displacement of the  $0,011 \text{ gkg}^{-1}$  contour line (Fig 4.7 a,b).

By 2100 UTC on 22 January the stronger south easterly winds along the west coast of South Africa expanded to cover the subcontinent. This increase in south easterly wind flow served to heighten the circulation both around the tropical low over Namibia, and the subtropical trough over the northeast of the country (Fig 4.8 a,b). Simulated instability followed the same pattern as indicated by the streamlines, with vertical velocities having a greater magnitude on the eastern limits of the subtropical trough, as well as over the area of modified sea-surface temperatures. Precipitation values continued to be higher over the central plateau and south eastern Namibia as a result of the stronger surface convergence over these areas.

The sensitivity simulation at 807 m showed only marginal circulation differences to the control experiment, which would suggest a longer period for the translation of circulation differences through the atmospheric levels than for the tropical Indian Ocean experiment. Southeasterly flow over the continent does however appear to strengthen as well as circulation around the subtropical trough. Vertical velocities over the south eastern portion of Namibia, the central plateau of South Africa, and

Control Run  
January 22 1981

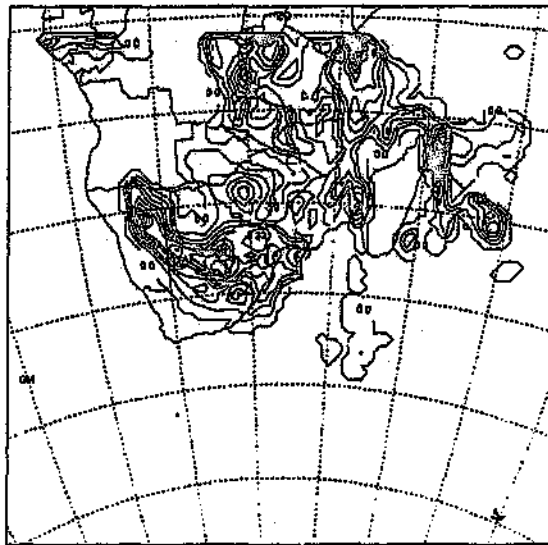


accum conv pcp

z = 148.4 m      t = 600 UTC

Scale 0.000000-10.0  
10.0 0.000000-10.0  
0.0 0.000000-10.0  
0.0 0.000000-10.0

Sensitivity Test 2  
January 22 1981



accum conv pcp

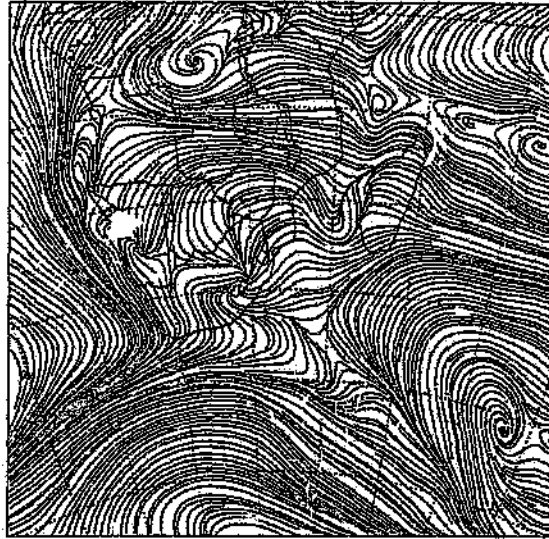
z = 148.4 m      t = 600 UTC

Scale 0.000000-10.0  
10.0 0.000000-10.0  
0.0 0.000000-10.0  
0.0 0.000000-10.0

Figure 4.4 Accumulated convective precipitation (in mm) for (a) the control and (b) the sensitivity simulations at the 146.4 m sigma level for 0600 UTC on 22 January 1981.

Control Run

January 22 1981

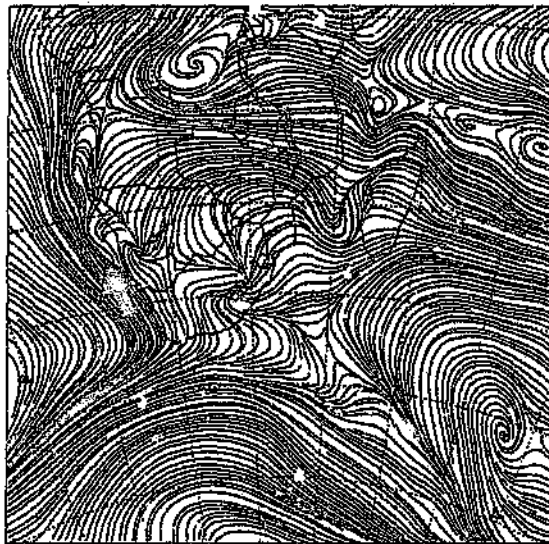


$z = 146.4 \text{ m}$

$t = 1500 \text{ UTC}$

Sensitivity Test 2

January 22 1981



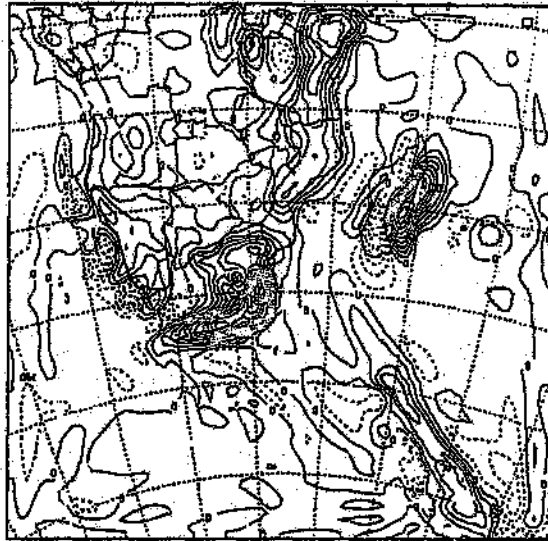
$z = 146.4 \text{ m}$

$t = 1500 \text{ UTC}$

Figure 4.5 Streamline diagrams for (a) the control and (b) the sensitivity simulations at the 146,4 m sigma level for 1500 UTC on 22 January 1981.

Control Run

January 22 1981



From: 180501  
To: 180501  
By: 180501  
Info: 180501-05

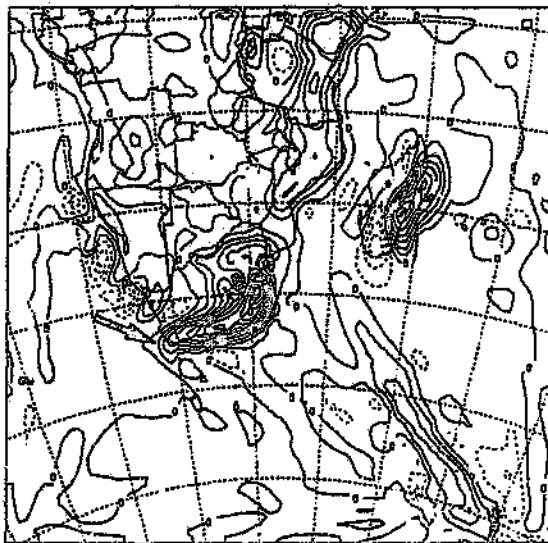
W

z = 146.4 m

t = 1500 UTC

Sensitivity Test 2

January 22 1981



From: 180501  
To: 180501  
By: 180501  
Info: 180501-05

W

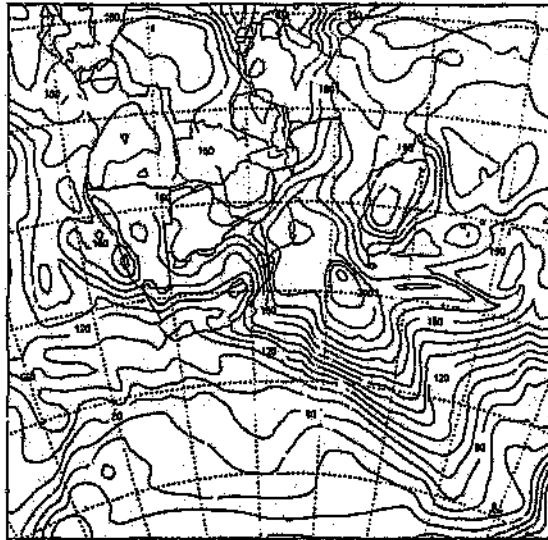
z = 146.4 m

t = 1500 UTC

Figure 4.6 Vertical velocities (in  $\text{cm.s}^{-1} \times 10^{-4}$ ) for (a) the control and (b) the sensitivity simulations at the 146.4 m sigma level for 1500 UTC on 22 January 1981.

Control Run

January 22 1981



VAPOUR AND CLOUDS

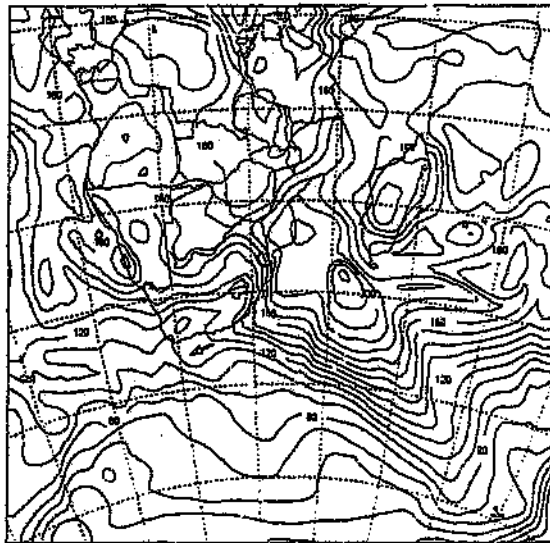
00000000-00  
00 000000-00  
00 000000-00  
0000 00 0000-00

z = 146.4 m

t = 1500 UTC

Sensitivity Test 2

January 22 1981



VAPOUR AND CLOUDS

00000000-00  
00 000000-00  
00 000000-00  
0000 00 0000-00

z = 146.4 m

t = 1500 UTC

Figure 4.7 Vapour and cloud mixing ratios (in  $\text{g}\cdot\text{kg}^{-1} \times 10^{-4}$ ) for (a) the control and (b) the sensitivity simulations at the 146.4 m sigma level for 1500 UTC on 22 January 1981.

Control Run

January 22 1981



$z = 146.4 \text{ m}$

$t = 2100 \text{ UTC}$

Sensitivity Test 2

January 22 1981



$z = 146.4 \text{ m}$

$t = 2100 \text{ UTC}$

Figure 4.8 Streamline diagrams for (a) the control and (b) the sensitivity simulations at the 146.4 m sigma level for 2100 UTC on 22 January 1981.

along the southeast coast are higher, with the simulated developing front exhibiting higher instability values aligned in a northwest to southeast direction, with values on the eastern limit of the subtropical trough showing a weakening trend for the same time period (Fig 4.9 a,b). At the 807,2 m level, cloud and vapour mixing ratios show the same trend as the 146,4 m level with marginal increases evident over the Western Cape and Cape south coast of  $0,0011 \text{ gkg}^{-1}$  to  $0,0010 \text{ gkg}^{-1}$  over the northern limit of the modified sea-surface temperature field (Fig 4.10 a,b).

### *Day three*

By the third day (0900 UTC) the Agulhas retroflection anomaly experiment at the 146,4 m level, began to exhibit a zonal strengthening over the area of modified sea-surface temperatures, with westerly wind components increasing from  $15 \text{ ms}^{-1}$  in the control experiment to  $16 \text{ ms}^{-1}$  in the sensitivity simulation. Westerly wind components over the initial westerly wave perturbation indicated a marginal decrease in strength at approximately  $48^{\circ}\text{S}$ ,  $70^{\circ}\text{E}$  (Fig 4.11 a,b), but exhibited heightened instability in this area with values of  $0,020 \text{ cms}^{-1}$  in the sensitivity simulation compared to control simulation values of  $0,016 \text{ cms}^{-1}$  (Fig 4.12 a,b).

Areas also experiencing heightened instability are found over the developing front and along the east coast. The origin of instability is found over the modified sea-surface temperature field and translated poleward by the predominant circulation (Fig 4.12 a,b). Vapour and cloud mixing ratios decreased over the southern Free State and northeastern Cape Province, but increased over southern Namibia and southwestern Botswana. Moisture availability remained high over the southeastern coast of South Africa and adjacent Indian Ocean. Precipitation increases in the simulation experiment coincide with the areas of heightened instability over the east coast of South Africa at  $30^{\circ}\text{S}$ , over the sea-surface temperature anomaly with a marginal increase from 2 mm in the sensitivity simulation compared to 1 mm in the control simulation, over eastern Namibia (18 mm versus 16 mm), and over southern Botswana (Fig 4.13 a,b).

Control Run

January 22 1981



W

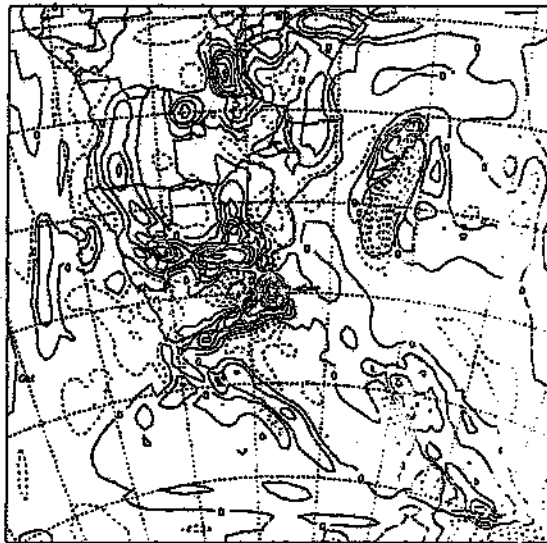
NOV 1 2008 05  
44 0 000000  
44 0 000000  
44 0 000000

z = 807.2 m

t = 2100 UTC

Sensitivity Test 2

January 22 1981



W

NOV 1 2008 05  
44 0 000000  
44 0 000000  
44 0 000000

z = 807.2 m

t = 2100 UTC

Figure 4.9 Vertical velocities (in  $\text{cm.s}^{-1} \times 10^{-4}$ ) for (a) the control and (b) the sensitivity simulations at the 807.2 m sigma level for 2100 UTC on 22 January 1981.

Control Run

January 22 1981



VAPOUR AND CLOUDS

From G12222-00  
to D 12222-01  
by B 12222-02  
Scheme \*G12222-02

z = 807.2 m

t = 2100 UTC

Sensitivity Test 2

January 22 1981



VAPOUR AND CLOUDS

From G12222-00  
to D 12222-01  
by B 12222-02  
Scheme \*B 12222-02

z = 807.2 m

t = 2100 UTC

Figure 4.10 Vapour and cloud mixing ratios (in  $\text{g kg}^{-1} \times 10^{-6}$ ) for (a) the control and (b) the sensitivity simulations at the 807.2 m sigma level for 2100 UTC on 22 January 1981.

Control Run

January 23 1981



$z = 146.4 \text{ m}$

$t = 900 \text{ UTC}$

Sensitivity Test 2

January 23 1981



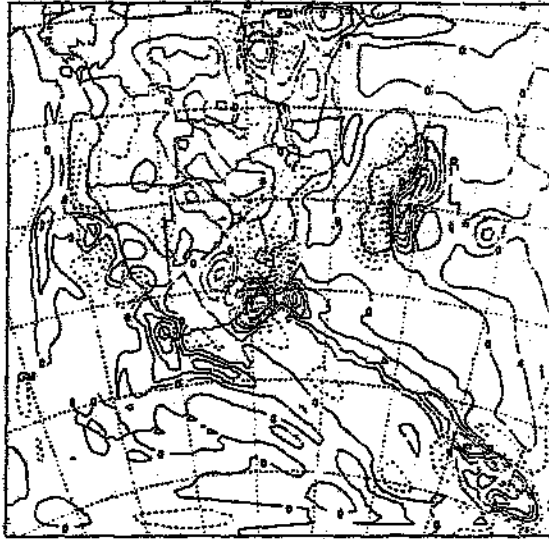
$z = 146.4 \text{ m}$

$t = 900 \text{ UTC}$

Figure 4.11 Streamline diagrams for (a) the control and (b) the sensitivity simulations at the 146,4 m sigma level for 0900 UTC on 23 January, 1981.

Control Run

January 23 1981



W

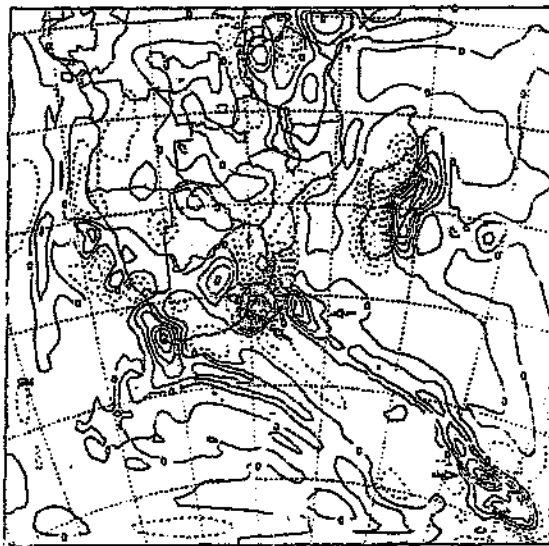
NOV 1980  
NOV 1980  
NOV 1980  
NOV 1980

z = 146.4 m

t = 900 UTC

Sensitivity Test 2

January 23 1981



W

NOV 1980  
NOV 1980  
NOV 1980  
NOV 1980

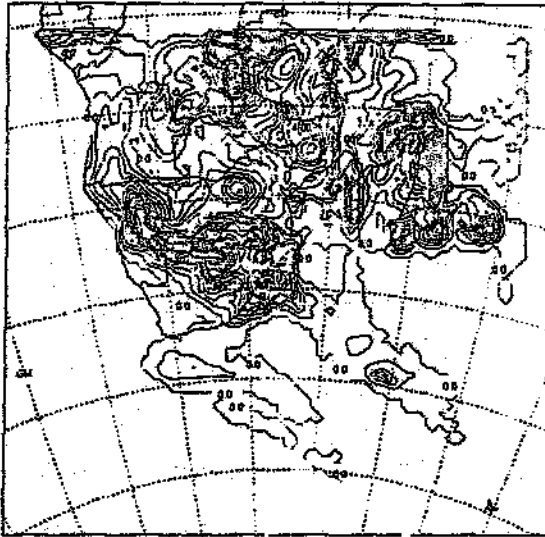
z = 146.4 m

t = 900 UTC

Figure 4.12 Vertical velocities (in  $\text{cm} \cdot \text{s}^{-1} \times 10^{-4}$ ) for (a) the control and (b) the sensitivity simulations at the 146.4 m sigma level for 0900 UTC on 23 January 1981.

Control Run

January 23 1981



accum conv pcp

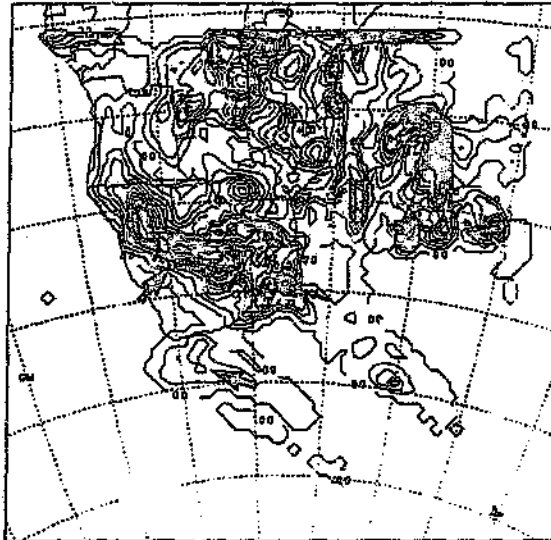
z = 146.4 m

t = 900 UTC

000000-00  
000000-00  
000000-00  
000000-00

Sensitivity Test 2

January 23 1981



accum conv pcp

z = 146.4 m

t = 900 UTC

000000-00  
000000-00  
000000-00  
000000-00

Figure 4.13 Accumulated convective precipitation (in mm) for (a) the control and (b) the sensitivity simulations at the 146.4 m sigma level for 0900 UTC on 23 January 1981.

Later on during the day (1500 UTC) the stronger convergence zone over the south coast of South Africa, indicated at the 146,4 m sigma level, moved eastwards to find a position along the eastern half of the country. The westerly winds over the northern parts of South Africa, and the southwesterly flow along the west coast of the continent appeared stronger than the control simulation, with stronger cyclonic circulation around the low pressure east of Durban over the Indian Ocean.

By the evening of 23 January 1981 (2100 UTC) the connection between the tropical and temperate regions was made possible by the coupling of the tropical low, the subtropical trough and the westerly wave perturbation. The magnitude of the westerly wind component was greater over the Cape south coast with values of  $16 \text{ ms}^{-1}$  compared to values of  $15 \text{ ms}^{-1}$ , poleward along the front, over the Northern Province, and over the Indian Ocean east of Durban (Fig 4.14 a,b). A secondary low pressure was simulated to the north of the subtropical trough in the sensitivity experiment (Fig 4.15 a,b). This feature is thought to be the product of reduced anticyclonic circulation over the northern parts of Namibia enabling greater north westerly wind flow towards the low. Vertical velocity showed higher instability over the Western Cape and along the cold front until the  $40^{\circ}\text{S}$  line of latitude. Accumulated convective precipitation values remained higher over the sea-surface temperature anomaly with sensitivity values of 6 mm compared to 4 mm in the control, eastern Namibia, southern Botswana (24 mm compared to 22 mm), and along the east coast of South Africa (Fig 4.16 a,b).

#### *Day four*

In the early morning (0600 UTC) of the last simulation day, the westerly winds continued to possess greater magnitude along the cold front down to approximately  $37^{\circ}\text{S}$ . The simulated lows over the eastern half of South Africa and over the Indian Ocean dissipated although instability remained higher over the south coast ( $0,45 \text{ cms}^{-1}$  compared to  $0,40 \text{ cms}^{-1}$ ) and along the receding cold front ( $15 \text{ cms}^{-1}$  compared to  $10 \text{ cms}^{-1}$ ) (Fig 4.17 a,b). At the end of the simulation period a strong westerly component moved along the south coast in the same direction as the receding cold front, with localised stronger flow remaining in situ over the Northern Province and

Control Run

January 23 1981



U

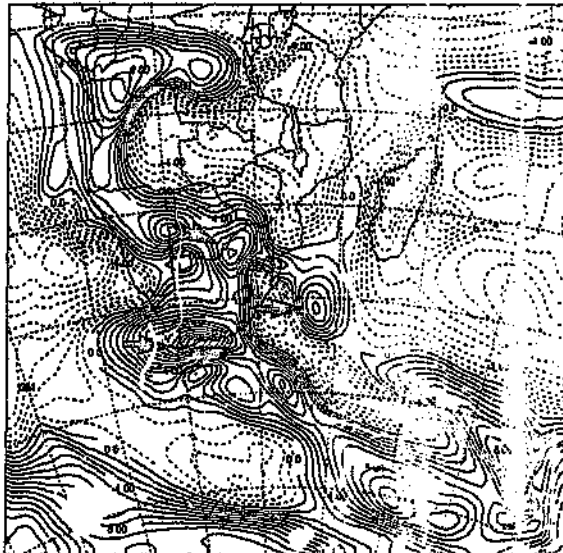
Item: 11025-01  
Rev: 010228-02  
By: 010228-01  
Scale: 1:0.0000-01

z = 146.4 m

t = 2100 UTC

Sensitivity Test 2

January 23 1981



U

Item: 11025-01  
Rev: 010228-02  
By: 010228-01  
Scale: 1:0.0000-01

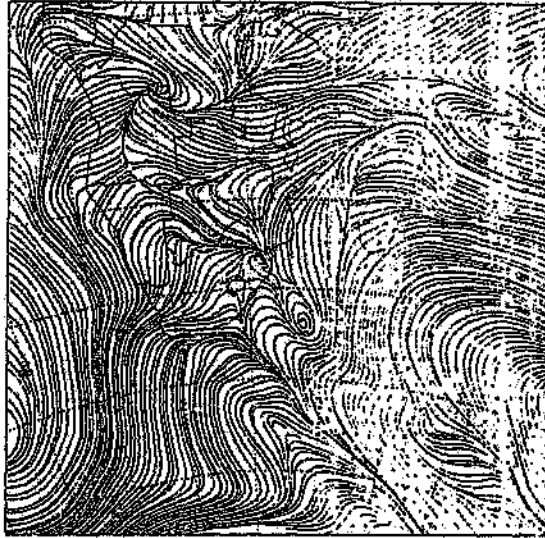
z = 146.4 m

t = 2100 UTC

Figure 4.14 U components (in m.s<sup>-1</sup>) for (a) the control and (b) the sensitivity simulations at the 146,4 m sigma level for 2100 UTC on 23 January 1981.

Control Run

January 23 1981

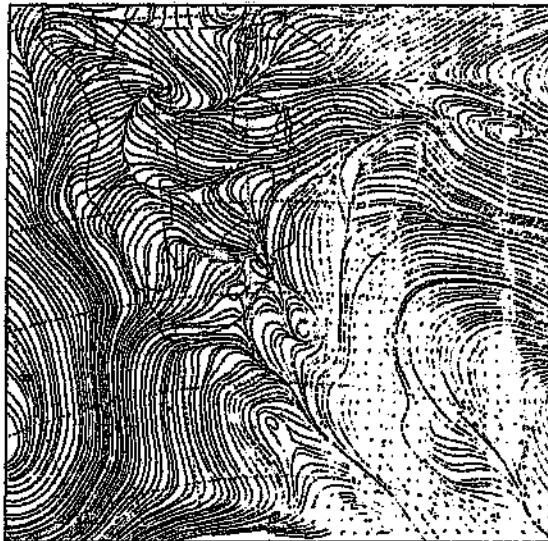


$z = 146.4 \text{ m}$

$t = 2100 \text{ UTC}$

Sensitivity Test 2

January 23 1981



$z = 146.4 \text{ m}$

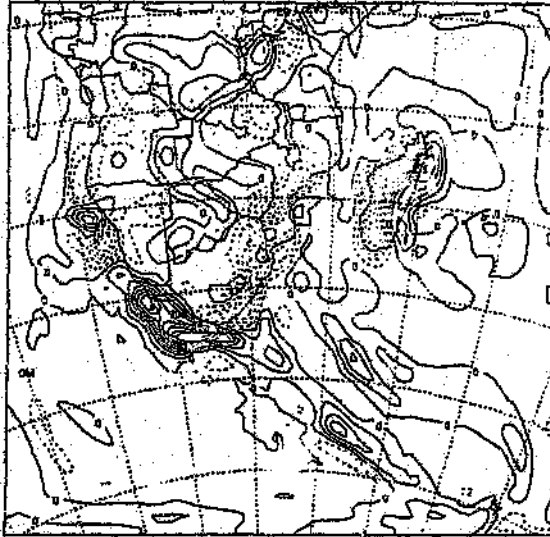
$t = 2100 \text{ UTC}$

Figure 4.15 Streamlines for (a) the control and (b) the sensitivity simulations at the 146.4 m sigma level for 2100 UTC on 23 January 1981.



Control Run

January 24 1981



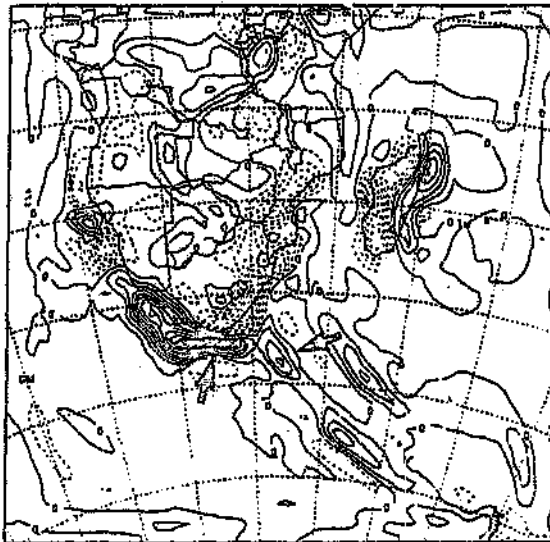
Jan 24 0600Z  
43 48282 01  
146.4 0000000  
146.4 10 146.4 00

z = 146.4 m

t = 600 UTC

Sensitivity Test 2

January 24 1981



Jan 24 0600Z  
43 48282 01  
146.4 0000000  
146.4 10 146.4 00

z = 146.4 m

t = 600 UTC

Figure 4.17 Vertical velocities (in  $\text{cm.s}^{-1} \times 10^{-4}$ ) for (a) the control and (b) the sensitivity simulations at the 146.4 m sigma level for 0600 UTC on 24 January 1981.

along the dissipating cold front (Fig 4.18 a,b). Once again streamlines indicate stronger southeasterly winds along the west coast of South Africa, with a concomitant increase in northwesterly winds over the Northern Province and Zimbabwe. Northerly winds along the east coast of South Africa also remained stronger, weakening the zone of convergence along the east coast (Fig 4.19 a,b). Instability remained higher along the west and south coasts, and northern parts of the east coast, coinciding with zones of heightened westerly flow. Precipitation maintained the same pattern as from early on 23 January. Accumulated values were markedly higher over the area of modified sea-surface temperatures with sensitivity values of 16 mm compared to control values of 8 mm. Similar differences are found over the eastern half of the country and adjacent Indian Ocean, as well as eastern Namibia and southern Botswana (Fig 4.20 a, b).

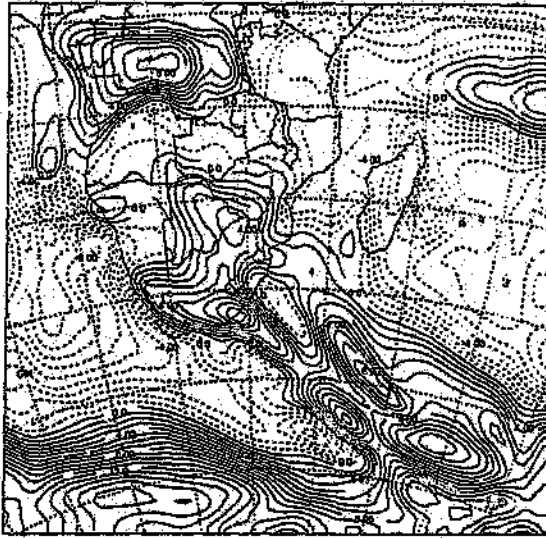
As at the near surface, the 810 m atmospheric level exhibits the same general trend of strengthening in the westerly component, from 23 January onwards (Fig 4.21 a,b). The streamlines at this level suggest a stronger shallow low pressure development over the Indian Ocean (Fig 4.22 a,b). Instability, as in the lower surface level remained higher over the west ( $0,049 \text{ cms}^{-1}$  compared to  $0,048 \text{ cms}^{-1}$ ) and south coast of South Africa ( $0,077 \text{ cms}^{-1}$  versus  $0,072 \text{ cms}^{-1}$ ) with, however, lower magnitudes along the dissipating front (Fig 4.23 a,b). Vapour and cloud mixing ratios, again indicated marginally higher moisture availability along the southeast coast and also east of Durban over the adjacent Indian Ocean, with control values of  $0,020 \text{ gkg}^{-1}$  and sensitivity values of  $0,021 \text{ gkg}^{-1}$  (Fig 4.24 a,b).

### Discussion

The atmospheric circulation changes brought about by the modification of sea-surface temperatures took longer to translate into the atmosphere than did the tropical Indian Ocean anomaly experiment. The explanation for this greater delay, lies in a comparison of the background sea-surface temperatures and moisture values over the two oceanic regions. In the tropical Indian Ocean background sea-surface

Control Run

January 24 1981



Item: 11026-02  
Date: 11/26/81  
By: R. 11026-01  
Scale: 1:1000000

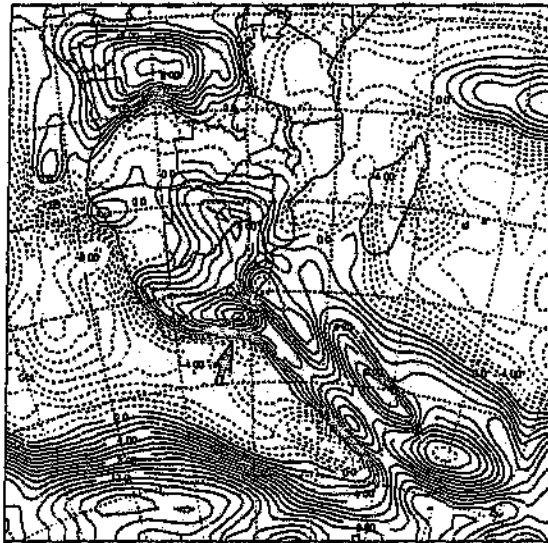
U

z = 146.4 m

t = 1200 UTC

Sensitivity Test 2

January 24 1981



Item: 11026-02  
Date: 11/26/81  
By: R. 11026-01  
Scale: 1:1000000

U

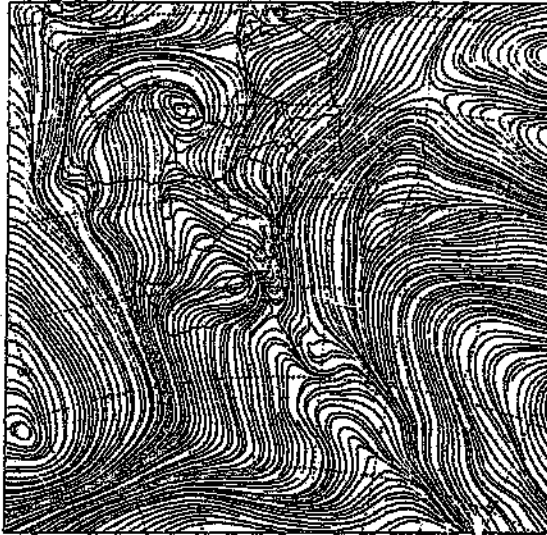
z = 146.4 m

t = 1200 UTC

Figure 4.18 U components (in  $m \cdot s^{-1}$ ) for (a) the control and (b) the sensitivity simulations at the 146.4 m sigma level for 1200 UTC on 24 January 1981.

Control Run

January 24 1981



$z = 146.4 \text{ m}$

$t = 1200 \text{ UTC}$

Sensitivity Test 2

January 24 1981



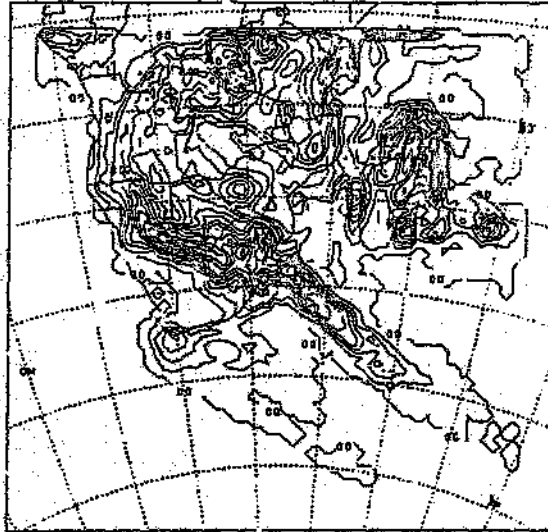
$z = 146.4 \text{ m}$

$t = 1200 \text{ UTC}$

Figure 4.19 Streamlines for (a) the control and (b) the sensitivity simulations at the 146,4 m sigma level for 1200 UTC on 24 January 1981.

Control Run

January 24 1981



accum conv ppt

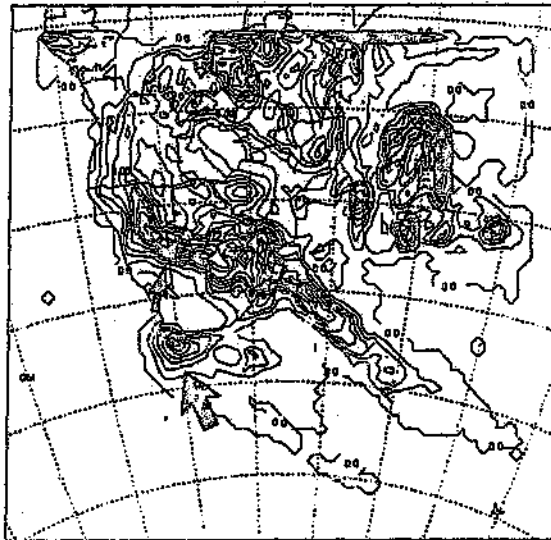
z = 146.4 m

t = 1200 UTC

NOAA-0100000-00  
NOAA-0100000-00  
NOAA-0100000-00  
NOAA-0100000-00

Sensitivity Test 2

January 24 1981



accum conv ppt

z = 146.4 m

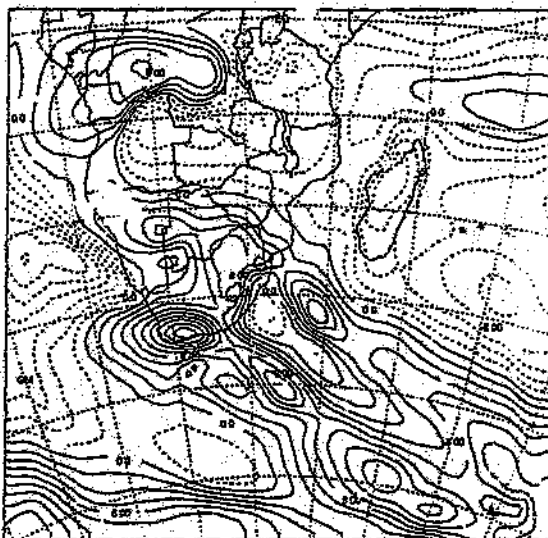
t = 1200 UTC

NOAA-0100000-00  
NOAA-0100000-00  
NOAA-0100000-00  
NOAA-0100000-00

Figure 4.20 Accumulated convective precipitation (in mm) for (a) the control and (b) the sensitivity simulations at the 146.4 m sigma level for 1200 UTC on 24 January 1981.

Control Run

January 23 1981



U

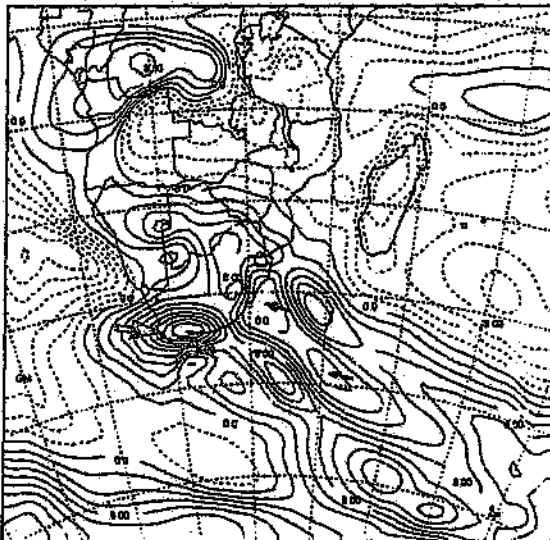
14228-02  
14228-02  
14228-02  
14228-02

z = 807.2 m

t = 2100 UTC

Sensitivity Test 2

January 23 1981



U

14228-02  
14228-02  
14228-02  
14228-02

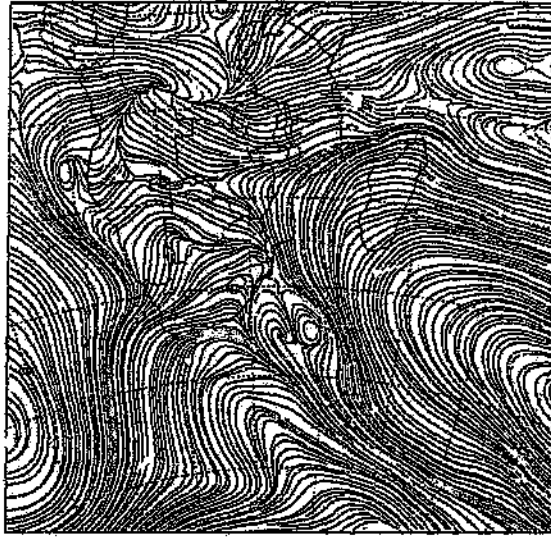
z = 807.2 m

t = 2100 UTC

Figure 4.21 U components (in m.s<sup>-1</sup>) for (a) the control and (b) the sensitivity simulations at the 807,2 m sigma level for 2100 UTC on 23 January 1981.

Control Run

January 23 1981



$z = 807.2 \text{ m}$

$t = 2100 \text{ UTC}$

Sensitivity Test 2

January 23 1981



$z = 807.2 \text{ m}$

$t = 2100 \text{ UTC}$

Figure 4.22 Streamlines for (a) the control and (b) the sensitivity simulations at the 807.2 m sigma level for 2100 UTC on 23 January 1981.

Control Run

January 24 1981



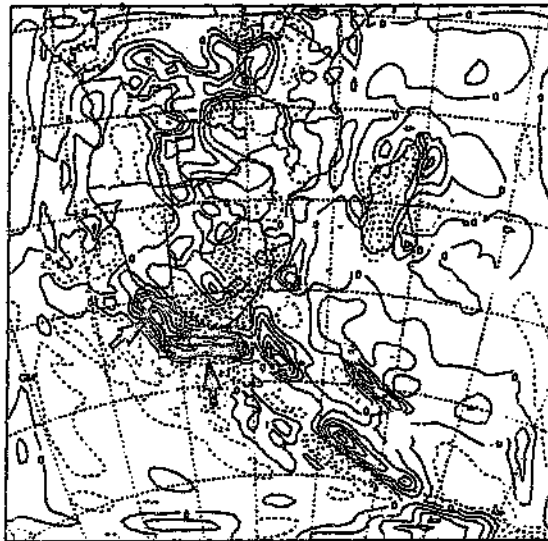
0000-0000-00  
1000000000  
1000000000  
1000000000

z = 807.2 m

t = 600 UTC

Sensitivity Test 2

January 24 1981



0000-0000-00  
1000000000  
1000000000  
1000000000

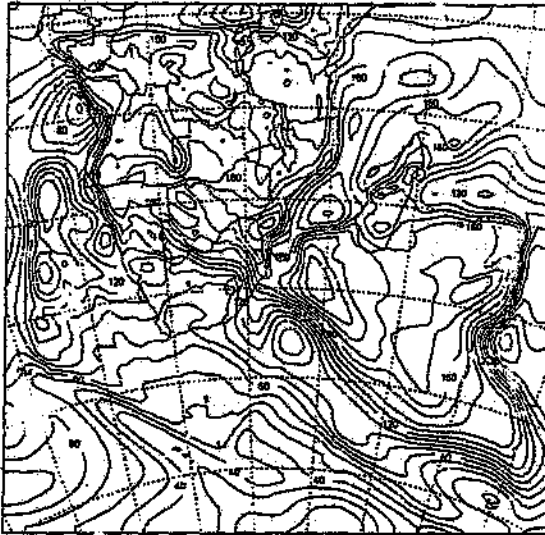
z = 807.2 m

t = 600 UTC

Figure 4.23 Vertical velocities ( $\text{in cm.s}^{-1} \times 10^{-4}$ ) for (a) the control and (b) the sensitivity simulations at the 807.2 m sigma level for 0600 UTC on 24 January 1981.

Control Run

January 24 1981



VAPOUR AND CLOUDS

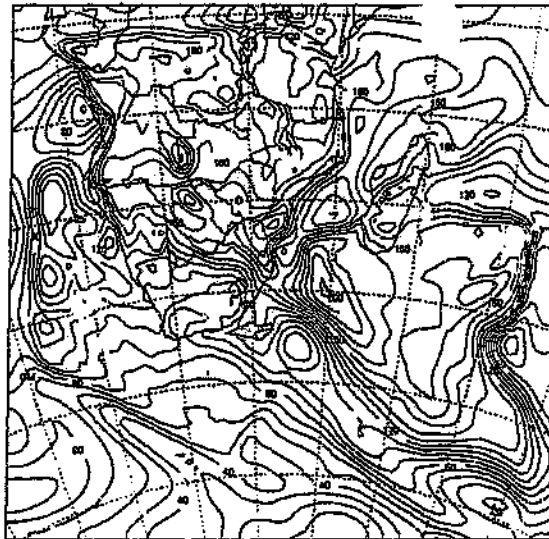
0.000000-00  
0.000000-00  
0.000000-00  
0.000000-00

z = 807.2 m

t = 1200 UTC

Sensitivity Test 2

January 24 1981



VAPOUR AND CLOUDS

0.000000-00  
0.000000-00  
0.000000-00  
0.000000-00

z = 807.2 m

t = 1200 UTC

Figure 4.24 Vapour and cloud mixing ratios (in  $\text{g kg}^{-1} \times 10^{-4}$ ) for (a) the control and (b) the sensitivity simulations at the 807.2 m sigma level for 1200 UTC on 24 January 1981.

temperatures are higher, with stronger boundary layer heat fluxes and thus greater atmospheric heating. The enhanced atmospheric temperatures over the anomaly region, and neighbouring ocean, allow for a greater moisture carrying capacity of the localised atmosphere. In the Agulhas Current retroflection region the lower background temperatures less readily affect moisture availability, instability and hence general circulation.

The circulation changes found for the anomaly experiment over the Agulhas Current retroflection closely resemble the ocean-atmosphere feedback mechanisms proposed by Walker (1989) for the southern Agulhas Current. As theorised (Fig 1.5), the development of sea temperature anomalies served to intensify the sea-surface temperature front, leading to a poleward shift in the surface westerlies. The strengthened heat fluxes enhanced low-level instability and produced a marginal amplification of the westerly troughs. The atmospheric differences that were found indicate that the origin of change lies over the modified sea-surface temperature field, and that the atmospheric circulation anomalies were translated both along the coast, from southwest to northeast by the passage of the westerly troughs, and also by the enhanced recurved westerly flow over eastern Namibia, southern Botswana and the Northern Province of South Africa. Higher instability values began over the modified sea-surface temperature field and migrated eastward along the coast, and poleward along the cold front. The greatest precipitation differences are found over the summer rainfall areas of South Africa, eastern Namibia and southern Botswana, with highest magnitude differences over the area of positive sea-surface temperature increase.

## Chapter V

### The Tropical Western Atlantic Sea-surface Temperature Anomaly (Sensitivity Test 3)

The tropical western Atlantic Ocean is a major source of moisture for the west African countries of Angola, Zaire, Gabon, Congo, and to a lesser extent South Africa in early summer. A combination of varying onshore flow and fluctuating sea-surface temperatures are, to a large extent, responsible for rainfall variability over this area (Hirst and Hastenrath, 1983; Hastenrath, 1984). Positive sea-surface temperature anomalies, in conjunction with stronger than normal westerly onshore flow, result in increased moisture transport into tropical west Africa and are thus linked with heavier rainfall events during the duration of the oceanic and atmospheric anomalies (Hirst and Hastenrath, 1983). The association between the tropical western Atlantic sea-surface temperature variability and rainfall over South Africa is poorly understood. The results of the third sensitivity experiment should illustrate some of the mechanisms involved in the association between the tropical western Atlantic Ocean and rainfall over South Africa. As for the previous two sensitivity experiments the model simulation was initialised using a modified long-term mean United Kingdom Meteorological Office sea-surface temperature data set, with positive anomalies of 2°C and 1°C respectively added to the background temperature field between 4°N and 20°S, with a longitudinal extent between 6°W and 14°E (Fig 5.1).

#### Results

##### *Day one*

The initial time-step of the tropical western Atlantic Ocean simulation once again confirmed the precise circulation patterns of the control simulation experiment. At the

146,4 m sigma level the position of the general synoptic features, as well as high vapour and cloud mixing ratios in the tropical Indian Ocean ( $0,022 \text{ gkg}^{-1}$ ) and lower mixing ratios of between  $0,007 \text{ gkg}^{-1}$  and  $0,016 \text{ gkg}^{-1}$  along the west coast were mirrored in the sensitivity simulation.

### Sensitivity Test 3 (African West Coast Atlantic Anomaly)

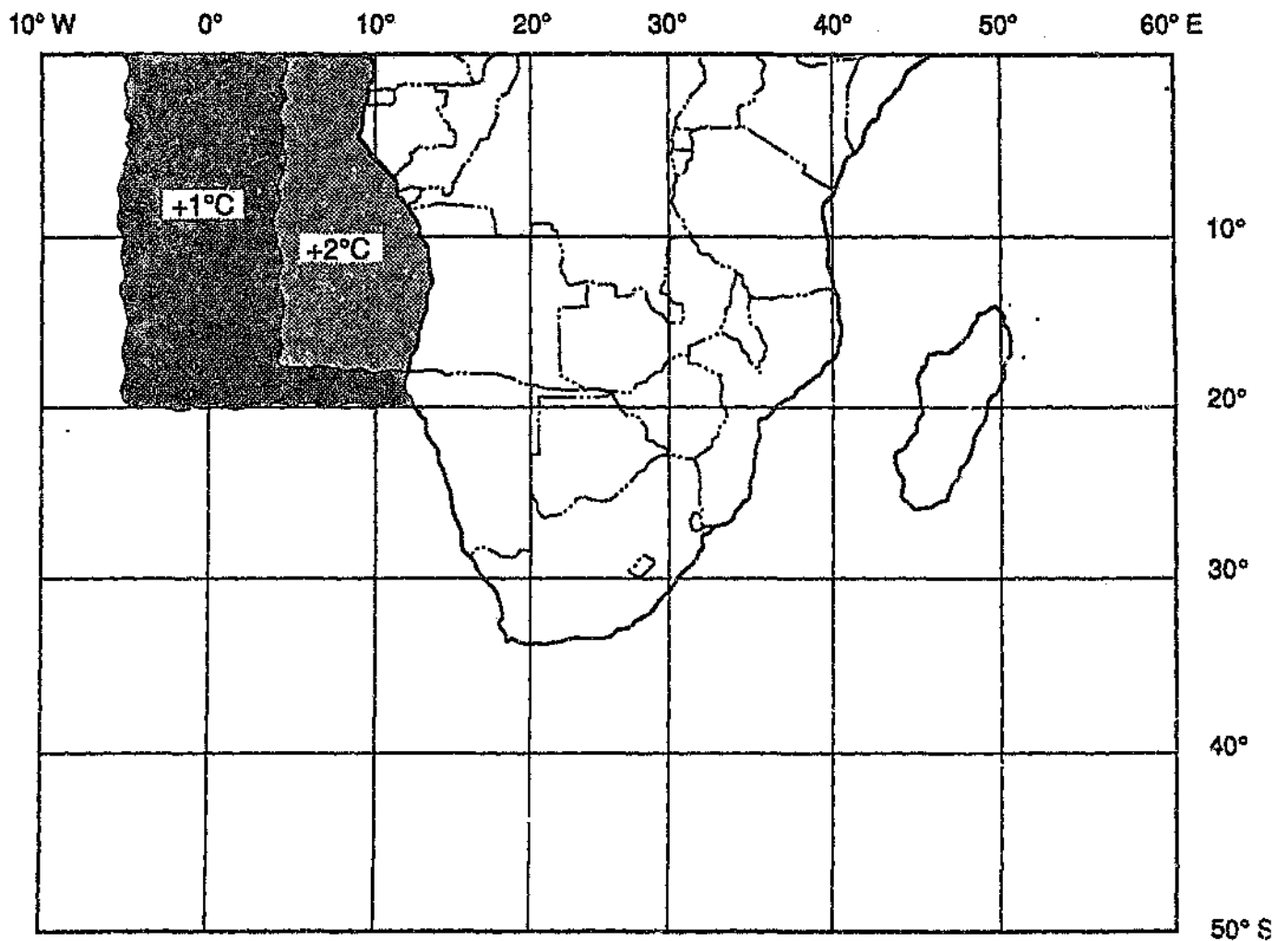


Figure 5.1 Representation of the third sensitivity test with anomalies placed between 4°N and 20°S, and from 6°W to the coast.

By 2100 UTC of 21 January the anomalous sea-surface temperatures in the tropical western Atlantic Ocean had been resident long enough to produce marginal circulation changes at the 146,4 m level. The increase in sea-surface temperatures in this region produced a concomitant increase in air temperature through heightened sensible

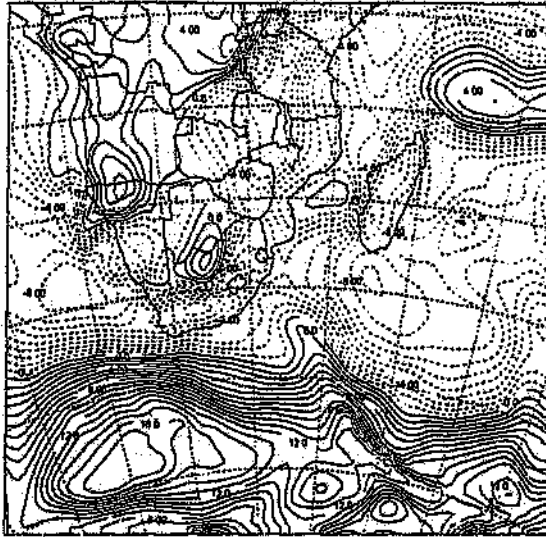
heating. This increase in air temperatures took place north of  $10^{\circ}\text{S}$  along the west coast, with the southerly extension of the 297 K isotherm. Over the Atlantic Ocean, adjacent to Angola, the westerly wind component strengthened, increasing onshore flow in the area (Fig 5.2 a,b). These differences are confirmed by the streamlines, where it is evident that over the northern half of Angola circulation became slightly more onshore, whereas over southern Congo flow became more southerly. The combination of strengthened onshore flow and warmer air temperatures produced vertical velocity increases along the Angolan coast from  $0,003 \text{ cms}^{-1}$  in the control simulation to  $0,006 \text{ cms}^{-1}$  in the sensitivity experiment (Fig 5.3 a,b). Precipitation values for 2100 UTC indicated a marginal increase over Gabon and Congo coast (Fig 5.4 a,b). The presence of heightened instability over Angola had not produced rainfall in this area as moisture levels were still relatively low.

#### *Day two*

On the morning of the second day (0600 UTC), the stronger westerly component simulated in the sensitivity experiment continued. The significance of this atmospheric circulation anomaly at the 146,4 m level was that the coastal regions of Gabon and Congo, along with parts of the Zaire basin, began to experience the greater availability of moisture, and thus the potential for precipitation increased. Later in the afternoon (1500 UTC) the westerly wind component or onshore flow remained stronger over Gabon and Congo with an intensification of convergence along the Angolan coast. Circulation around the tropical low strengthened, due to the behaviour of the westerly wind component, as well as the development of higher atmospheric temperatures (297 K) extending from the north (Fig 5.5 a,b), heightened moisture availability over Gabon and the Congo (control values are less than  $0,016 \text{ cms}^{-1}$  and sensitivity values are greater than  $0,016 \text{ cms}^{-1}$ ) (Fig 5.6 a,b). Higher precipitation values of 6 mm in the sensitivity experiment compared to 4 mm in the control simulation were found adjacent to the sea-surface temperature anomaly (Fig 5.7 a,b). Rainfall over the Gauteng region, however, showed a decrease from between 5 mm to 6 mm in the control simulation to less than 4 mm in the sensitivity experiment (Fig 5.7 a,b).

Control Run

January 21 1981



U

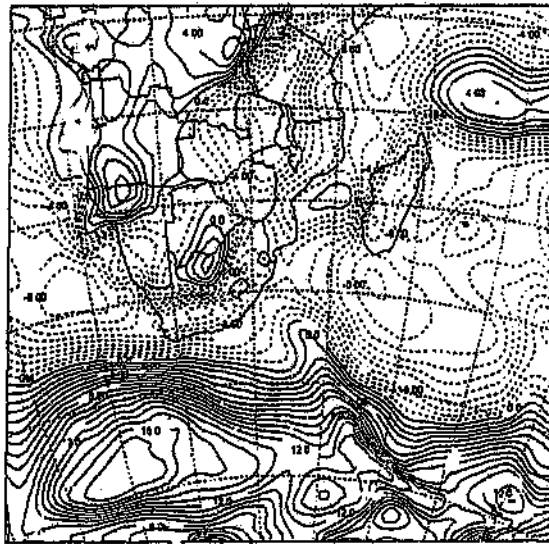
Scale: 10000-00  
10.0 10000-02  
10.0 10000-04  
10.0 10000-06

z = 146.4 m

t = 2100 UTC

Sensitivity Test 3

January 21 1981



U

Scale: 10000-00  
10.0 10000-02  
10.0 10000-04  
10.0 10000-06

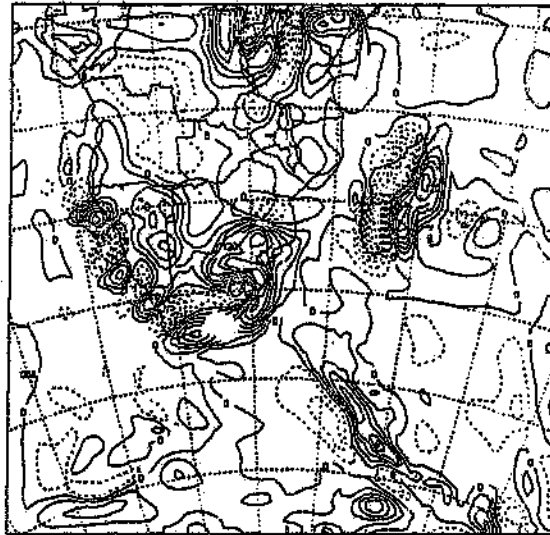
z = 146.4 m

t = 2100 UTC

Figure 5.2 U components (in  $m.s^{-1}$ ) for (a) the control and (b) the sensitivity simulations at the 146.4 m sigma level for 2100 UTC on 21 January 1981.

Control Run

January 21 1981



w

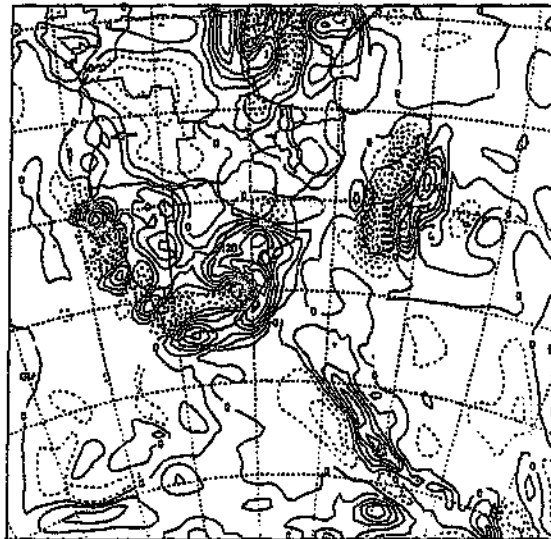
Apr - 22288.01  
ca 0 211028.01  
by C 22288.01  
scale \* 10000.00

z = 146.4 m

t = 2100 UTC

Sensitivity Test 3

January 21 1981



w

Apr - 22288.01  
ca 0 211028.01  
by C 22288.01  
scale \* 10000.00

z = 146.4 m

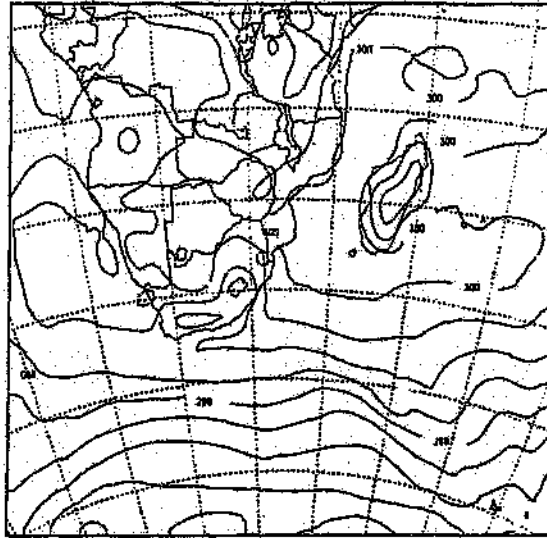
t = 2100 UTC

Figure 5.3 Vertical velocities (in  $\text{cm.s}^{-1} \times 10^{-4}$ ) for (a) the control and (b) the sensitivity simulations at the 146.4 m sigma level for 2100 UTC on 21 January 1981.



Control Run

January 22 1981



Temperature

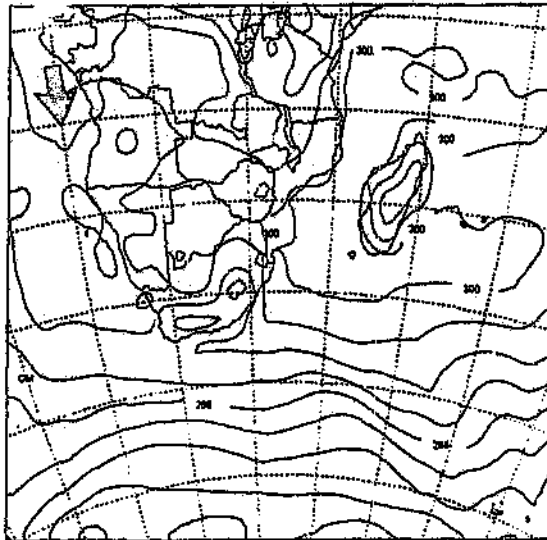
z = 146.4 m

t = 1500 UTC

Page 071228-03  
File 030228-03  
By 030228-01  
Date 12 10 2008-03

Sensitivity Test 3

January 22 1981



Temperature

z = 146.4 m

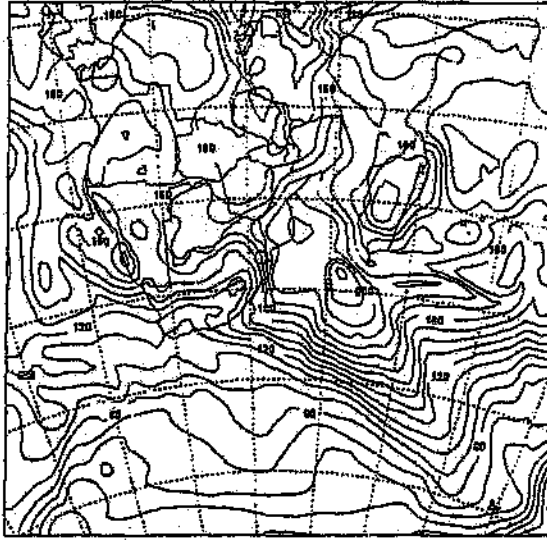
t = 1500 UTC

Page 071228-03  
File 030228-03  
By 030228-01  
Date 12 10 2008-03

Figure 5.5 Temperature contours (in K) for (a) the control and (b) the sensitivity simulations at the 146.4 m sigma level for 1500 UTC on 22 January 1981.

Control Run

January 22 1981



VAPOUR AND CLOUDS

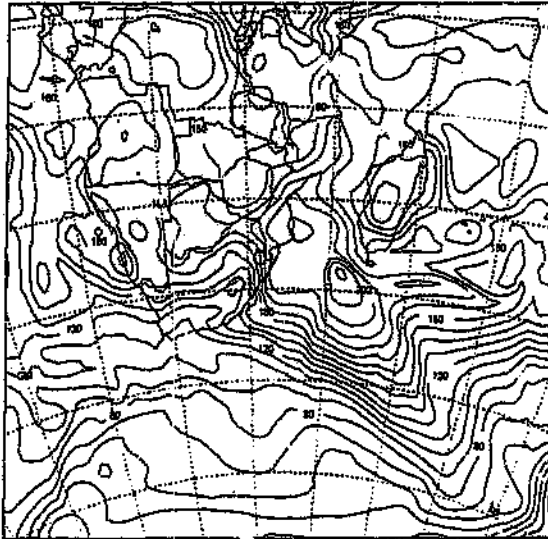
z = 146.4 m

t = 1500 UTC

0.000000  
0.000000  
0.000000  
0.000000

Sensitivity Test 3

January 22 1981



VAPOUR AND CLOUDS

z = 146.4 m

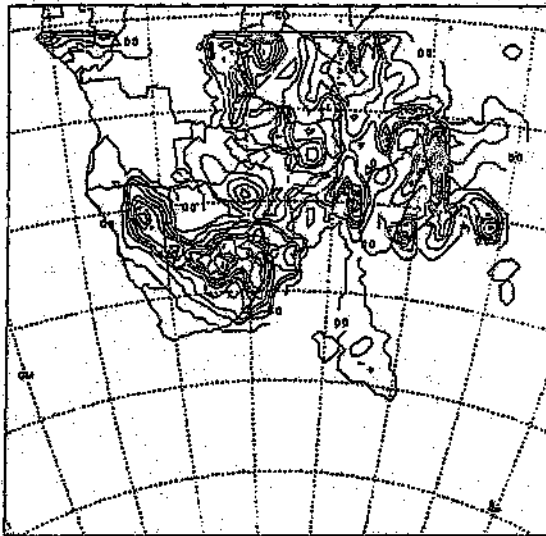
t = 1500 UTC

0.000000  
0.000000  
0.000000  
0.000000

Figure 5.6 Vapour and cloud mixing ratios (in  $\text{g kg}^{-1} \times 10^{-4}$ ) for (a) the control and (b) the sensitivity simulations at the 146.4 m sigma level for 1500 UTC on 22 January 1981.

Control Run

January 1981



accum conv pop

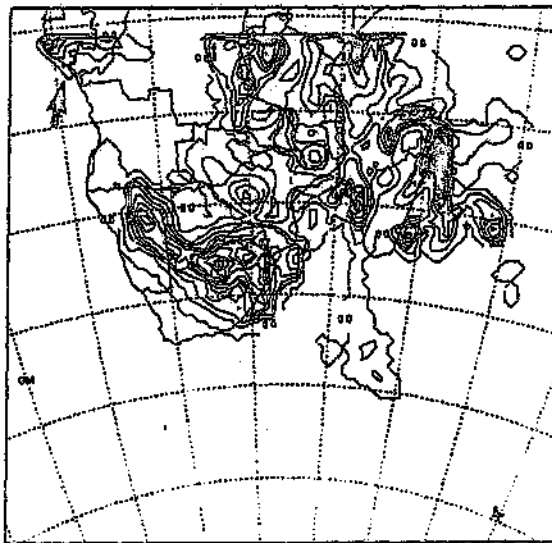
z = 146.4 m

t = 1500 UTC

000 0 0000-00  
00 0 0000-00  
00 0 0000-00  
0000 0 0000-00

Sensitivity Test 3

January 22 1981



accum conv pop

z = 146.4 m

t = 1500 UTC

000 0 0000-00  
00 0 0000-00  
00 0 0000-00  
0000 0 0000-00

Figure 5.7 Accumulated convective precipitation (in mm) for (a) the control and (b) the sensitivity simulations at the 146.4 m sigma level for 1500 UTC on 22 January 1981.

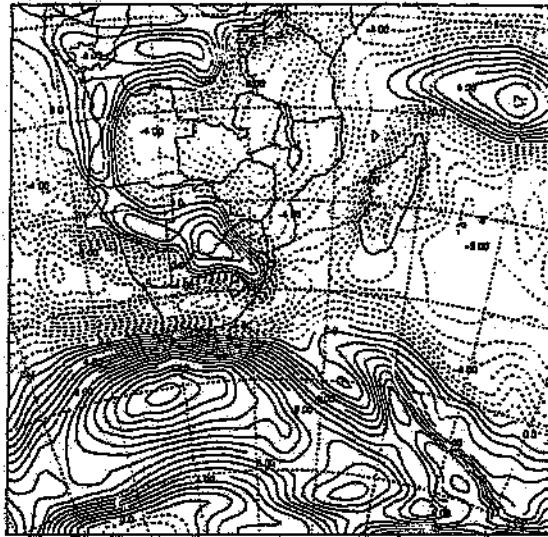
By the evening of 22 January the westerly wind component at the 146,6 m sigma level showed a slight increase over the Mpumalanga region, with the sensitivity experiment simulating values of  $6 \text{ ms}^{-1}$  over the southern Congo and northern Angola regions as opposed to values of  $5 \text{ ms}^{-1}$  for the control simulation (Fig 5.8 a,b). Circulation differences appeared to become prominent over South Africa with both stronger circulation and heightened instability present around the subtropical trough. Vertical velocities over the Indian Ocean east of Durban exhibit sensitivity values of  $0,040 \text{ cms}^{-1}$  compared to control values of  $0,036 \text{ cms}^{-1}$  (Fig 5.9 a,b). Circulation around the subtropical trough strengthened with higher vertical velocities present over the Indian Ocean east of Durban of  $0,040 \text{ cms}^{-1}$  compared to  $0,036 \text{ cms}^{-1}$  (Fig 5.9 a,b). In spite of the periodic reduction of the onshore component over Gabon and Congo simulated precipitation values for the sensitivity test remained higher with 7 mm in the sensitivity experiment compared 5 mm in the control simulation (Fig 5.10 a,b). Over the Gauteng region and eastern Namibia precipitation values showed a decrease from 16 mm in the control simulation to 13 mm in the sensitivity experiment (Fig 5.10 a,b).

Until 1500 UTC on 22 January very few of the atmospheric circulation changes brought about by the inclusion of the positive sea-surface temperature field had translated to the higher 807,2 m level. The only differences that are evident were vapour and cloud mixing ratios, which exhibited the same trend of increase as at the lower sigma level.

By 1500 UTC on 22 January sufficient simulation time had passed to allow for the vertical translation of the atmospheric circulation anomalies to take place. Again, the differences at the 807,2 m level were consistent with the 146,6 m level, with stronger westerly component north of  $10^{\circ}\text{S}$  (Fig 5.11 a,b), which served to increase moisture availability over Gabon, Congo and the Zaire basin (Fig 5.12 a,b), as well as to encourage stronger cyclonic circulation around the tropical low to the west of Angola (Fig 5.13 a,b). Later in the day (2100 UTC) the simulated cyclonic circulation around the tropical low continued to be stronger (Fig 5.14 a,b).

Control Run

January 22 1981



U

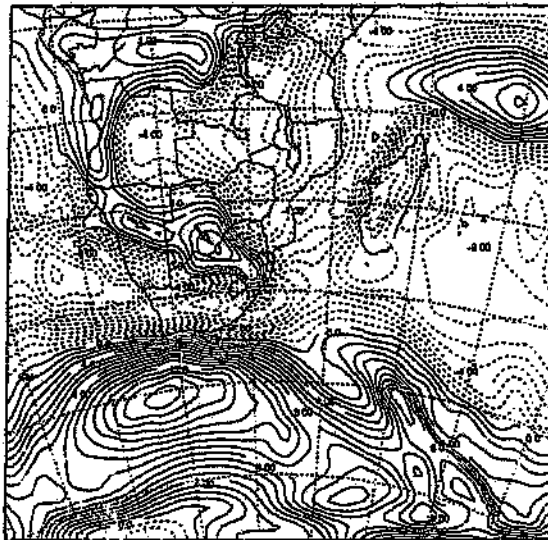
Run: Y2201-02  
File: U2201-02  
By: J. G. J. G.  
Date: 22 JAN 1981

z = 146.4 m

t = 2100 UTC

Sensitivity Test 3

January 22 1981



U

Run: Y2201-02  
File: U2201-02  
By: J. G. J. G.  
Date: 22 JAN 1981

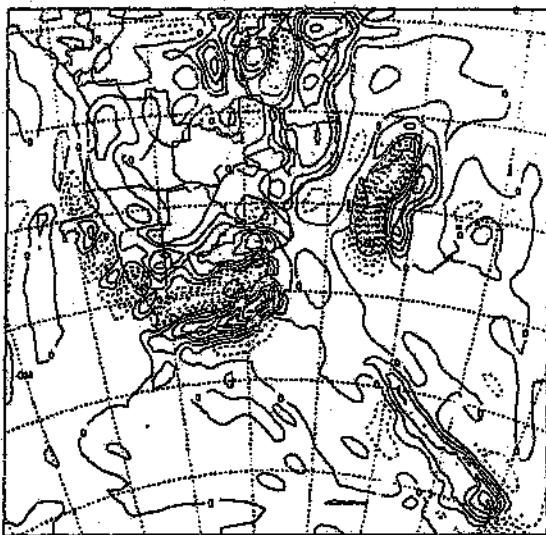
z = 146.4 m

t = 2100 UTC

Figure 5.8 U components (in  $\text{m.s}^{-1}$ ) for (a) the control and (b) the sensitivity simulations at the 146.4 m sigma level for 2100 UTC on 22 January 1981.

Control Run

January 22 1981



w

File: 432547  
14 0 3028 01  
by 01 432547  
month: 01 1981-01

z = 146.4 m

t = 2100 UTC

Sensitivity Test 3

January 22 1981



w

File: 432547  
14 0 3028 01  
by 01 432547  
month: 01 1981-01

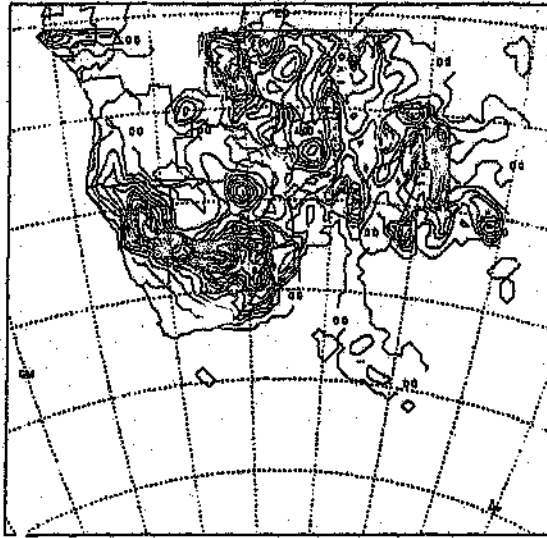
z = 146.4 m

t = 2100 UTC

Figure 5.9 Vertical velocities (in  $\text{cm.s}^{-1} \times 10^{-4}$ ) for (a) the control and (b) the sensitivity simulations at the 146.4 m sigma level for 2100 UTC on 22 January 1981.

Control Run

January 22 1981



accum conv pop

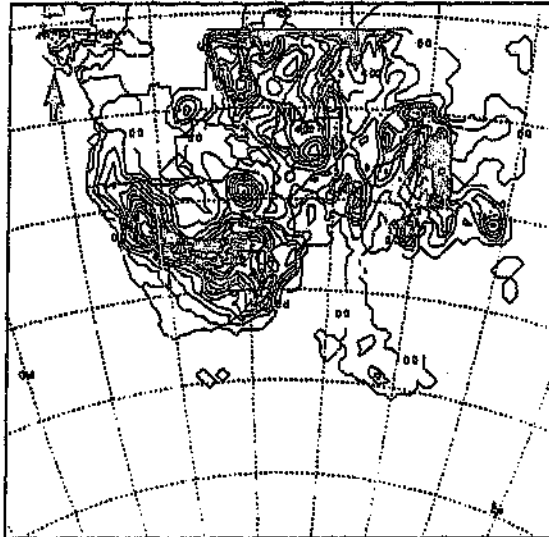
FILE: 012021-01  
P: 012021-01  
BY: 012021-01  
DATE: 012021-01

z = 146.4 m

t = 2100 UTC

Sensitivity Test 3

January 22 1981



accum conv pop

FILE: 012021-01  
P: 012021-01  
BY: 012021-01  
DATE: 012021-01

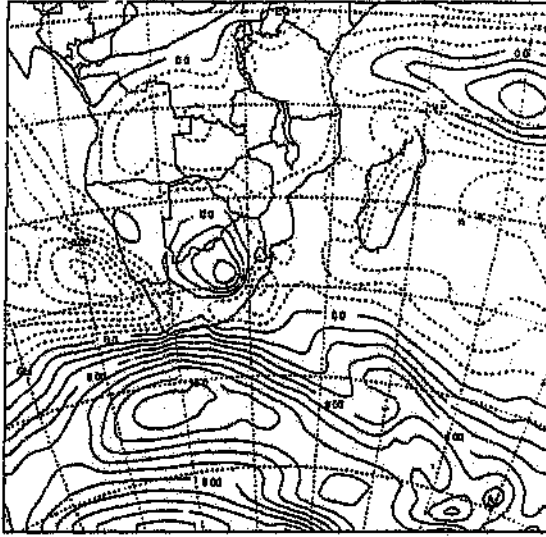
z = 146.4 m

t = 2100 UTC

Figure 5.10 Accumulated convective precipitation (in mm) for (a) the control and (b) the sensitivity simulations at the 146.4 m sigma level for 2100 UTC on 22 January 1981.

Control Run

January 22 1981



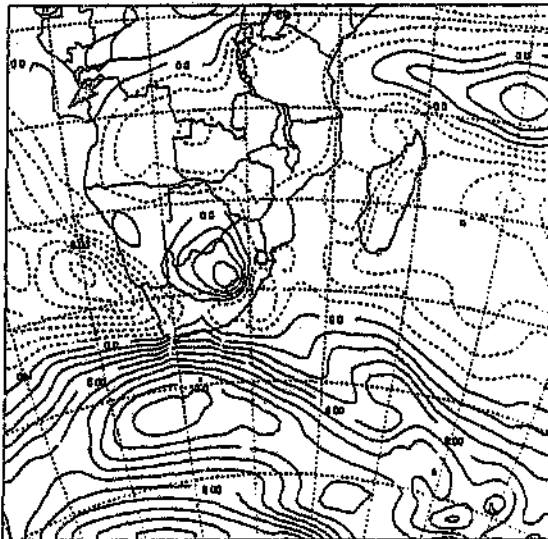
NOV 1 1981-01  
14 00 1981-01  
15 00 1981-01  
16 00 1981-01

z = 807.2 m

t = 1500 UTC

Sensitivity Test 3

January 22 1981



NOV 1 1981-01  
14 00 1981-01  
15 00 1981-01  
16 00 1981-01

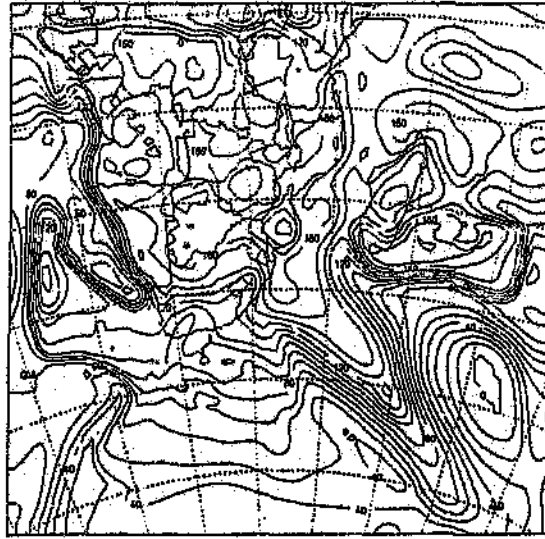
z = 807.2 m

t = 1500 UTC

Figure 5.11 U components (in m.s<sup>-1</sup>) for (a) the control and (b) the sensitivity simulations at the 807.2 m sigma level for 1500 UTC on 22 January 1981.

Control Run

January 22 1981



VAPOUR AND CLOUDS

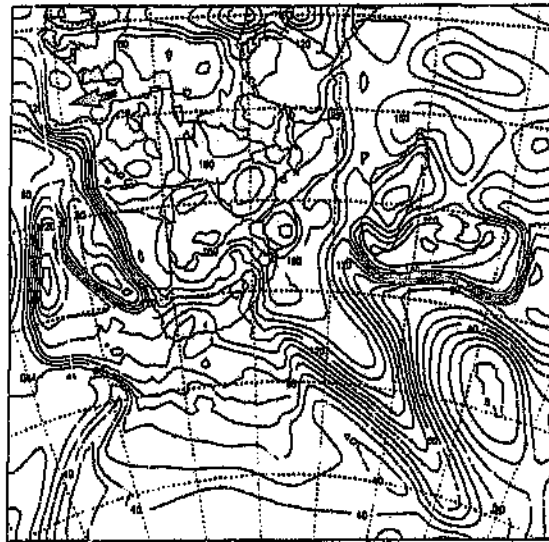
From 000000-00  
to 010000-01  
by 010000-00  
interval 00 0000-00

z = 807.2 m

t = 1500 UTC

Sensitivity Test 3

January 22 1981



VAPOUR AND CLOUDS

From 000000-00  
to 010000-01  
by 010000-00  
interval 00 0000-00

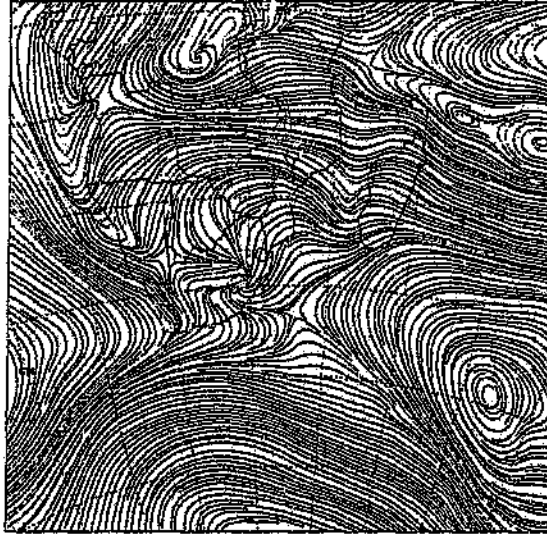
z = 807.2 m

t = 1500 UTC

Figure 5.12 Vapour and cloud mixing ratios (in  $\text{g.kg}^{-1} \times 10^{-4}$ ) for (a) the control and (b) the sensitivity simulations at the 807.2 m sigma level for 1500 UTC on 22 January 1981.

Control Run

January 22 1981



$z = 807.2 \text{ m}$

$t = 1500 \text{ UTC}$

Sensitivity Test 3

January 22 1981



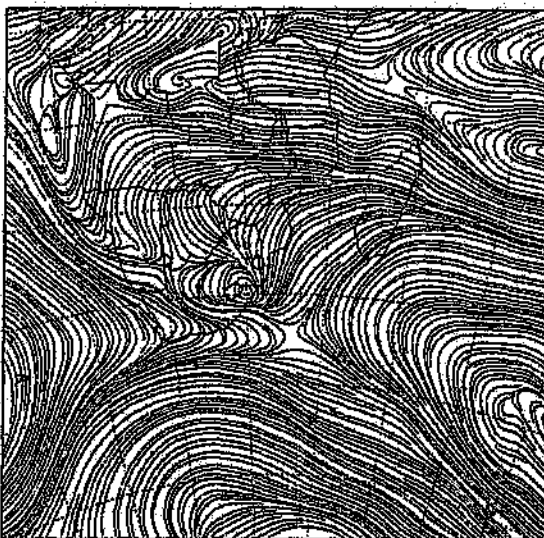
$z = 807.2 \text{ m}$

$t = 1500 \text{ UTC}$

Figure 5.13 Streamlines for (a) the control and (b) the sensitivity simulations at the 807,2 m sigma level for 1500 UTC on 22 January 1981.

Control Run

January 22 1981

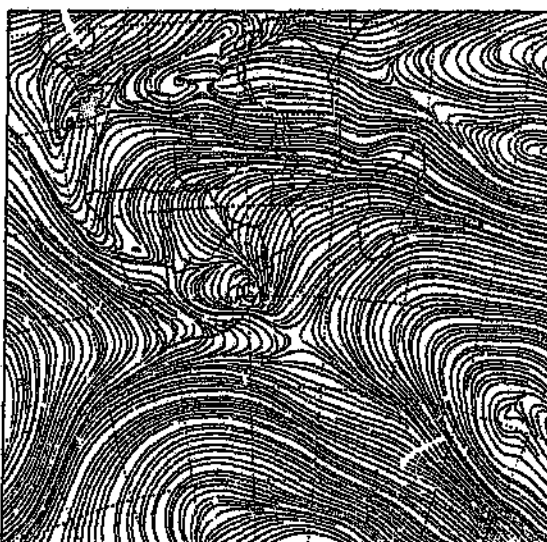


$z = 807.2 \text{ m}$

$t = 2100 \text{ UTC}$

Sensitivity Test 3

January 22 1981



$z = 807.2 \text{ m}$

$t = 2100 \text{ UTC}$

Figure 5.14 Streamlines for (a) the control and (b) the sensitivity simulations at the 807.2 m sigma level for 2100 UTC on 22 January 1981.

### *Day three*

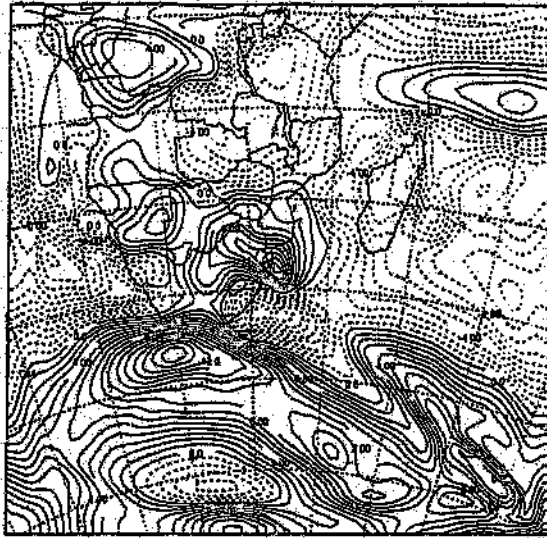
On the third day of the simulation (23 January 0900 UTC), the 146,4 m sigma level showed strong westerly components north of 10°S (Fig 5.15 a,b). The heightened onshore flow began to not only influence circulation in coastal, or near-coastal regions, but also further inland. The influence of the circulation on the interior can be seen in the intensification of cyclonic circulation over southern Zaire (Fig 5.16 a,b). Moisture availability was also greater over the western coastline north of 15°S (with the greater extent of the 0,017 gkg<sup>-1</sup>), and over northwestern Botswana (with greater extent of the 0,020 gkg<sup>-1</sup>) (Fig 5.17 a,b). The greater availability of moisture and hence heightened latent instability continued to produce higher accumulated precipitation values over Gabon, Congo, southern Zaire, Zimbabwe and in the vicinity of the Namibia/Botswana border (Fig 5.18 a,b).

By 2100 UTC the strong westerly wind component became prevalent over the Northern Provinces of South Africa with a simulated increase from 7 ms<sup>-1</sup> in the control to 8 ms<sup>-1</sup> in the sensitivity experiment (Fig 5.19 a,b). The strong simulated onshore flow that has been evident since 22 January has served to enhance convergence over Angola, and also east-west aligned convergence over the west coast of the continent and the immediate interior north of 12°S (Fig 5.20 a,b).

The comparison of accumulated convective precipitation with the control simulation shows the influence of the modified sea-surface temperature field limited predominantly to the western half of the continent and having little or no effect on the westerly wave perturbation. Simulated precipitation continued to be lower over the Mpumalanga, but remained higher over Gabon, Congo and in the vicinity of the Namibia/Botswana border. Precipitation increases are also noted for the first time over the southern portion of Zaire (Fig 5.21 a,b).

Control Run

January 23 1981



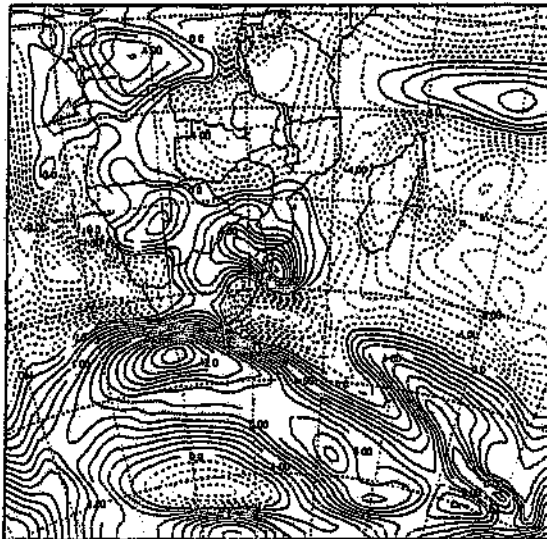
File: J23C-02  
in: 0 10000-02  
by: 0 10000-01  
date: 0 10000-01

z = 146.4 m

t = 900 UTC

Sensitivity Test 3

January 23 1981



File: J23C-02  
in: 0 10000-02  
by: 0 10000-01  
date: 0 10000-01

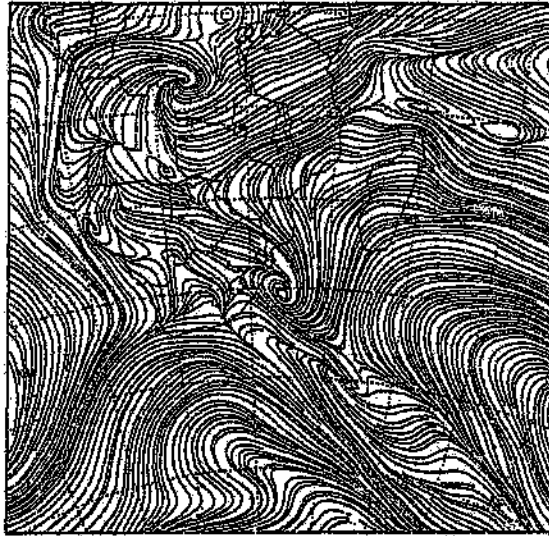
z = 146.4 m

t = 900 UTC

Figure 5.15 U components (in  $m \cdot s^{-1}$ ) for (a) the control and (b) the sensitivity simulations at the 146.4 m sigma level for 0900 UTC on 23 January 1981.

Control Run

January 23 1981



$z = 146.4 \text{ m}$

$t = 900 \text{ UTC}$

Sensitivity Test 3

January 23 1981



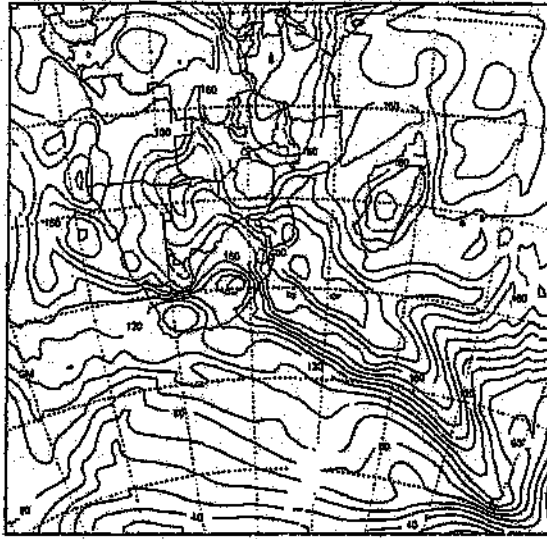
$z = 146.4 \text{ m}$

$t = 900 \text{ UTC}$

Figure 5.16 Streamlines for (a) the control and (b) the sensitivity simulations at the 146,4 m sigma level for 0900 UTC on 23 January 1981.

Control Run

January 23 1981



VAPOUR AND CLOUDS

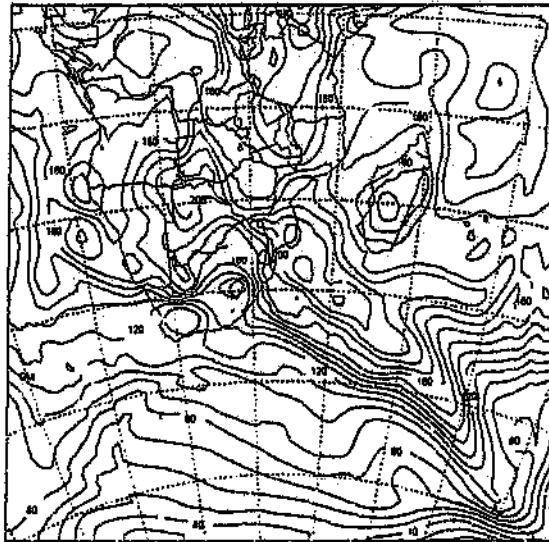
z = 146.4 m

t = 900 UTC

From 0 10000 01  
to 0 10000 01  
by 0 10000 01  
using 70 10000 01

Sensitivity Test 3

January 23 1981



VAPOUR AND CLOUDS

z = 146.4 m

t = 900 UTC

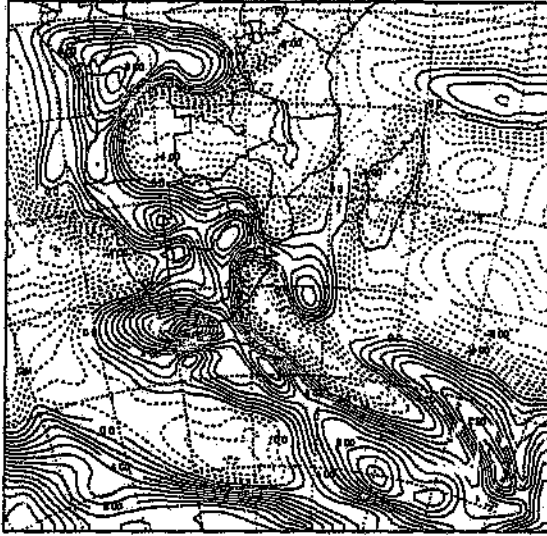
From 0 10000 01  
to 0 10000 01  
by 0 10000 01  
using 70 10000 01

Figure 5.17 Vapour and cloud mixing ratios (in  $\text{g kg}^{-1} \times 10^{-4}$ ) for (a) the control and (b) the sensitivity simulations at the 146.4 m sigma level for 0900 UTC on 23 January 1981.



Control Run

January 23 1981



Jan - 1 1981-01  
12 0 146.4 m  
12 0 146.4 m  
12 0 146.4 m

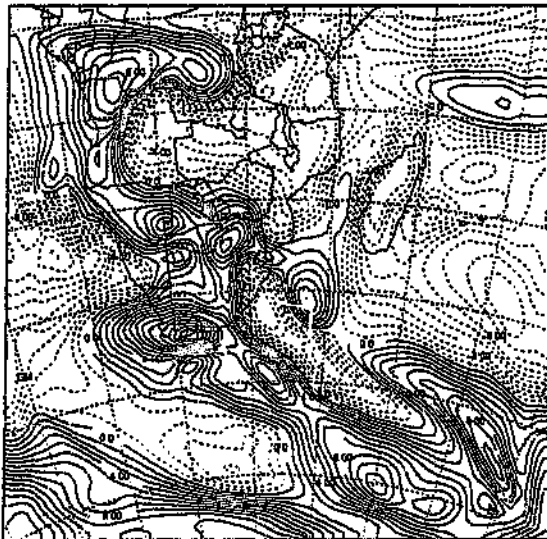
U

z = 146.4 m

t = 2100 UTC

Sensitivity Test 3

January 23 1981



Jan - 1 1981-01  
12 0 146.4 m  
12 0 146.4 m  
12 0 146.4 m

U

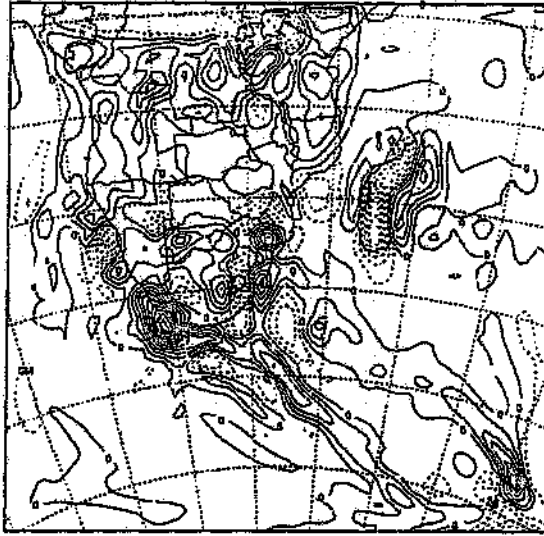
z = 146.4 m

t = 2100 UTC

Figure 5.19 U components in (m.s<sup>-1</sup>) for (a) the control and (b) the sensitivity simulations at the 146.4 m sigma level for 2100 UTC on 23 January 1981.

Control Run

January 23 1981



W

Contour interval  
= 0.50000  
= 0.50000  
= 0.50000

z = 146.4 m

t = 2100 UTC

Sensitivity Test 3

January 23 1981



W

Contour interval  
= 0.50000  
= 0.50000  
= 0.50000

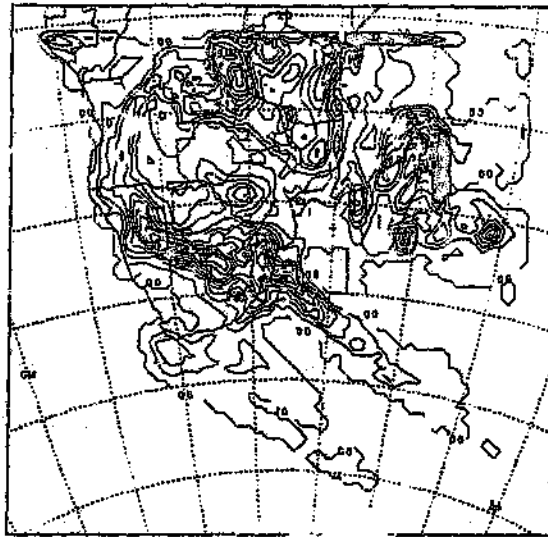
z = 146.4 m

t = 2100 UTC

Figure 5.20 Vertical velocities (in  $\text{cm.s}^{-1} \times 10^{-4}$ ) for (a) the control and (b) the sensitivity simulations at the 146.4 m sigma level for 2100 UTC on 23 January 1981.

Control Run

January 23 1981



accum conv prcp

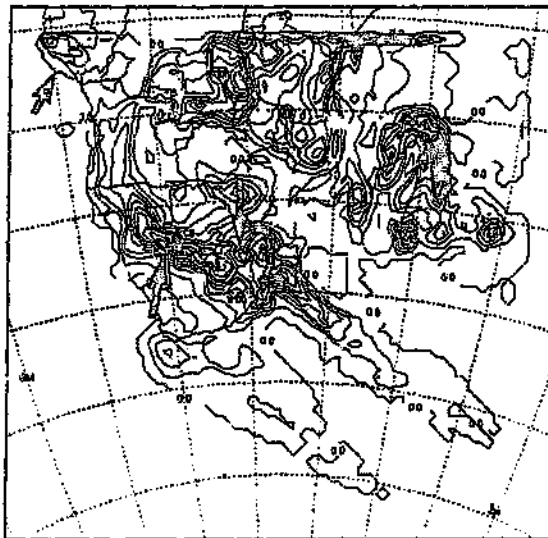
0.0000-0.0000  
0.0000-0.0000  
0.0000-0.0000  
0.0000-0.0000

z = 146.4 m

t = 2100 UTC

Sensitivity Test 3

January 23 1981



accum conv prcp

0.0000-0.0000  
0.0000-0.0000  
0.0000-0.0000  
0.0000-0.0000

z = 146.4 m

t = 2100 UTC

Figure 5.21 Accumulated convective precipitation (in mm) for (a) the control and (b) the sensitivity simulations at the 146.4 m sigma level for 2100 UTC on 23 January 1981.

#### *Day four*

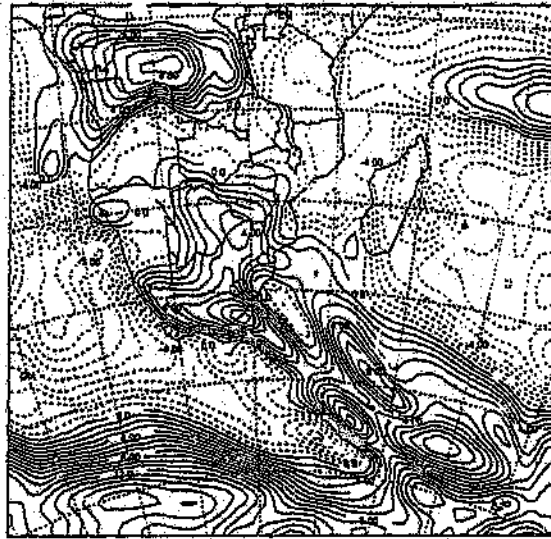
By the mid-day on 24 January the 146,4 m sigma level simulated the dissipation of the tropical-temperate trough through the eastward propagation of the westerly wave. Onshore winds remained strong north of 12°S with the extent of the 9 ms<sup>-1</sup> westerly wind component greater in the sensitivity simulation (Fig 5.22 a,b). The effects of the sea-surface temperature anomaly became visible in the westerly wave perturbation only on the fourth day of the sensitivity simulation, with stronger westerly component values evident at 40°S to 50°S with 10 ms<sup>-1</sup> compared to 9 ms<sup>-1</sup> (Fig 5.22 a,b). The greater onshore flow north of 12°S ensured the amplification of the tropical low over southern Zaire for the past 15 hours (Fig 5.23 a,b).

Total accumulated precipitation values showed continually higher precipitation over Gabon, Congo and the Namibia/Botswana border, along with marginally lower values over the Mpumalanga region. Precipitation over the southern portion of Zaire indicated increased falls for the past 15 hours (Fig 5.24 a,b). This is linked with the intensification of the tropical low and southerly return flow from this synoptic feature.

An overview of the upper level circulation changes from 2100 UTC on 23 January to the end of the simulation (1200 UTC on 24 January), continued to exhibit a progression of circulation differences brought about by the presence of the sea-surface temperature anomaly within the tropical west Atlantic Ocean. By 2100 UTC on 23 January the 807,2 m sigma level continued to show stronger onshore flow north of 10°S (Fig 5.25 a,b). The stronger onshore flow in turn enhanced cyclonic circulation around the tropical low centered over southern Zaire and caused the pattern of moisture availability to vary along the African west coast, north of 10°S. Maximum control values over Congo exhibited moisture ratios of 0,014 gkg<sup>-1</sup> compared to maximum sensitivity values of 0,016 gkg<sup>-1</sup> (Fig 5.25 a,b). These patterns continued well into the fourth day of the simulation and to the conclusion of the sensitivity experiment (Fig 5.27 a,b).

Control Run

January 24 1981



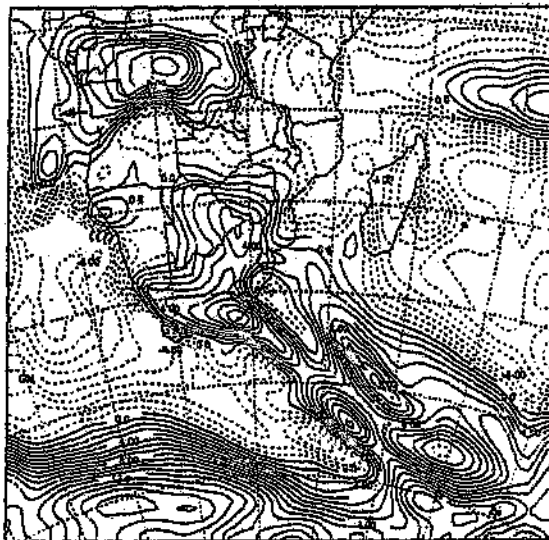
Jan - 11200-01  
10 11200-02  
11 11200-03  
12 11200-04

z = 146.4 m

t = 1200 UTC

Sensitivity Test 3

January 24 1981



Jan - 11200-01  
10 11200-02  
11 11200-03  
12 11200-04

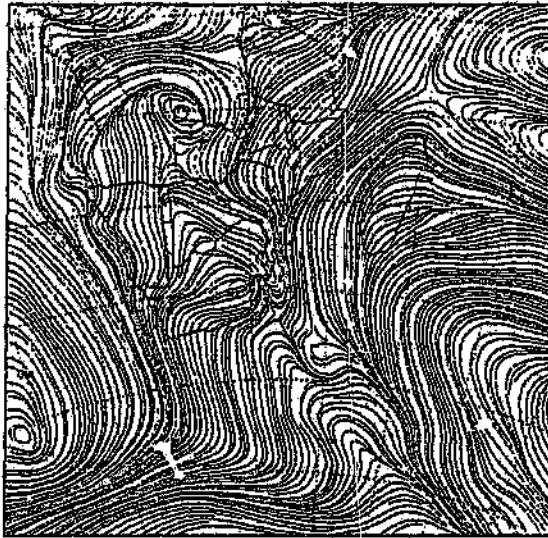
z = 146.4 m

t = 1200 UTC

Figure 5.22 J components in  $(m.s^{-1})$  for (a) the control and (b) the sensitivity simulations at the 146.4 m sigma level for 1200 UTC on 24 January 1981.

Control Run

January 24 1981

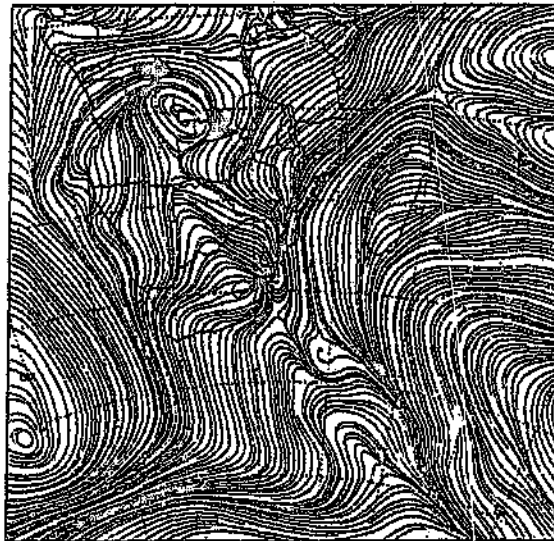


$z = 146.4 \text{ m}$

$t = 1200 \text{ UTC}$

Sensitivity Test 3

January 24 1981



$z = 146.4 \text{ m}$

$t = 1200 \text{ UTC}$

Figure 5.23 Streamlines for (a) the control and (b) the sensitivity simulations at the 146,4 m sigma level for 1200 UTC on 24 January 1981.



Control Run

January 23 1981



$z = 807.2 \text{ m}$

$t = 2100 \text{ UTC}$

Sensitivity Test 3

January 23 1981



$z = 807.2 \text{ m}$

$t = 2100 \text{ UTC}$

Figure 5.25 Streamlines for (a) the control and (b) the sensitivity simulations at the 807.2 m sigma level for 2100 UTC on 23 January 1981.

Control Run

January 23 1981



VAPOUR AND CLOUDS

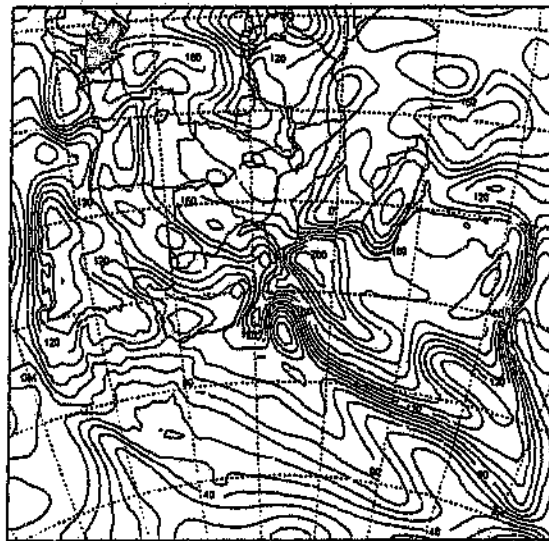
z = 807.2 m

t = 2100 UTC

0.000000  
0.000000  
0.000000  
0.000000

Sensitivity Test 3

January 23 1981



VAPOUR AND CLOUDS

z = 807.2 m

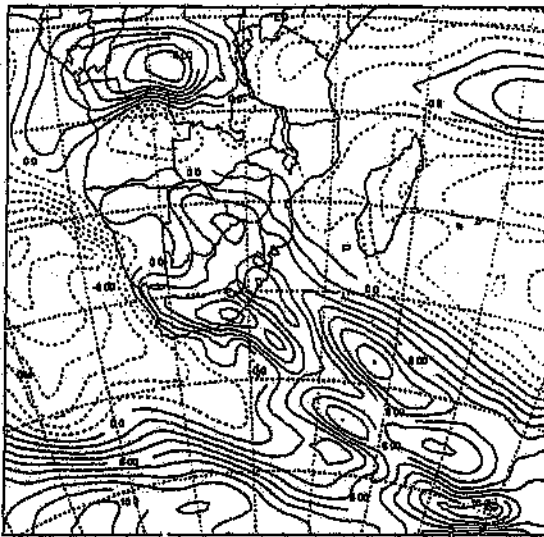
t = 2100 UTC

0.000000  
0.000000  
0.000000  
0.000000

Figure 5.26 Vapour and cloud mixing ratios ( $\mu\text{g kg}^{-1} \times 10^{-4}$ ) for (a) the control and (b) the sensitivity simulations at the 807.2 m sigma level for 2100 UTC on 23 January 1981.

Control Run

January 24 1981

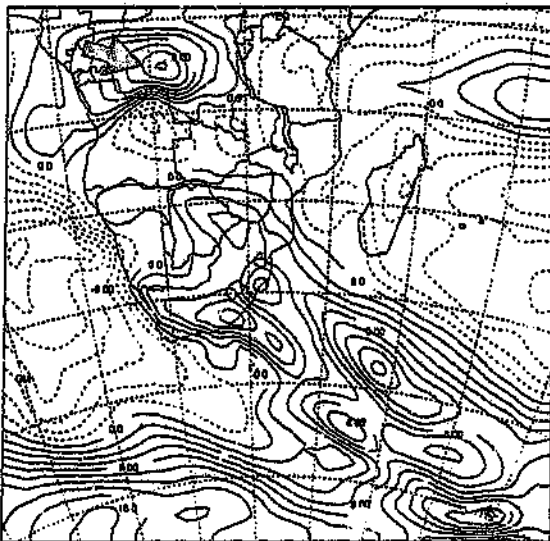


Run - 14228-02  
by D 14228-02  
by D 14228-02  
14228-02 14228-02

U  
z = 807.2 m      t = 1200 UTC

Sensitivity Test 3

January 24 1981



Run - 14228-02  
by D 14228-02  
by D 14228-02  
14228-02 14228-02

U  
z = 807.2 m      t = 1200 UTC

Figure 5.27 U components (in m.s<sup>-1</sup>) for (a) the control and (b) the sensitivity simulations at the 807.2 m sigma level for 1200 UTC on 24 January 1981.

## Discussion

Previous investigations of inter-annual variation in large-scale circulation over the tropical western Atlantic Ocean, using water level values of the Zaire river, showed that these values were positively related to sea-surface temperatures in the above mentioned area (Hirst and Hastenrath, 1983; Hastenrath, 1984). Positive anomalous sea-surface temperatures were found to strengthen zonal westerly circulation over Zaire, Gabon, and Congo regions, and in this way modulate the moisture content of the flow (Hirst and Hastenrath, 1983; Hastenrath, 1984). A comparison of hypotheses and theoretical observations of the effect of positive sea-surface temperature development on southern African atmospheric circulation with the numerical model simulation, a number of over-lapping similarities occur.

Onshore westerly flow over the west coast has been observed during periods of positive sea-surface temperature anomalies, and is consistent with the numerical model simulation. By 2100 UTC on 21 January stronger onshore flow was simulated north of  $10^{\circ}\text{S}$ . As this strengthened westerly zonal flow persisted, simulated moisture availability increased due to the influx of air over the warmer ocean. The simulation of heightened moisture availability and stronger onshore flow had a two-fold effect on the simulated circulation over the African west coast. Firstly the greater moisture availability served to increase instability north of  $10^{\circ}\text{S}$ . Secondly the increased westerly component produced strong convergence east of Angola. The combination of all these factors positively influenced rainfall, particularly over Gabon, Congo and southern Zaire. These circulation changes simulated in the sensitivity experiment were slowly translated southward along the west coast of Africa by the strengthened return flow from the tropical low and surface convergence east of Angola. It is still unclear as to the direct link of the tropical western Atlantic sea-surface temperature anomalies and circulation differences over South Africa.

## Chapter VI

### Synthesis and Conclusions

As water forms the major link between the atmospheric, economic and ecological environments of South Africa it is critical that the nature and controls on rainfall variability be understood. Most attempts at explaining rainfall variations over southern Africa have been limited to statistical, regional and planetary-scale investigations of the atmosphere and oceans over seasonal time frames. With the advent of mesoscale numerical models a more powerful means of investigating the atmosphere over southern Africa, at higher space and time resolutions, has become available. In particular the Regional Atmospheric Modelling System has proved to be a most successful tool in the investigation of the characteristics of tropical-temperate troughs during wet and dry years over southern Africa (van den Heever, 1995). Simulations of wet and dry case studies provided substantiation of a number of previous hypotheses and allowed the development of new insights, along with the refinement and extension of existing ideas (van den Heever, 1995; Mason and Jury, 1996).

The use of mesoscale models is new in South Africa, and thus many atmospheric research opportunities still exist. At present the focus of many research bodies in South Africa is the improvement of atmospheric circulation analysis. Until recently statistical approaches have been the sole method of analysing the effects of sea-surface temperature anomalies on atmospheric circulation, but the accuracy has been low due to the failure of statistical methods to take into account the complex and dynamic nature of boundary layer interactions with the ocean surface. It is only through numerical modelling and long term observation of boundary interactions that dramatic improvements can be made in the analysis of atmospheric circulation changes produced by the development of sea temperature anomalies. With this in mind the research presented in this dissertation will form a platform from which to begin such studies, as

the Regional Atmospheric Modelling System has proved to be adequately sensitive to positive modifications of sea-surface temperature and that the simulated response closely parallels the theoretical expectations and observations over a climatological time scale.

The control simulation, used as a comparison to the three sensitivity experiments, in itself provided an accurate simulation of the observed synoptic circulation for the period 21 to 24 January 1981. The approximate position of all the major circulation features were simulated, as well as the full development of the tropical-temperate trough on 23 January 1981. When the individual sensitivity experiments were compared to the control simulation each of the three initial simulation time-steps showed no differences from the control. This indicated that the numerical model requires a certain time-period in which to allow for circulation differences to be produced. The response magnitude of the individual experiments differed, with most pronounced results found in the tropical Indian Ocean anomaly experiment. The degree of response was found to be related to the average temperature of the particular ocean in which the anomaly developed. Comparing the average temperatures of the tropical Indian Ocean with those of the Agulhas Current retroflexion and the tropical western Atlantic Ocean it was found that the values were on average higher in the tropical Indian ocean. The addition of positive sea-surface temperature anomalies to a region of already high temperature values will affect the flux equations of the numerical model to a far greater degree than positive anomalies added to a region of colder background temperatures. Although the atmospheric circulation changes produced by the Agulhas Current anomaly inclusions were less dramatic than the tropical Indian Ocean anomaly experiment, the results are by no means insignificant. In the following subsections the atmospheric circulation changes produced by the tropical Indian Ocean, the Agulhas Current retroflexion, and the tropical western Atlantic anomaly experiments are discussed

### **Tropical Indian Ocean Anomaly (Sensitivity Test 1)**

- For the first sensitivity test, the initial circulation differences became detectable after nine hours with changes in near-surface windfields, and accumulated convective precipitation. The general pattern of circulation change indicated the development of stronger easterly winds to the east of Madagascar, with precipitation increases in the same area, and to the north.
- The continued simulation of strong easterly flow to the east of Madagascar, for the remainder of the experiment, served to maintain higher vertical instability over the island.
- Less than twelve hours into the simulation (0600 UTC, 22 January 1981), cyclogenesis began to occur west of the modified sea-surface temperatures. The combination of higher sea-surface temperatures, moisture availability, and vertical instability initiated the development of cyclogenesis to the north of Madagascar.
- Other features such as the westward expansion of anticyclonic flow north of  $10^{\circ}\text{S}$  and the development of surface divergence along  $40^{\circ}\text{E}$  reduced the moisture inflow into the subcontinent by deflecting moisture to the region of developing cyclogenesis.
- By the time the numerical model simulated the full development of the tropical-temperate trough over southern Africa, the reduction of moisture availability over the subcontinent produced lower widespread precipitation values over the country.

- Although the positive modification of sea-surface temperatures to the north and east of Madagascar had little effect on the formation and dissipation of the tropical-temperate trough, the simulated promotion of cyclogenesis over the area of sea-surface temperature modification served to reduce precipitation within the tropical-temperate trough.
- The simulated changes produced by the first sensitivity experiment coincide with the seasonal observations of atmospheric circulation modulation under similar anomalous sea-surface temperature conditions.

#### **Agulhas Current Retroflexion Anomaly Experiment (Sensitivity Test 2)**

- The modification of the sea-surface temperature field within the region of the Agulhas current retroflexion caused the numerical model to simulate a weakened onshore flow over the southern coast of South Africa, with heightened zonal or westerly flow to the south of the Agulhas Current retroflexion anomaly. This type of atmospheric circulation change was proposed by Walker (1989) who stated that the development of sea-surface temperature anomalies in this region serves to intensify the sea-surface temperature front towards the poles and thus shifting the surface westerlies in a poleward direction.
- Later in the simulation the positive sea-surface temperature anomalies aided in the enhancement of surface and near-surface convergence along the Angolan and Namibian coast, by increasing moisture inflow to the area. The anticyclonic circulation around the semi-permanent South Atlantic High pressure passes over the anomaly and flowed equatorward along the west coast of the subcontinent. The positive sea-surface temperatures would slowly have allowed moisture transfer from the anomaly source to the convergence zone along the west coast.

- As the first westerly wave perturbation passed over the sea-surface temperature anomaly, greater instability was imparted to the disturbance. The same was true for the second westerly wave disturbance.
- The initial enhancement of convergence along the southern African west coast produced higher convective precipitation values over the Namibia/Botswana border, with the westerly wave disturbances increasing precipitation values along the South African east coast.
- The sea-surface temperature anomalies served as a source of instability for the tropical low and the westerly wave disturbances.
- The addition of the anomalous sea-surface temperatures in the Agulhas Current retroflexion region had no effect on the general formation and dissipation of the tropical-temperate trough. The results of the Agulhas Current anomaly simulation closely resemble the circulation changes proposed by Walker (1989). The development of the anomaly produced higher sea-surface temperatures in the southern Agulhas region. This in turn intensified the sea-surface temperature gradient thus enhancing westerly flow further southwards. The warmer sea temperature anomaly strengthened ocean-atmosphere heat fluxes increasing baroclinicity within the boundary layer and reducing static stability over the anomaly. The reduction of stability influences both the structure of the westerly troughs and meridional flow along the west coast, that in turn enhanced precipitation.

### **The Tropical Western Atlantic Ocean Anomaly (Sensitivity Test 3)**

- The origin of circulation differences for the third sensitivity experiment was found directly over the area in which the sea-surface temperature anomalies were placed. The variation in atmospheric circulation and atmospheric parameters began with the modification of local surface wind-fields and surface

air temperatures. The surface wind fields showed a strengthening of westerly zonal circulation along with air temperatures increasing from the north.

- The positive modification of air temperatures enhanced the moisture carrying capacity of the onshore flow, which in turn encouraged vertical instability and local precipitation.
- These changes in atmospheric circulation were translated over time to the Zaire Air Boundary and southwards through return flow to Namibia and Botswana.
- The effect of the sea-surface temperature anomaly on South Africa is much less clearly defined although stronger westerly flow and instability was present over the Northern Province.
- The modification of atmospheric circulation was limited, for the most part, to the localised coastal regions and immediate interior of the African west coast.
- As with the previous two sensitivity experiments, the tropical western Atlantic Ocean anomalies have no direct impact on the formation and dissipation of the tropical-temperate trough. The effect of the anomaly was very localised with enhanced precipitation found over the regions of Gabon, Congo and southern Zaire. Strengthened onshore flow over the coast, adjacent to the sea-surface temperature anomaly, served to enhance convergence within the Zaire Air Boundary (ZAB). The impact on South Africa is less well defined although stronger westerly wind components and instability are found over the Northern Province and to the east of Durban.

The Regional Atmospheric Modelling System demonstrates the capability to run successful sensitivity simulations, over the tropical Indian Ocean, the Agulhas Current retroflection, and the tropical western Atlantic Ocean. Both the control and the sensitivity iterations identify quasi-stationary and transient synoptic scale features for the period 21 to 24 January 1981. The addition of positive sea-surface temperatur-

anomalies to the three designated areas revealed only localised sensitivity to these changes, with a slow transmission to other regions of the study domain. A general increase in vertical instability and convective precipitation were recorded for each of the three sensitivity tests. RAMS proved to be an effective tool by providing a mesoscale three-dimensional perspective of the influence of sea-surface temperature anomalies on the meteorology of a tropical-temperate trough over southern Africa. Even though the time scale of the experiment was limited, the small perturbations that were found in the simulated meteorological response, in each case were consistent with the expected climatic response to anomalously warm sea-surface temperatures.

## References

- Barclay, J.J., Jury, M.R. and Landman, W., 1993. Climatological and structural differences between wet and dry troughs over southern Africa in the early summer, *Meteorology and Atmospheric Physics*, 51, 41-51.
- Bell, L.D., 1986. The northwest Australian cloud band, *Preprints of the 2<sup>nd</sup> International Conference on Southern Hemisphere Meteorology*, American Meteorological Society, 42-45.
- Brundit, G.B. and Shannon, L.V., 1989. Cape Storms and the Agulhas current: a glimpse of the future?, *So. th African Journal of Science*, 85, 619-620.
- Bjerknes, J., 1969. Atmospheric teleconnections from the equatorial Pacific, *Monthly Weather Review*, 97, 163-172.
- Cione, J.J. and Raman, S., 1995. A numerical investigation of surface-induced mesocyclogenesis near the Gulf Stream, *Tellus*, 47A, 815-833.
- Clark, T.L., 1977. A small-scale dynamic model using a terrain-following co-ordinate transformation, *Journal of Computational Physics*, 24, 186-215.
- Cotton, W.R., Thompson, G., and Mielke, P.W., 1994. Real-time mesoscale prediction on workstations, *Bulletin of the American Meteorological Society*, 75, 349-362.

D'Abreton, P.C., 1993. The dynamics and energetics of tropical-temperate troughs over southern Africa, Unpublished Ph.D Thesis, University of the Witwatersrand, 231pp.

D'Abreton, P.C. and Lindesay, J.A., 1993. Water vapour transport over southern Africa during wet and dry early and late summer months, *International Journal of Climatology*, 13, 151-170.

D'Abreton, P.C. and Tyson, P.D., 1995. Divergent and non-divergent water vapour transport over southern Africa during wet and dry conditions, *Meteorology and Atmospheric Physics*, 55, 47-59

Davies, H.C., 1983. Limitations of some common lateral boundary schemes used in the regional NWP models, *Monthly Weather Review*, 111, 1002-1012.

Diab, R.D., Preston-Whyte, R.A. and Washington, R., 1991. Distribution of rainfall by synoptic type over Natal, South Africa, *International Journal of Climatology*, 11, 877-888.

Doyle, J.D., 1995. Coupled ocean wave/atmosphere mesoscale model simulations of cyclogenesis, *Tellus*, 47A, 766-778.

Druryan, L.M. and Hastenrath, S., 1991. Modelling the differential impact of 1984 and 1950 sea-surface temperatures on Sahell rainfall, *International Journal of Climatology*, 11, 367-380.

Dyer, T.G.J., 1979. Rainfall along the east coast of southern Africa, the Southern Oscillation, and the latitude of the subtropical high pressure belt, *Quarterly Journal of the Royal Meteorological Society*, **105**, 445-451.

Flatau, P., Tripoli, G.J., Verlinde, J., and Cotton, W.R., 1989. The CSU-RAMS cloud microphysics module: general theory and code documentation, Atmospheric Science Paper No. 451, Colorado State University, 88pp.

Fourie, M., 1981. Weer van die Maand, *South African Weather Bureau News Letter*, No. 382, 76-79.

Fox-Rabinovitz, M.S., 1991. Computational dispersion properties of horizontal staggered grids for atmospheric and ocean models, *Monthly Weather Review*, **119**, 1624-1639.

Gal-Chen, T. and Somerville, R.C.J., 1975. Numerical solution of the Navier-Stokes equations with topography, *Journal of Computational Physics*, **17**, 267-310.

Gates, D.M., 1980. *Biophysical Ecology*. Springer-Verlag, New York, 611pp.

Gillooly, J.F. and Walker, N.D., 1984. Spatial and temporal behaviour of sea-surface temperatures in the South Atlantic, *South African Journal of Science*, **80**, 97-100.

- Gründlingh, M.L., 1987. On the seasonal temperature variation in the southwestern Indian Ocean, *South African Geographical Journal*, 69, 129-138.
- Gordon, H.B. and Hunt, B.G., 1991. Droughts, floods, and sea-surface temperature anomalies: a modelling approach, *International Journal of Climatology*, 11, 347-365.
- Hamilton, K. and Garcia, R.R., 1986. El Niño/Southern Oscillation events and their associated midlatitude teleconnections, *Bulletin of the American Meteorological Society*, 67, 1354-1361.
- Harangozo, S. and Harrison, M.S.J., 1983. On the use of synoptic data in indicating the presence of cloud bands over southern Africa, *South African Journal of Science*, 79, 413-414.
- Harangozo, S., 1989. Circulation characteristics of some South African rainfall systems, Unpublished Msc Dissertation, University of the Witwatersrand, 123pp.
- Harrison, M.S.J., 1984a. A generalised classification of South African summer rain-bearing synoptic systems, *Journal of Climatology*, 4, 547-560.
- Harrison, M.S.J., 1984b. The annual rainfall cycle over the central interior of South Africa, *South African Geographical Journal*, 66, 47-74.

- Harrison, M.S.J., 1986. A synoptic climatology of South African rainfall variations, Unpublished PhD Thesis, University of the Witwatersrand, 341pp.
- Hastenrath, S., 1984. Inter-annual variability and annual cycle: mechanisms of circulation and climate in the tropical Atlantic sector, *Monthly Weather Review*, **112**, 1097-1107.
- Hastenrath, S., Greischar, L. and van Heerden, J., 1995. Prediction of the summer rainfall over South Africa, *Journal of Climate*, **8**, 1511-1518.
- Hirst, A.C. and Hastenrath, S., 1983. Diagnostics of hydrometeorological anomalies in the Zaïre (Congo) Basin, *Quarterly Journal of the Royal Meteorological Society*, **109**, 881-892.
- Hunt, H.A., Taylor, G. and Qualey, E.T., 1913. The climate and weather of Australia, *Bureau of Meteorology*, Melbourne.
- Janjic, T.Z. and Janjic, Z.I., 1993. Spectral distributions of the pressure gradient force errors in  $\sigma$ -coordinate spectral and grid-point models in an idealized case, *Meteorology and Atmospheric Physics*, **52**, 129-135.
- Jury, M.R. and Reason, C.J.C., 1989. Extreme subsidence in the Agulhas-Benguela air mass transition, *Boundary-Layer Meteorology*, **46**, 35-51.

- Jury, M.R. and Pathack, B., 1991. A study of climate and weather variability over the tropical southwest Indian Ocean, *Meteorology and Atmospheric Physics*, 47, 37-48.
- Jury, M.R., Pathack, B., Campbell, G., Wang, B. and Landman, W., 1991. Transient convective waves in the tropical southwest Indian Ocean, *Meteorology and Atmospheric Physics*, 47, 27-36.
- Jury, M.R., Pathack, B. and Sohn, B.J., 1992. Spatial structure and interannual variability of summer convection over southern Africa and the SW Indian Ocean, *South African Journal of Science*, 88, 275-280.
- Jury, M.R., 1993. A thermal front within the marine atmospheric boundary layer over the Agulhus Current south of Africa: Composite aircraft observations, *Journal of Geophysical Research*, 99 C2, 3297-3304.
- Jury, M.R. and Pathack, B., 1993. Composite climatic patterns associated with extreme modes of summer rainfall over southern Africa: 1975-1984, *Theoretical and Applied Climatology*, 47, 137-145.
- Jury, M.R., 1996. Regional teleconnection patterns associated with summer rainfall over South Africa, Namibia and Zimbabwe, *International Journal of Climatology*, 16, 135-153.

- Kershaw, R., 1988. The effect of a sea surface temperature anomaly on a prediction of the onset of the south-west monsoon over India, *Quarterly Journal of the Royal Meteorological Society*, 114, 325-345.
- Kiladis, G.N. and Diaz, H.F., 1986. An analysis of the 1977-78 ENSO episode and comparison with 1982-83, *Monthly Weather Review*, 114, 1035-1047.
- Klemp, J.B. and Wilhelmson, R.B., 1978a. The simulation of three-dimensional convective storm dynamics, *Journal of the Atmospheric Sciences*, 35, 1070-1056.
- Klemp, J.B. and Wilhelmson, R.B., 1978b. Simulations of right- and left-moving storms produced through storm-splitting, *Journal of the Atmospheric Sciences*, 35, 1097-1110.
- Kuhnel, I., 1959. Tropical-extratropical cloudband climatology based on satellite data, *International Journal of Climatology*, 9, 441-463.
- Lindesay, J.A., Harrison, M.S.J. and Haffner, M.P., 1986. The Southern Oscillation and South African rainfall, *South African Journal of Science*, 82, 196-198.
- Lindesay, J.A., 1988. The Southern Oscillation and atmospheric circulation changes over southern Africa, Unpublished PhD Thesis, University of the Witwatersrand, 284pp.
- Lindesay, J.A., 1988. South African rainfall, the Southern Oscillation and a Southern Hemisphere semi-annual cycle, *Journal of Climatology*, 8, 17-30.

- Lindesay, J.A. and Vogel, C.H., 1990. Historical evidence for Southern Oscillation-southern African rainfall relationships, *International Journal of Climatology*, 10, 679-689.
- Lindesay, J.A. and Jury, M.R., 1991. Atmospheric circulation controls and characteristics of a flood event in central South Africa, *International Journal of Climatology*, 11, 609-627.
- Mahrer, Y. and Pielke, R.A., 1977. A numerical study of the airflow over irregular terrain, *Beiträge zur Physik der Atmosphäre*, 50, 98-113.
- Manton, M.J. and Cotton, W.R., 1977. Parameterization of the atmospheric surface layer, *Journal of Atmospheric Sciences*, 34, 331-334.
- Mason, S.J., 1990. Temporal variability of sea surface temperatures around southern Africa: a possible forcing mechanism for the 18-year rainfall oscillation?, *South African Journal of Science*, 86, 243-252.
- Mason, S.J., 1992. Sea surface temperatures and South African rainfall variability. Unpublished Ph.D. Thesis, University of the Witwatersrand. 235pp.
- Mason, S.J., 1995. Sea-surface temperature - South African rainfall associations, 1910-1989, *International Journal of Climatology*, 15, 119-135.

- Mason, S.J. and Tyson, P.D., 1992. The modulation of sea surface temperature and rainfall associations over southern Africa with solar activity and the Quasi-Biennial Oscillation, *Journal of Geophysical Research*, 97 D5, 5847-5856.
- Mason, S.J. and Lindesay, J.A., 1993. A note on the modulation of Southern Oscillation-southern African associations with the Quasi-Biennial Oscillation, *Journal of Geophysical Research*, 98 D5, 8847-8850.
- Mason, S.J., Lindesay, J.A. and Tyson, P.D., 1994. Simulating drought in southern Africa using sea surface temperature variations, *Water SA*, 20, 15-22.
- Mason, S.J. and Jury, M.R., 1996. Climatic variability and change over southern Africa: a reflection on underlying processes, *Progress in Physical Geography*, (in press).
- McCumber, M.C. and Pielke, R.A., 1981. Simulation of the effects of surface fluxes of heat and moisture in a mesoscale numerical model, *Journal of Geophysical Research*, 86 C10, 9929-9938.
- Mechoso, C.R., Kitoh, A., Moorthi, S. and Arakawa, A., 1987. Numerical simulations of the atmospheric response to a sea surface temperature anomaly over the equatorial eastern Pacific Ocean, *Monthly Weather Review*, 115, 2936-2956.
- Meehl, G.A., 1988. Tropical-midlatitude interactions in the Indian and Pacific sectors of the Southern Hemisphere, *Monthly Weather Review*, 116, 472-484.

- Mesinger, F. and Arakawa, A., 1976. Numerical methods used in atmospheric models, GARP Publication Series No. 17, WMO/ICSU Joint Organising Committee, 64pp.
- Mesinger, J., Janjic, Z.I., Nickovic, S., Gavrilov, D. and Deaven, D.G., 1988. The step-mountain co-ordinate: model description and performance for cases of Alpine lee cyclogenesis and for a case of an Appalachian redevelopment, *Monthly Weather Review*, **116**, 1493-1518.
- Mey, R.D., Walker, N.D. and Jury, M.R., 1990. Surface heat fluxes and marine boundary layer modification in the Agulhus retroflection region, *Journal of Geophysical Research*, **95** C9, 15 997-16 015.
- Miron, O. and Tyson, P.D., 1984. Wet and dry conditions and pressure anomaly fields over South Africa and the adjacent oceans, 1963-79, *Monthly Weather Review*, **112**, 2127-2132.
- Mo, K.C. and Kalnay, E., 1991. Impact of sea surface temperature anomalies on the skill of monthly forecasts, *Monthly Weather Review*, **119**, 2771-2793.
- Mo, K.C., Wang, X.L., and Tracton, M.S., 1994. Tropical and extratropical interaction and its impact on extended-range forecasting. Part I: the impact of sea surface temperature anomalies, *Monthly Weather Review*, **122**, 274-290.

- Newell, R.E., 1979. Climate and the ocean, *American Scientist*, **67**, 405-416.
- Nicholson, S.E., 1986. The spatial coherence of African rainfall anomalies: interhemispheric teleconnections, *Journal of Climate and Applied Meteorology*, **25**, 1365-1381.
- Parker, D.E., 1987. The Meteorological Office historical sea-surface temperature data set, *Meteorological Magazine*, **116**, 250-254.
- Parker, D.E. and Folland, C.K., 1988. The Meteorological Office historical sea surface temperature data set, in *Recent Climatic Change*, Ed. Gregory, S., Belhaven Press, London, 41-50.
- Perkey, D.J. and Kreitzberg, C.W., 1976. A time-dependent lateral boundary scheme for limited-area primitive equation models, *Monthly Weather Review*, **104**, 744-755.
- Physick, W.L., Abbs, D.J., and Pielke, R.A., 1989. Formulation of the thermal internal boundary layer in a mesoscale model, *Boundary-Layer Meteorology*, **49**, 99-111.
- Pielke, R.A., Cotton, W.R., Walko, R.L., Tremback, C.J., Lyons, W.A., Grasso, L.D., Nicholls, M.E., Moran, M.D., Wesely, D.A., Lee, T.J. and Copeland, J.H., 1992. A comprehensive meteorological modelling system - RAMS, *Meteorology and Atmospheric Physics*, **49**, 69-91.
- Preston-Whyte, R.A. and Tyson, P.D., 1988. *The Atmosphere and Weather of Southern Africa*, Oxford University Press, Cape Town, 374pp.

- Rouault, M. and Lutjeharms, J.R.E., 1994. Air-sea interaction in the marine atmospheric boundary layer: a new South African research venture, *South African Journal of Science*, 90, 11-12.
- Soden, B.J. and Bretherton, F.P., 1994. Evaluation of water vapour distribution in general circulation models using satellite observations, *Journal of Geophysical Research*, 99 D1, 1187-1210.
- Sonka, S.T., Lamb, P.J., Hollinger, S.E. and Mjelde, J.W., 1986. Economic use of weather and climate information: concepts and an agricultural example, *Journal of Climatology*, 6, 447-457.
- Snook, J.S., Cram, J.M. and Schmidt, J.M., 1995. LAPS/RAMS. A nonhydrostatic mesoscale numerical modeling system configured for operational use, *Tellus*, 47A, 864-875.
- Streten, N.A., 1973. Some characteristics of satellite-observed bands of persistent cloudiness over the Southern Hemisphere. *Monthly Weather Review*, 101, 486-495.
- Taljaard, J.J., 1986. Contrasting atmospheric circulation during dry and wet summers in South Africa, *South African Weather Bureau News Letter*. No. 445, 1-5.

- Tapp, R.G. and Barrell, S.L., 1984. The north-west Australian cloud band: climatology, characteristics and factors associated with development, *Journal of Climatology*, 4, 411-424.
- Thompson, G., 1993. Prototype real-time mesoscale prediction during the 1991-92 winter season and statistical verification of model data, Unpublished Msc Dissertation, Colorado State University, 105pp.
- Tremback, C.J., Tripoli, G.J. and Cotton, W.R., 1985. A Regional Atmospheric Modelling System, in *Proceedings of the International Conference on the Development and Application of Computer Techniques to Environmental Studies*, Ed. Zannetti, P., Computational Mechanics Publications, Boston, 601-607.
- Tremback, C.J. and Kessler, R., 1985. A surface temperature and moisture parameterisation for use in mesoscale numerical models, Reprints of the 7<sup>th</sup> Conference of the American Meteorological Society, Boston, 355-358.
- Tripoli, G.J. and Cotton, W.R., 1980. A numerical investigation of several factors leading to the observed variable intensity of deep convection over South Florida, *Journal of Applied Meteorology*, 19, 1037-1063.
- Tripoli, G.J. and Cotton, W.R., 1982. The Colorado State University three-dimensional cloud/mesoscale model - 1982. Part I: general theoretical framework and sensitivity experiments, *Journal de Atmosphériques*, 16, 185-219.

- Tyson, P.D., 1981. Atmospheric circulation variations and the occurrence of extended wet and dry spells over southern Africa, *Journal of Climatology*, 1, 115-131.
- Tyson, P.D., 1984. The atmospheric modulation of extended wet and dry spells over South Africa, 1958-1978, *Journal of Climatology*, 4, 627-635.
- Tyson, P.D., 1986. *Climatic Change and Variability in Southern Africa*, Oxford University Press, Cape Town, 220pp.
- Van den Heever, S.C., 1995. Modelling tropical-temperate troughs over southern Africa, Unpublished M.Sc Dissertation, University of the Witwatersrand, 216pp.
- Walker, N.D., 1990. Links between South African summer rainfall and temperature variability of the Agulhas and Benguela Current Systems, *Journal of Geophysical Research*, 95 C3, 3297-3319.
- Walko, R.L. and Tremback, C.J., 1991. RAMS. The Regional Atmospheric Modelling System Version 2C, User's Guide, STeR Inc., Fort Collins, 89pp.
- Wright, W.J., 1988. The low latitude influence on winter rainfall in Victoria, south-eastern Australia - I. Climatological aspects, *Journal of Climatology*, 8, 437-462.

Handwritten text, possibly a signature or a list of names, located in the upper right quadrant of the page. The text is faint and difficult to decipher.

1. The first part of the document discusses the importance of maintaining accurate records of all transactions and activities. It emphasizes that this is essential for ensuring transparency and accountability in the organization's operations.

2. The second part of the document outlines the various methods and tools used to collect and analyze data. It highlights the need for consistent data collection procedures and the use of advanced analytical techniques to derive meaningful insights from the data.

3. The third part of the document focuses on the implementation of data-driven decision-making processes. It provides a detailed overview of the steps involved in identifying key performance indicators, setting targets, and monitoring progress against these targets.

4. The fourth part of the document discusses the challenges and risks associated with data management and analysis. It identifies common pitfalls such as data quality issues, privacy concerns, and the potential for misinterpretation of data, and offers strategies to mitigate these risks.

5. The fifth part of the document concludes by summarizing the key findings and recommendations. It emphasizes the importance of a continuous and iterative process of data collection, analysis, and decision-making to drive organizational success and growth.

**Author: Crimp, Steven Jeffrey.**

**Name of thesis: Simulating sea-surface temperature effects on Southern African rainfall using a mesoscale numerical model.**

***PUBLISHER:***

University of the Witwatersrand, Johannesburg

©2015

***LEGALNOTICES:***

**Copyright Notice:** All materials on the University of the Witwatersrand, Johannesburg Library website are protected by South African copyright law and may not be distributed, transmitted, displayed or otherwise published in any format, without the prior written permission of the copyright owner.

**Disclaimer and Terms of Use:** Provided that you maintain all copyright and other notices contained therein, you may download material (one machine readable copy and one print copy per page) for your personal and/or educational non-commercial use only.

The University of the Witwatersrand, Johannesburg, is not responsible for any errors or omissions and excludes any and all liability for any errors in or omissions from the information on the Library website.